

The non-linear evolution of jet quenching

Edmond Iancu

Institut de Physique Théorique de Saclay, F-91191 Gif-sur-Yvette, France

E-mail: edmond.iancu@cea.fr

ABSTRACT: We construct a generalization of the JIMWLK Hamiltonian, going beyond the eikonal approximation, which governs the high-energy evolution of the scattering between a dilute projectile and a dense target with an arbitrary longitudinal extent (a nucleus, or a slice of quark–gluon plasma). Different physical regimes refer to the ratio L/τ between the longitudinal size L of the target and the lifetime τ of the gluon fluctuations. When $L/\tau \ll 1$, meaning that the target can be effectively treated as a shockwave, we recover the JIMWLK Hamiltonian, as expected. When $L/\tau \gg 1$, meaning that the fluctuations live inside the target, the new Hamiltonian governs phenomena like the transverse momentum broadening and the radiative energy loss, which accompany the propagation of an energetic parton through a dense QCD medium. Using this Hamiltonian, we derive a non-linear equation for the dipole amplitude (a generalization of the BK equation), which describes the high-energy evolution of jet quenching. As compared to the original BK–JIMWLK evolution, the new evolution is remarkably different: the plasma saturation momentum evolves much faster with increasing energy (or decreasing Bjorken’s x) than the corresponding scale for a shockwave (nucleus). This widely opens the transverse phase-space for the evolution and implies the existence of large radiative corrections, enhanced by the double logarithm $\ln^2(LT)$, with T the temperature of the medium. This confirms and explains from a physical perspective a recent result by Liou, Mueller, and Wu (arXiv:1304.7677). The dominant, double-logarithmic, corrections are smooth enough to be absorbed into a renormalization of the jet quenching parameter \hat{q} . This renormalization is controlled by a linear equation supplemented with a saturation boundary, which emerges via controlled approximations from the generalized BK equation alluded to above.

Contents

1	Introduction	1
2	The evolution Hamiltonian in the high-energy approximation	7
2.1	The evolution Hamiltonian	7
2.2	Virtual corrections and probability conservation	11
3	A shockwave target: recovering the JIMWLK Hamiltonian	14
3.1	Performing the time integrations	14
3.2	The Balitsky–Kovchegov equation	18
4	The high-energy evolution of transverse momentum broadening	21
4.1	The tree-level approximation	22
4.2	The dipole evolution equation	25
4.3	The single scattering approximation	30
4.3.1	The BFKL equation	30
4.3.2	The double logarithmic approximation	33
4.3.3	The phase-space for the high-energy evolution	36
4.4	Gluon evolution and saturation in the medium	39
4.5	Comments on the effects of multiple scattering	42
5	The high-energy evolution of the radiative energy loss	45
5.1	The tree-level approximation: the BDMPSZ formalism	45
5.2	The dominant radiative corrections	49
6	Conclusions and perspectives	52
A	A succinct derivation of the evolution Hamiltonian	54
B	The background field gluon propagator	57
C	A sum rule for the light-cone gauge propagator	58
D	Finite-N_c corrections within the mean field approximation	59

1 Introduction

The concept of jet quenching globally denotes the modifications in the properties of a ‘hard probe’ (an energetic parton, or the jet generated by its evolution) which occur when this ‘jet’ propagates through the dense QCD matter (‘quark–gluon plasma’) created in the intermediate stages of a ultrarelativistic nucleus–nucleus collision [1–5]. This encompasses several related phenomena like

the transverse momentum broadening, the (radiative) energy loss, or the jet fragmentation via medium-induced gluon branching, and also the associated observables, like the nuclear modification factor, or the di-jet asymmetry. A common denominator of these phenomena is that, within most of their theoretical descriptions to date, they depend upon the medium properties via a single parameter : a transport coefficient known as the ‘jet quenching parameter’ \hat{q} . This explains the importance of this quantity \hat{q} for both theory and phenomenology, and motivates the recent attempts to obtain better estimates for it from first principles, at least in special cases [6–11].

Roughly speaking, the jet quenching parameter measures the dispersion in transverse momentum¹ accumulated by a fast parton after crossing the medium over a distance L : $\langle p_{\perp}^2 \rangle \simeq \hat{q}L$. At weak coupling, the dominant mechanism responsible for this dispersion is multiple scattering off the medium constituents. At leading order in α_s , \hat{q} can be computed as the second moment of the ‘collision kernel’ (the differential cross-section for elastic scattering in the medium; see Sect. 4.1 for details). Beyond leading order, one needs a non-perturbative definition for the transverse momentum broadening. The one that we shall adopt here and which is often used in the literature involves the ‘color dipole’, a light-like Wilson loop in the color representation of the fast parton. Physically, this Wilson loop describes the S -matrix for a small ‘color dipole’ (a quark-antiquark pair, or a set of two gluons, in a color singlet state) which propagates through the medium. Via unitarity, the Fourier transform of this S -matrix determines the cross-section $dN/d^2\mathbf{p}$ for transverse momentum broadening [12, 13]. At tree-level, these definitions imply $\langle p_{\perp}^2 \rangle^{(0)} \simeq \hat{q}^{(0)}(L)L$, with $\hat{q}^{(0)}(L)$ logarithmically dependent upon the medium size L . This dependence enters via the resolution of the scattering process: the transverse momenta transferred by the medium can be as large as the ‘saturation momentum’ $Q_s^2 \equiv \hat{q}L$ (see Sect. 4.1). Beyond leading order, it is a priori unclear whether the notion of ‘jet quenching parameter’ (as a quasi-local transport coefficient) is still useful, or even well-defined. Our criterion in that sense will be to check whether a formula like $\langle p_{\perp}^2 \rangle \simeq \hat{q}(L)L$ does still hold, with $\hat{q}(L)$ a reasonably slowly-varying function. But even when this appears to be the case, we shall see that the L -dependence of \hat{q} is generally enhanced by the radiative corrections, due to the intrinsic non-locality of the quantum fluctuations.

So far, two different classes of next-to-leading order corrections, which correspond to very different kinematical regimes, have been computed at weak coupling [7, 9]. In Ref. [7], Caron-Huot considered a medium which is a weakly-coupled quark-gluon plasma (QGP) with temperature T and computed the corrections of $\mathcal{O}(g)$ to the ‘collision kernel’, as generated by the soft, highly-populated (and hence semi-classical), thermal modes, with energies and momenta $\lesssim gT$. (The corresponding leading-order value has been computed by Arnold and Xiao [6].) These corrections do not modify the logarithmic dependence of \hat{q} upon the medium size L , which is rather introduced by the hardest collisions, with transferred momenta $k_{\perp} \sim Q_s$. (We implicitly assume that $Q_s \gg T$.)

By contrast, in Ref. [9], Liou, Mueller, and Wu have studied the relatively hard and nearly on-shell gluon fluctuations, with large transverse momenta $p_{\perp} \gg T$ and even larger longitudinal momenta, $p^3 \simeq p^0 \gg p_{\perp}$ (in the plasma rest frame). Such fluctuations, which are most naturally viewed as bremsstrahlung by the projectile, are not sensitive to the detailed properties of the medium. They depend upon the latter only via the tree-level value $\hat{q}^{(0)}$ of the jet quenching parameter and via two basic scales — the longitudinal extent L of the medium and the wavelength

¹By ‘transverse’ we mean the two dimensional plane $\mathbf{x} = (x^1, x^2)$ orthogonal to the parton direction of motion, conventionally chosen along x^3 .

λ of its typical constituents (with $\lambda = 1/T$ for the QGP) — which constrain the phase-space for bremsstrahlung. Ref. [9] found large one-loop corrections² to $\langle p_{\perp}^2 \rangle$, of relative order $\alpha_s N_c \ln^2(L/\lambda)$, where the double logarithm comes from the phase-space: one logarithm is generated by integrating over the lifetime $\tau \sim p^0/p_{\perp}^2$ of the fluctuations, over the range $\lambda \ll \tau \ll L$, and the other one comes from the respective transverse momenta, within the interval $\hat{q}\tau \ll p_{\perp}^2 \ll Q_s^2$ (for a given value of τ). The lower limit $\hat{q}\tau$ on p_{\perp}^2 refers to multiple scattering: the condition $p_{\perp}^2 \gg \hat{q}\tau$ means that the relevant fluctuations are hard enough to suffer only one scattering during their lifetime.

Note that this ‘single scattering’ property refers to a color *dipole*, and not to a charged parton. That is, the large radiative corrections identified in Ref. [9] should not be viewed as a renormalization of the collision kernel above mentioned, which represents the differential cross-section for individual scatterings in the plasma, but rather as a change in the *transport* cross-section relevant for transverse momentum broadening, which is controlled by the relatively rare collisions involving a sufficiently large momentum transfer (which can be as large as Q_s).

For what follows, it is important to notice that the medium size L sets the upper limit on the lifetime τ of the fluctuations, and hence on their energy p^0 . Accordingly, when increasing L , one opens the phase-space for fluctuations which are more and more energetic. Such fluctuations can then evolve towards lower energies, via soft gluon emissions. This evolution is represented by Feynman graphs of higher-loop order (gluon cascades which are strongly ordered in energy), which are enhanced by the phase-space: the powers of $\bar{\alpha} \equiv \alpha_s N_c/\pi$ associated with soft gluon emissions can be accompanied by either double, or at least single, logarithms of L/λ , depending upon the kinematics of the emissions. Ref. [9] not only computed the first step in this evolution, for both the double-logarithmic and the single-logarithmic corrections, but also provided a simple recipe for resumming the corrections enhanced by double-logarithms to all orders.

Yet, already the one-loop calculation of the single-logarithmic corrections in Ref. [9] has met with serious difficulties, which reflect the lack of a systematic theoretical framework for addressing this complicated, non-linear, high-energy evolution. Namely, in order to compute the effects of order $\bar{\alpha} \ln(L/\lambda)$, one had to estimate the effects of multiple scattering beyond the eikonal approximation and also to heuristically include the ‘virtual’ corrections, which were truly missed by that analysis, but were essential for that purpose. Vice-versa, the only reason why the double-logarithmic corrections appear to be comparatively simple, is because they are neither sensitive to multiple scattering (except for the restriction on their phase-space), nor to the effects of the ‘virtual’ corrections (which are generally important to ensure probability conservation³, but become irrelevant at double-logarithmic accuracy). Remarkably, it appears that the subset of radiative corrections which are enhanced by powers of $\ln^2(L/\lambda)$ forms an ‘island’ of effectively linear evolution, which besides being structurally simple, it also plays a major physical role, in that it gives the dominant contributions in the limit of a large medium $L \gg \lambda$.

By itself, the prominence of a double-logarithmic approximation in the context of pQCD evolution is not new — other familiar examples include the fragmentation of a virtual jet in the vacuum [15], or the evolution of the parton distribution in the ‘double-leading-log-approximation’ (a common limit of the DGLAP and BFKL equations [16]). What is a bit surprising though, is

²See also Ref. [14] for a similar but earlier observation, which has motivated the more elaborate analysis in Ref. [9].

³The ‘virtual’ terms express the reduction in the probability that the evolving system remain in its original state, as it was prior to the evolution. They become negligible to double-logarithmic accuracy because, in that limit, the scattering of the original projectile is much weaker than that of the evolved system including additional gluons.

the importance of such an approximation in the context of a *non-linear* evolution. All the other examples listed above refer to linear processes. And in the only other example of a non-linear pQCD evolution at our disposal — the BK–JIMWLK evolution of the gluon distribution in a large nucleus (or of particle production in proton–nucleus collisions) [17–27] —, it is well known that the ‘double–logarithmic approximation’ (DLA) is not a good approximation at high energy.

For instance, the high–energy scattering between a small dipole and a dense nucleus is described by the non–linear BK equation or, at least (in the single scattering regime), by a linear approximation to it that can be described as ‘the BFKL equation supplemented with a saturation boundary’ [28–30]. The ‘saturation boundary’ expresses the reduction in the phase–space for linear evolution introduced by multiple scattering (or, equivalently, by gluon saturation in the nucleus). Both the saturation effects and the ‘virtual’ BFKL corrections are essential for that dynamics and together they lead to a dramatic change in the behavior of the scattering amplitude for small dipole sizes $r \lesssim 1/Q_s$: they introduce a non–perturbative anomalous dimension (the amplitude behaves like $r^{2\gamma_s}$ with $\gamma_s \simeq 0.63$, instead of the tree–level result $\propto r^2$). If a similar change was to occur in the context of transverse momentum broadening, it would have important consequences for the phenomenology : such corrections could not be simply absorbed into a redefinition of \hat{q} , unlike the comparatively smooth corrections introduced by the DLA (see below). We thus see that the prominence of the DLA in the problem of jet quenching is a remarkable simplification, which is unusual in the context of the non–linear evolution and is important for the phenomenology.

Such considerations invite us to a deeper understanding of the high–energy evolution of jet quenching from first principles. It is our main purpose in this paper to provide a general framework in that sense — that is, a theory for the non–linear evolution of jet quenching to leading order in perturbative QCD at high energy — and then use this framework to address some of the questions aforementioned. In particular, we shall try to clarify issues like the comparison with the BK–JIMWLK evolution, the origin and calculation of the virtual corrections (which is particularly tricky for an extended target), the physics of gluon evolution and saturation in the plasma, the emergence of the double–logarithmic approximation (including the precise phase–space), the possibility to include the radiative corrections into a renormalization of the jet quenching parameter, and the consequences of such a renormalization for the related problem of the radiative energy loss.

In developing the general formalism below, it will be convenient to assume that the projectile enters the medium from the outside and that it was on–shell prior to the collision. This guarantees that the quantum fluctuations which matter for the evolution of the S –matrix are generated exclusively via interactions in the target⁴. Then the main difference between the problem of jet quenching and the BK–JIMWLK formalism for pA collisions refers to the longitudinal extent L of the target and, more precisely, to the ratio between L and the lifetime τ of the typical gluon fluctuations. In pA collisions, the center–of–mass energy is so high that the nuclear target looks effectively like a shockwave ($L \ll \tau$), due to Lorentz contraction. Then the multiple scattering can be treated in the strict eikonal approximation, which assumes that the transverse coordinates of the projectile partons are not affected by the interactions. By contrast, in the context of jet quenching, the energies are much lower and the fluctuations live fully inside the medium ($L \gtrsim \tau$), so the effects of the multiple scattering can accumulate during their whole lifetime. Then the strict

⁴If the projectile is produced by a hard process occurring inside the medium or at some finite distance from it, then there is additional radiation, associated with the initial virtuality, that would mix with the evolution that we are here interested in (see e.g. the discussion in [31]) By choosing an on–shell projectile, we avoid this mixing.

eikonal approximation is not applicable anymore, although the individual scatterings are still soft: one cannot ignore the transverse motion of the fluctuations during their lifetime.

These considerations also show that the two problems aforementioned (pA collisions and jet quenching) can be viewed as limiting situations of a common set-up: the high-energy scattering between a dilute projectile and a dense target *with an arbitrary longitudinal extent*. This is the first problem that we shall address and solve in this paper. Specifically, in Sect. 2 and Appendix A, we shall construct an effective Hamiltonian which, when acting on the S -matrix of the projectile (a gauge-invariant product of Wilson lines), generates one additional soft gluon emission in the background of a strong color field representing the medium. (The medium correlations are reproduced by averaging over this background field, in the spirit of the color glass condensate [32, 33].) This Hamiltonian may be viewed as a generalization of the JIMWLK Hamiltonian beyond the strict eikonal approximation. It looks compact and simple, but it is less explicit than the JIMWLK Hamiltonian, in the sense that the integrals over the emission times cannot be performed in general (i.e. for an arbitrary target). Accordingly, the general Hamiltonian is non-local both in the transverse coordinates and in the light-cone (LC) times. The formal manipulations with this Hamiltonian are complicated by potential (infrared and ultraviolet) divergences which require prescriptions at the intermediate steps and cancel only in the final results. In Sect. 2.2, we demonstrate a general mechanism ensuring such cancellations — this involves a particular ‘sum-rule’ for the gluon propagator in the LC gauge, Eq. (2.13) — and clarify its connexion to probability conservation. In particular, we show that the ‘virtual’ corrections can be alternatively implemented as a local ‘counter-term’, which is particularly convenient when the target is an extended medium.

As a first test of the new Hamiltonian and of our ability to use it for explicit calculations, we consider in Sect. 3 the example of a shockwave target ($L \ll \tau$). Then the integrals over the emission times can be explicitly performed (the adiabatic prescription for regulating the large time behavior turns out to be important for that purpose) and, as a result, we recover the JIMWLK Hamiltonian [19–27], as expected. We also show that the ‘counter-term’ alluded to above generates the ‘virtual’ piece in the BK equation, as it should.

Starting with Sect. 4, we turn to the case of an extended target ($L \gg \tau$), as appropriate for the physics of jet quenching and related phenomena. The general equations generated by the evolution Hamiltonian in that case are extremely complicated (see the discussion in Sect. 4.2): they are *non-local in LC time* (because gluon emissions can occur anywhere inside the medium and they can have any lifetime τ) and also *functional* (the transverse trajectories of the gluons are random, due to the quantum diffusion, and they are distributed according to a path-integral). A useful approximation is to assume that the medium correlations are Gaussian and local in LC time. (A similar mean field approximation proved to be successful in the case of the BK–JIMWLK equations [32, 34–41].) Under this assumption, the equation obeyed by the dipole S -matrix takes the form shown in Eq. (4.22), which is recognized as a functional generalization of the BK equation. The solution to this equation resums all the corrections enhanced by at least one power of the large logarithm $\ln(L/\lambda)$. It remains as an open question whether such a functional equation can be solved via numerical methods. Our main point though is that, for the present purposes — i.e. for a study of the leading-order evolution of the jet quenching in the limit $L \gg \lambda$ —, one can drastically simplify this equation and even obtain analytic results.

This is based on the following two observations. First, in order to compute the transverse momentum broadening $\langle p_{\perp}^2 \rangle$, one needs the dipole S -matrix $\mathcal{S}(r)$ for dipole sizes in the vicinity of

the *plasma saturation line* ; that is, when increasing the medium size L , one must simultaneously decrease the typical dipole size, according to $r \sim 1/Q_s(L)$, with $Q_s^2(L) = \hat{q}L$. Second, the dominant radiative corrections in the interesting regime at $L/\lambda \gg 1$ and $r \sim 1/Q_s(L)$ are those which are enhanced by a *double* logarithm $\ln^2(L/\lambda)$. They can be resummed to all orders by solving a simplified, *linear*, equation, namely Eq. (4.42), which emerges from the generalized BK equation aforementioned and is equivalent to the resummation proposed in Ref. [9]. This equation, that can be described as ‘the DLA equation supplemented with a saturation boundary’, is different from ‘the BFKL equation with a saturation boundary’ alluded to before — it is actually simpler and in particular it does not lead to a (non-perturbative) anomalous dimension. That is, the scattering amplitude obtained by solving this equation is still proportional to r^2 up to a slowly varying function, as it would be at tree-level⁵ (see Sect. 4.3 for details). This in turn implies that the dominant corrections to $\langle p_\perp^2 \rangle$ can be absorbed into a renormalization $\delta\hat{q}(L)$ of the jet quenching parameter, which thus becomes mildly non-local.

Given the central role played by the DLA, it is interesting to understand the emergence of this approximation on physical grounds. As we explain in Sect. 4.4, this is related to the specificity of the high-energy evolution of the gluon distribution in the medium, that we here address for the first time. Namely, we show that the non-linear effects in the generalized BK equation (4.22) can be also understood as gluon saturation in the medium, but with a saturation scale $Q_s^2(x)$ which increases very fast when decreasing $x \equiv \lambda/\tau$ (the longitudinal momentum fraction carried by the gluons) — much faster than the corresponding scale in a shockwave. Specifically, one has $Q_s^2(x) \propto 1/x$ already at *tree-level* and this growth becomes even faster after including the effects of the small- x evolution. The physical explanation is quite simple: the quantity $Q_s^2(x)$ is proportional with the longitudinal size of the region where the gluons can overlap with each other. For gluons inside the medium, this region is their wavelength $\tau \simeq \lambda/x$; hence, $Q_s^2 \propto \tau \sim 1/x$, as anticipated. In turn, this rapid growth of $Q_s^2(x)$ with $1/x$ widely opens the *transverse* phase-space and thus favors a *double-logarithmic evolution* : when increasing L/λ , one opens not only the longitudinal phase-space at $\lambda \ll \tau \ll L$, but also the transverse one at $Q_s^2(x) \ll p_\perp^2 \ll Q_s^2$. The upper limit $Q_s^2 = \hat{q}L$ (the conventional ‘saturation momentum’ in the literature on jet quenching) is simply the largest value of $Q_s^2(x)$, corresponding to $x_{\min} = \lambda/L$. This situation should be contrasted to the more familiar case of a shockwave, where the variation of $Q_s^2(x)$ with $1/x$ is a parametrically small effect, of order α_s (a pure effect of the evolution), so the transverse phase-space increases much slower than the longitudinal one in the approach towards saturation. Incidentally, this explains why, in that context, the DLA is generally not a good approximation [28–30].

Such considerations will allow us to recover the double-logarithmic corrections of Ref. [9] from a more fundamental perspective and with a transparent physical interpretation. An additional clarification refers to the phase-space for the high-energy evolution: as we shall discuss in Sect. 4.3.3, the original argument in that sense in Ref. [9] must be supplemented with the kinematical constraint $p^0 > p_\perp$. This has consequences when the medium is a weakly-coupled QGP (more generally, whenever $\hat{q}\lambda^3 \ll 1$): in that case, the validity of the high-energy approximations requires the stronger constraint $L/\lambda \gg 1/\alpha_s^2 \ln(1/\alpha_s)$ (and not just $L/\lambda \gg 1$). In more suggestive terms, the necessary condition can be written as $Q_s^2 \gg T^2$.

⁵But a *perturbative* anomalous dimension, of $\mathcal{O}(g)$, can be generated by the all-order resummation of the double-logarithmic corrections; this is the ‘saturation exponent’ to be discussed in Sect. 4.4.

As a further application, we consider in Sect. 5 the evolution of the radiative energy loss, within the framework of the BDMPSZ mechanism for medium-induced gluon radiation [42–52]. Within the approximations of interest, this problem is closely related to that of the transverse momentum broadening and in Sect. 5 we shall merely emphasize the differences. Once again, the cross-section (and its evolution) can be related to the dipole S -matrix, which obeys the equations established in Sect. 4. The new feature is that, now, the eikonal approximation fails not only for the soft gluon fluctuation responsible for the evolution, but also for its relatively hard parent gluon, which is responsible for the energy loss. Yet, this failure poses no difficulty for the calculation of the high-energy evolution, because of the strong separation in lifetime between the fluctuations and the radiation. In particular, to double-logarithmic accuracy, the evolution of the radiative energy loss is obtained by simply using the renormalized value of \hat{q} (the solution to Eq. (4.42)) within the respective formula at tree-level. Similar conclusions have been independently reached in Ref. [53], where Eq. (4.42) has been obtained via a different method (namely, via the direct calculation of the relevant Feynman graphs to DLA accuracy).

Finally, Sect. 6 summarizes our results and conclusions, together with some open problems.

2 The evolution Hamiltonian in the high-energy approximation

Throughout this paper, we shall consider the high-energy evolution of the scattering amplitude for the collision between a dilute projectile and a dense target. The projectile is a set of partons in an overall color singlet state (the prototype being a color dipole), while the target can be either a large nucleus, or the dense partonic medium created in the intermediate stage of an ultrarelativistic heavy ion collision. In both cases, the target is characterized by a dense gluon distribution, which for the present purposes will be described in the spirit of the CGC formalism, that is, as a random distribution of strong, classical, color fields. The interactions between the projectile and the target will be treated in a generalized eikonal approximation, which allows one to resum the multiple scattering between the partons in the projectile and the strong color fields in the target to all orders, via Wilson lines, while also keeping trace of the transverse motion of the partons.

One step in the high-energy evolution consists in the emission of a relatively soft gluon by one of the partons in the projectile and in the background of the target field. Such an emission modifies the partonic content of the projectile and hence the S -matrix for the elastic scattering between the projectile and the target. In this section we shall present and motivate a rather compact expression for the Hamiltonian which ‘generates this evolution’, that is, which describes the change in the S -matrix induced by one soft gluon emission. A more formal derivation of this Hamiltonian from the QCD path integral is given in Appendix A.

2.1 The evolution Hamiltonian

To be specific, let us assume that the projectile propagates in the positive x^3 direction and introduce light-cone (LC) vector notations: $x^\mu = (x^+, x^-, \mathbf{x})$, with $x^+ = (x^0 + x^3)/\sqrt{2}$, $x^- = (x^0 - x^3)/\sqrt{2}$, and $\mathbf{x} = (x^1, x^2)$. Each parton in the projectile has a color current oriented in the LC ‘plus’ direction, which couples to the A_a^- component of the target color field. If the parton energy is sufficiently high (see below for the precise condition), its transverse coordinate \mathbf{x} is not affected by the interaction. Then the only effect of the latter is a rotation of the parton color state, as encoded

in the Wilson line :

$$U^\dagger(\mathbf{x}) = \text{P exp} \left\{ ig \int dx^+ A_a^-(x^+, \mathbf{x}) T^a \right\}. \quad (2.1)$$

The T^a 's are the color group generators in the appropriate representation and P stands for path ordering w.r.t. x^+ (the LC 'time' for the projectile) : with increasing x^+ , matrices are ordered from right to left. The integral over x^+ formally extends along the whole real axis, but in practice it is limited to the support of the target field. The x^- coordinate has been omitted in Eq. (2.1) since it is understood that $x^- \simeq 0$ for the ultrarelativistic projectile, by Lorentz contraction.

The elastic S -matrix for a color-singlet projectile involves the trace of a product of such Wilson lines, one for each parton (quark, antiquark, or gluon) in the projectile. For more clarity, in what follows we shall keep the notations T^a and U^\dagger for the color group generators and the Wilson lines in the adjoint representation, and use t^a and respectively V^\dagger for quarks in the fundamental representation. As anticipated, most of the examples below will refer to a color dipole, for which the S -matrix reads (in the fundamental representation, for definiteness)

$$\hat{S}_{\mathbf{x}\mathbf{y}} \equiv \frac{1}{N_c} \text{tr} [V_{\mathbf{x}}^\dagger V_{\mathbf{y}}], \quad (2.2)$$

where \mathbf{x} and \mathbf{y} are the transverse coordinates of the quark and the antiquark, respectively, and $V_{\mathbf{x}}^\dagger \equiv V^\dagger(\mathbf{x})$, etc. This dipole enters the calculation of a variety of physical processes, like the total cross-section for deep inelastic scattering, the cross-section for single inclusive hadron production in proton-nucleus (pA) collisions, or the transverse momentum broadening of a 'hard probe' (here an energetic quark) propagating through the dense partonic medium ('quark-gluon plasma') created at the intermediate stages of a nucleus-nucleus (AA) collision.

Below we shall refer to Eq. (2.1) as the *strict* eikonal approximation. For a quantum particle, this is correct only so long as the target is 'sufficiently thin' — namely, so long as the duration of the interaction (which is the same as the extent L of the target in the x^+ direction) is small enough for the effects of the quantum diffusion to remain negligible. Indeed, a high energy particle with longitudinal momentum p^+ is similar to a non-relativistic quantum particle with mass equal to p^+ and living in two spatial dimensions, in that it undergoes a Brownian motion in the transverse plane: the dispersion Δx_\perp^2 in its transverse position grows with time according to $\Delta x_\perp^2 \simeq \Delta x^+ / 2p^+$. (This transverse dynamics is explicit in Eq. (2.9) below.) The dispersion thus accumulated during the interaction time $\Delta x^+ = L$ can be neglected so long as it remains smaller than the respective quantum uncertainty $1/p_\perp^2$ (with $p_\perp = |\mathbf{p}|$ the particle transverse momentum). This requires⁶ $L < \tau_{coh} \equiv 2p^+ / p_\perp^2$, a condition which is indeed satisfied when the target is a shockwave, but not also for the case of an extended medium. Hence, in the case of the medium, we shall need the generalization of Eq. (2.1) to an arbitrary trajectory $\mathbf{x}(t)$ in the transverse plane, where $t \equiv x^+$ is the LC time. This reads

$$U_{t_2 t_1}^\dagger[\mathbf{x}(t)] = \text{P exp} \left\{ ig \int_{t_1}^{t_2} dt A_a^-(t, \mathbf{x}(t)) T^a \right\}, \quad (2.3)$$

and is a functional of the trajectory. As compared to Eq. (2.1) we have also generalized the definition in Eq. (2.3) to trajectories which start at some generic (light-cone) time t_1 and end up at a later time t_2 .

⁶In evaluating the coherence time τ_{coh} one should use the maximal value of p_\perp accumulated by the particle via rescattering in the target, that is, the saturation momentum Q_s to be later introduced.

We are now in a position to present the operator which generates the emission of a soft gluon by the dilute projectile in the presence of the strong color field of the target. This operator acts on gauge-invariant operators built with products of Wilson lines, like that in Eq. (2.2), and reads

$$\Delta H = \frac{1}{2} \int_{\text{strip}} \frac{dp^+}{2\pi} \int dt_1 \int dt_2 \int d^2\mathbf{r}_2 \int d^2\mathbf{r}_1 J^a(t_2, \mathbf{r}_2) G_{ab}^{--}(t_2, \mathbf{r}_2; t_1, \mathbf{r}_1; p^+) J^b(t_1, \mathbf{r}_1), \quad (2.4)$$

in notations to be explained below.

The variable p^+ is the LC longitudinal momentum of the emitted gluon; by assumption this is much smaller than the respective momentum of the parent parton (to be below denoted as Λ), but much larger than any ‘plus’ component that can be transferred by the target in the collision process. Accordingly, the component p^+ is conserved by the interactions, which makes it useful to use the mixed Fourier representation (t, \mathbf{x}, p^+) , as we did above. The ‘strip integral’ in Eq. (2.4) runs over an interval in p^+ which is symmetric around $p^+ = 0$:

$$\int_{\text{strip}} \frac{dp^+}{2\pi} f(p^+) \equiv \left(\int_{x\Lambda}^{\Lambda} + \int_{-\Lambda}^{-x\Lambda} \right) \frac{dp^+}{2\pi} f(p^+) = \int_{x\Lambda}^{\Lambda} \frac{dp^+}{2\pi} [f(p^+) + f(-p^+)], \quad (2.5)$$

Here Λ is the typical ‘plus’ momentum of the emitters, which is the relevant ‘hard’ scale, whereas x , with $x \ll 1$, is the smallest longitudinal fraction of the emitted, ‘soft’, gluon. In what follows, we shall be mostly concerned with situations where the above integral is logarithmic, $\int (dp^+/p^+)$; in such a case, the evolution operator takes of the form $\Delta H = H_{\text{evol}} \ln(1/x)$, with H_{evol} playing the role of a Hamiltonian for the evolution with ‘time’ $Y \equiv \ln(1/x)$ (the rapidity difference between the valence partons in the projectile and the softest evolution gluons).

Furthermore, $J^a(t, \mathbf{r})$ denotes the functional derivative w.r.t. the component $A_a^-(t, \mathbf{r})$ of the gauge field and plays the role of the color charge density operator. When acting on a Wilson line like that in Eq. (2.3), this operator generates the emission of a soft gluon from the parton represented by that Wilson line:

$$\begin{aligned} J^a(t, \mathbf{r}) U_{t_2 t_1}^\dagger[\mathbf{x}] &\equiv \frac{\delta}{\delta A_a^-(t, \mathbf{r})} U_{t_2 t_1}^\dagger[\mathbf{x}] \\ &= ig\theta(t_2 - t)\theta(t - t_1)\delta^{(2)}(\mathbf{r} - \mathbf{x}(t)) U_{t_2 t}^\dagger[\mathbf{x}] T^a U_{t t_1}^\dagger[\mathbf{x}]. \end{aligned} \quad (2.6)$$

As visible on this equation, each functional derivative brings a factor of g , so ΔH starts at order $g^2 = 4\pi\alpha_s$ (but in general includes effects of higher order in g , via the background field; see below). The operator $J^a(t, \mathbf{x})$ is also the generator of the infinitesimal color rotations. Using (2.6), one can check the following equal-time commutation relation (with f^{abc} the structure constants for $\text{SU}(N_c)$ and $\delta_{\mathbf{x}\mathbf{y}} \equiv \delta^{(2)}(\mathbf{x} - \mathbf{y})$)

$$[J^a(t, \mathbf{x}), J^b(t, \mathbf{y})] = -g\delta_{\mathbf{x}\mathbf{y}} f^{abc} J^c(t, \mathbf{x}), \quad (2.7)$$

which confirms that these operators obey the color group algebra, as they should.

The last ingredient in Eq. (2.4) is the background field propagator G^{--} of the emitted gluon. This is a functional of the target field A^- , via Wilson lines. Its construction is well documented in the literature and will be briefly discussed in Appendix B, where we show that

$$G_{ab}^{--}(x^+, \mathbf{x}; y^+, \mathbf{y}; p^+) = \frac{1}{(p^+)^2} \partial_x^i \partial_y^i G_{ab}(x^+, \mathbf{x}; y^+, \mathbf{y}; p^+) + \frac{i}{(p^+)^2} \delta_{ab} \delta(x^+ - y^+) \delta_{\mathbf{x}\mathbf{y}}. \quad (2.8)$$

Here, G_{ab} is the ‘scalar’ propagator, defined as the solution to the following equation

$$[2ip^+(\partial_x^- - igA^-(x)) + \nabla_{\perp x}^2]_{ac} G_{cb}(x^+, \mathbf{x}; y^+, \mathbf{y}; p^+) = i\delta_{ab}\delta(x^+ - y^+)\delta_{\mathbf{x}\mathbf{y}}, \quad (2.9)$$

with Feynman prescription for the pole at the mass-shell. This prescription ensures that modes with positive (negative) values of p^+ propagate forward (backward) in time (see e.g. Eq. (B.8)). For definiteness, we shall refer to the two pieces in the r.h.s. of Eq. (2.8) as the ‘radiative piece’ and respectively the ‘Coulomb piece’ of the gluon propagator.

Eq. (2.9) exhibits the eikonal coupling between the large component p^+ of the 4-momentum of the gluon and the conjugate component A^- of the color field of the target, and also the transverse dynamics responsible for quantum diffusion. Given the formal analogy between this equation and the Schrödinger equation for a non-relativistic particle in two spatial dimensions, it is clear that its solution can be written as a path integral. Namely, for $p^+ > 0$ and hence $x^+ > y^+$, one has⁷

$$G(x^+, \mathbf{x}; y^+, \mathbf{y}; p^+) = \frac{1}{2p^+} \mathcal{G}(x^+, \mathbf{x}; y^+, \mathbf{y}; p^+),$$

$$\mathcal{G}(x^+, \mathbf{x}; y^+, \mathbf{y}; p^+) = \int [\mathcal{D}\mathbf{r}(t)] \exp\left\{i\frac{p^+}{2} \int_{y^+}^{x^+} dt \dot{\mathbf{r}}^2(t)\right\} U_{x^+y^+}^\dagger[\mathbf{r}(t)], \quad (2.10)$$

where one integrates over paths $\mathbf{r}(t)$ with boundary conditions $\mathbf{r}(y^+) = \mathbf{y}$ and $\mathbf{r}(x^+) = \mathbf{x}$. For $p^+ < 0$ (and hence $x^+ < y^+$), the propagator can be computed by using the following symmetry property, which follows from Eq. (2.9) together with the Feynman prescription:

$$G_{ab}(x^+, \mathbf{x}; y^+, \mathbf{y}; p^+) = G_{ba}(y^+, \mathbf{y}; x^+, \mathbf{x}; -p^+), \quad (2.11)$$

By exploiting the above properties, one can limit the time integrals in Eq. (2.4) to $-\infty < t_1 < t_2 < \infty$, while simultaneously restricting the p^+ integral to the positive side of the strip, $x\Lambda < p^+ < \Lambda$, and multiplying the result by two. More precisely, we have here in mind the integral over the ‘radiation’ piece of the propagator (2.8), which is non-local in time. The local, Coulomb, piece must be treated separately.

Note finally that there is no ambiguity concerning the ordering of the various factors within the integrand of Eq. (2.4): (i) the two charge operators act at different times, t_1 and t_2 , so they commute with each other; (ii) the radiation piece of the propagator involves the background field $A^-(t)$ only at intermediate times t , between t_1 and t_2 , so it commutes with any of the two functional derivatives; (iii) the Coulomb piece is local not only in time, but also in color.

The structure of the evolution Hamiltonian (2.4) looks both simple and intuitive: this operator does precisely what it is expected to do, namely, it generates the evolution of an S -matrix like (2.2) via the emission and the reabsorption of a soft gluon by any of the color sources within the projectile. But this apparent simplicity hides several subtleties which show up when trying to use this Hamiltonian in practice. These subtleties will be discussed in the next subsection, where we shall derive an alternative form for the evolution Hamiltonian — more precisely, for its action on a generic operator $\hat{\mathcal{O}}[A^-]$ — which is more convenient in practice, especially for an extended target.

⁷The ‘reduced propagator’ \mathcal{G} is formally the same as the non-relativistic evolution operator.

2.2 Virtual corrections and probability conservation

The purpose of this subsection is to render the Hamiltonian (2.4) ‘less formal’. First, we shall argue that, in order to be well defined, this operator must be supplemented with an adiabatic prescription for switching off the interactions at large times. Second, we shall discuss a sum–rule for the free LC gauge propagator, which ensures probability conservation and also the cancellation of ultraviolet and infrared divergences between the ‘radiative’ piece and the ‘Coulomb’ piece of the Hamiltonian. Finally, we shall derive an alternative expression for the action of ΔH where this cancellation occurs locally in time and probability conservation becomes manifest.

Throughout this paper, we shall assume that the target is localized in x^+ , within the longitudinal⁸ strip at $0 < x^+ < L$, so the collision has a finite duration $\Delta x^+ \sim L$. The scattering amplitude can only be affected by gluon emissions which occur sufficiently close to this interaction region, within a time interval $\Delta x^+ \sim \tau_{coh}$. (We recall that the ‘coherence time’ $\tau_{coh} \equiv 2p^+/p_{\perp}^2$ is the typical lifetime of the fluctuation.) Vice–versa, virtual fluctuations in the wave function of the projectile which occur very far away from the interaction region, either in the remote past or the remote future, should have no influence on the evolution of the S –matrix. As we shall see, this property is correctly encoded in the present formalism, but it involves delicate cancellations between various terms, which might be invalidated by careless manipulations at intermediate stages. It turns out that a proper way to deal with this problem is to adiabatically switch off the interactions at very large times $|x^+| \gg \tau_{coh}$ [13, 54]. (Other, less smooth, prescriptions, like a sharp cutoff on $|x^+|$, could induce spurious radiation and thus alter the Fock space of the projectile.) To that aim, we shall supplement each functional derivative within ΔH with an exponential attenuation factor,

$$J^a(t, \mathbf{r}) \rightarrow J^a(t, \mathbf{r}) e^{-\epsilon|t|}, \quad (2.12)$$

where ϵ should be much smaller than $1/\tau_{coh}$. The physical predictions will not be sensitive to the precise value of ϵ because the limit $\epsilon \rightarrow 0$ of the final results, as obtained after performing the integrals over the emission times t_1 and t_2 , is indeed well defined.

With this adiabatic switch–off, the free LC gauge propagator G_0^{--} , Eq. (B.7), obeys the following sum–rule, with paramount consequences for what follows:

$$\int dt_1 \int dt_2 G_0^{--}(t_2 - t_1, \mathbf{r}; p^+) e^{-\epsilon(|t_1| + |t_2|)} = 0. \quad (2.13)$$

This will be demonstrated in Appendix C, where we show that the l.h.s. of Eq. (2.13) is a quantity of $\mathcal{O}(\epsilon)$ and hence vanishes when $\epsilon \rightarrow 0$. A simple way to understand this cancellation is to notice that the integral over $\Delta t \equiv t_2 - t_1$ isolates the Fourier component with $p^- = 0$, which vanishes because $G_0^{--}(p) \propto p^-$, cf. Eq. (B.7). But this property holds only for the *complete* propagator, $G_0^{--} = G_{0,rad}^{--} + G_{0,Coul}^{--}$, as obtained after adding its radiative and Coulomb pieces. In the presence of a background field, we have to distinguish between these two pieces, since they are differently dressed by the background, cf. Eq. (2.8). Taken separately, the radiative piece $G_{0,rad}^{--}$ and the Coulomb piece $G_{0,Coul}^{--}$ generate contributions $\propto 1/\epsilon$ to the l.h.s. of Eq. (2.13), which however cancel, together with the finite terms of $\mathcal{O}(1)$, in their sum (see Appendix C).

⁸An interval Δx^+ is ‘longitudinal’ from the viewpoint of the target (a left mover), but ‘temporal’ from that of the projectile (a right mover). In what follows, we shall often mix the two viewpoints and the respective terminologies. The precise meaning should be clear from the context.

In view of the above, the sum–rule (2.13) is expected to be important for the limit $A^- \rightarrow 0$ of our formalism. In that limit, it ensures an important property, that we now explain. As previously mentioned, quantum fluctuations which are not measured by the collision should not matter for the evolution of the S –matrix. Consider in particular the situation where, after acting with ΔH on some generic S –matrix \hat{O} (to produce the fluctuation), one sets $A^- = 0$, so that there is no scattering. Without scattering, the evolution cannot be measured (the S –matrix must be equal to one both before and after the evolution), hence the action of ΔH must vanish :

$$\Delta H \hat{O} \Big|_{A^-=0} = 0. \quad (2.14)$$

This is precisely ensured by the identity (2.13), as it can be easily seen: the action of the functional derivatives on \hat{O} becomes independent of time after we set $A^- = 0$ (since all the Wilson lines are replaced by the unity matrix). Accordingly, the result of first acting with ΔH on any \hat{O} and then letting $A^- \rightarrow 0$ is indeed proportional to the integral in the l.h.s. of Eq. (2.13).

These properties, Eqs. (2.13) and (2.14), allows one to compute the action of ΔH on \hat{O} in an alternative way, where the Coulomb piece of the propagator is not explicitly present anymore and the cancellation of would–be divergent contributions occurs quasi–locally in time. Namely, Eq. (2.14) implies, with obvious notations,

$$\Delta H_{Coul} \hat{O} \Big|_{A^-=0} = -\Delta H_{rad} \hat{O} \Big|_{A^-=0}. \quad (2.15)$$

Also, as we shall shortly demonstrate, the action of the Coulomb piece of the Hamiltonian on any observable \hat{O} amounts to

$$\Delta H_{Coul} \hat{O} = \left(\Delta H_{Coul} \hat{O} \Big|_{A^-=0} \right) \hat{O} = -\left(\Delta H_{rad} \hat{O} \Big|_{A^-=0} \right) \hat{O}, \quad (2.16)$$

where the second equality follows after using Eq. (2.15). By using the above, one can write

$$\Delta H \hat{O} = [\Delta H_{rad} + \Delta H_{Coul}] \hat{O} = \left[\Delta H_{rad} - \left(\Delta H_{rad} \hat{O} \Big|_{A^-=0} \right) \right] \hat{O}, \quad (2.17)$$

or, less formally,

$$\Delta H \hat{O}[A^-] = \int_{x\Lambda}^{\Lambda} \frac{dp^+}{2\pi} \int_{-\infty}^{\infty} dt_2 \int_{-\infty}^{t_2} dt_1 e^{-\epsilon(|t_1|+|t_2|)} \int d^2\mathbf{r}_2 \int d^2\mathbf{r}_1 \left[\mathcal{H} - \left(\mathcal{H} \hat{O} \Big|_{A^-=0} \right) \right] \hat{O}, \quad (2.18)$$

where \mathcal{H} is a Hamiltonian density built with the ‘radiation’ piece of the propagator alone:

$$\mathcal{H}(t_2, \mathbf{r}_2; t_1, \mathbf{r}_1; p^+) [A^-] \equiv \frac{1}{(p^+)^2} J^a(t_2, \mathbf{r}_2) \left[\partial_{\mathbf{r}_2}^i \partial_{\mathbf{r}_1}^i G_{ab}(t_2, \mathbf{r}_2; t_1, \mathbf{r}_1; p^+) \right] J^b(t_1, \mathbf{r}_1). \quad (2.19)$$

In Eq. (2.19), the transverse derivatives act only on the ‘scalar’ propagator. In particular,

$$\mathcal{H} \hat{O} \Big|_{A^-=0} = \frac{1}{(p^+)^2} \left[\partial_{\mathbf{r}_2}^i \partial_{\mathbf{r}_1}^i G_0(t_2 - t_1, \mathbf{r}_2 - \mathbf{r}_1; p^+) \right] \left(J^a(t_2, \mathbf{r}_2) J^a(t_1, \mathbf{r}_1) \hat{O} \Big|_{A^-=0} \right), \quad (2.20)$$

with G_0 the free propagator (B.8). Notice that the r.h.s. of Eq. (2.18) cannot be written as the action of a linear operator on \hat{O} . Hence, this equation does not provide an alternative expression for the Hamiltonian ΔH , but rather a new method for computing its action on a generic observable.

Using $\hat{\mathcal{O}}|_{A^-=0} = 1$, one sees that the property (2.14) is now satisfied *locally* in time, that is, it is already verified by the integrand in Eq. (2.18). This allows for a natural probabilistic interpretation: the term $\mathcal{H}\hat{\mathcal{O}}$ describes the change in the S -matrix associated with a *real* emission which occurs during the time interval from t_1 to t_2 ; the *virtual* term $-(\mathcal{H}\hat{\mathcal{O}}|_{A^-=0})\hat{\mathcal{O}}$ represents the *reduction* in the probability that the projectile remain in its original state during that time interval. The local (in time) version of (2.14) is then the expression of probability conservation.

To better appreciate the advantages of Eq. (2.18) over the direct use of Eq. (2.4), let us consider the action of ΔH_{Coul} in more detail. (This will also allow us to verify the first equality in Eq. (2.16).) What we would like to show is that any operator $\hat{\mathcal{O}}$ is an eigenstate of ΔH_{Coul} , but with an ill-define eigenvalue, which suffers from both infrared (large time and small p^+) and ultraviolet (small $|\mathbf{r}_2 - \mathbf{r}_1|$, or high p_\perp) divergences. Chosing $\hat{\mathcal{O}} = \hat{S}_{\mathbf{x}\mathbf{y}}$ for definiteness (this brings no loss in generality), we can write (cf. Eq. (2.8))

$$\begin{aligned} \Delta H_{Coul}\hat{S}_{\mathbf{x}\mathbf{y}} &= \int_{x\Lambda}^{\Lambda} \frac{dp^+}{2\pi} \int_{t_1, t_2} \int_{\mathbf{r}_1, \mathbf{r}_2} e^{-\epsilon(|t_1|+|t_2|)} \frac{i}{(p^+)^2} \delta_{t_2 t_1} \delta_{\mathbf{r}_1 \mathbf{r}_2} J^a(t_2, \mathbf{r}_2) J^a(t_1, \mathbf{r}_1) \hat{S}_{\mathbf{x}\mathbf{y}} \\ &= -\frac{ig^2 C_F}{2\pi} \int_{x\Lambda}^{\Lambda} \frac{dp^+}{(p^+)^2} \int dt e^{-2\epsilon|t|} \int d^2\mathbf{r} (\delta_{\mathbf{r}\mathbf{x}} + \delta_{\mathbf{r}\mathbf{y}}) \delta_{\mathbf{r}\mathbf{r}} \hat{S}_{\mathbf{x}\mathbf{y}} \\ &= -\frac{ig^2 C_F}{\pi} \left[\delta_{\mathbf{r}\mathbf{r}} \frac{1}{\epsilon} \int_{x\Lambda}^{\Lambda} \frac{dp^+}{(p^+)^2} \right] \hat{S}_{\mathbf{x}\mathbf{y}} . \end{aligned} \quad (2.21)$$

Because of the ultra-local nature of the Coulomb propagator $\propto \delta_{t_2 t_1} \delta_{\mathbf{r}_1 \mathbf{r}_2}$, the two functional derivatives must act on a same Wilson line within $\hat{S}_{\mathbf{x}\mathbf{y}}$, either the quark one at \mathbf{x} or the antiquark one at \mathbf{y} . This feature, together with identities like

$$J^a(t, \mathbf{r}_2) J^a(t, \mathbf{r}_1) V_{\mathbf{x}}^\dagger = -g^2 C_F \delta_{\mathbf{r}_1 \mathbf{x}} \delta_{\mathbf{r}_2 \mathbf{x}} V_{\mathbf{x}}^\dagger , \quad (2.22)$$

explains why the result is again proportional to $\hat{S}_{\mathbf{x}\mathbf{y}}$. But for the very same reason, the proportionality coefficient exhibits several types of divergences, as anticipated: a large-time divergence as $\epsilon \rightarrow 0$, a small- p^+ divergence when $x \rightarrow 0$, and a transverse ‘tadpole’ $\delta_{\mathbf{r}\mathbf{r}} = \int [d^2\mathbf{p}/(2\pi^2)]$. Being independent of A^- , this coefficient is necessarily the same as the limit $A^- \rightarrow 0$ of $\Delta H_{Coul}\hat{S}_{\mathbf{x}\mathbf{y}}$, in agreement with Eq. (2.16). Clearly, a similar argument holds for any observable $\hat{\mathcal{O}}$.

The above discussion shows that the action of the Coulomb piece of ΔH generates severe divergences. By virtue of Eq. (2.13), these divergences are guaranteed to cancel against similar ones generated by the radiation piece, but only after performing the two time integrations. This cancellation can be explicitly verified whenever one is able to perform the time integrations, as in the case of a shockwave target to be discussed in Sect. 3. But even in such a case, the calculation of the finite terms is quite subtle and relies in an essential way on the use of the adiabatic prescription (see e.g. Sect. 3.1). By contrast, the calculations based on Eq. (2.18) are more robust, because the potential divergences cancel between the ‘real’ and ‘virtual’ terms quasi-locally in time, so one is not sensitive to the regularization prescription used for the time integrations. This second method becomes particularly useful in those cases where one is not able to explicitly perform the time integrals, like that of an extended target to be discussed in Sect. 4.

3 A shockwave target: recovering the JIMWLK Hamiltonian

In this section, we shall specialize the general formalism developed so far to the case where the target is a ‘shockwave’. By this, we more precisely mean a target which looks localized in x^+ on the resolution scale set by the lifetime of the quantum fluctuations. For this case, we will be able to explicitly perform the time integrations which appear in Eq. (2.4) and thus recover the JIMWLK Hamiltonian [19–27], as expected. Besides giving us more confidence with the use of Eq. (2.4) in practice, the subsequent manipulations will also illustrate some of the subtleties discussed in Sect. 2.2, notably the role of the adiabatic prescription and the cancellation of the ill-defined contributions between the ‘radiation’ piece and the ‘Coulomb’ piece of ΔH .

More precisely, the physical problem that we here have in mind is ‘dense–dilute’ (e.g. proton–nucleus) scattering in the high–energy regime where the longitudinal extent $\Delta x^+ \equiv L$ of the dense target is much smaller than the coherence time $\tau_{coh} = 2p^+/p_\perp^2$ of the typical gluons fluctuations associated with the evolution of the projectile : $\tau_{coh} \gg L$. This condition involves both the ‘energy’ (actually, LC longitudinal momentum) p^+ and the transverse momentum p_\perp of the gluon fluctuations. In practice, p_\perp is at least as large as the target saturation momentum Q_s , since this is the typical transverse momentum acquired by either the soft gluon, or its parent parton, via interactions with the target (see e.g. [12, 32, 33]). Hence, the ‘shockwave condition’ can be written as a lower limit on the gluon energy : $p^+ \gg \omega_c$, with

$$\omega_c \equiv Q_s^2 L. \quad (3.1)$$

This limiting energy ω_c is an intrinsic scale of the target and grows with the target size like $\omega_c \sim L^2$ (since $Q_s^2 \propto L$). To have a significant phase–space for the high–energy evolution, the energy $p_0^+ \equiv E$ of the incoming projectile must be considerably larger than ω_c , namely such that $\bar{\alpha} \ln(E/\omega_c) \gtrsim 1$ with $\bar{\alpha} \equiv \alpha_s N_c/\pi$ assumed to be small ($\bar{\alpha} \ll 1$).

3.1 Performing the time integrations

What is special about the shockwave (SW) target, is that the probability for a gluon to be emitted or absorbed inside the target is negligible⁹, since suppressed by a factor $L/\tau_{coh} \ll 1$. This physical statement is boost invariant, but the mathematics becomes simpler by working in the ‘target infinite momentum frame’, i.e. a frame in which the nucleus is ultrarelativistic and it looks like a ‘pancake’ (our intuitive representation of a SW). In such a frame, the target can be effectively treated as a δ –function at $x^+ = 0$. This drastically simplifies the structure of the background field propagator and the action of the functional derivatives on the Wilson lines.

Namely, assuming the SW to be localized near $x^+ = 0$, one can easily show that the path integral in Eq. (2.10) reduces to (for $p^+ > 0$ and hence $x^+ > y^+$; see Appendix B for details)

$$\begin{aligned} G(x^+, \mathbf{x}; y^+, \mathbf{y}; p^+ > 0) &= G_0(x^+ - y^+, \mathbf{x} - \mathbf{y}; p^+) [\theta(x^+) \theta(y^+) + \theta(-x^+) \theta(-y^+)] \\ &\quad + 2p^+ \theta(x^+) \theta(-y^+) \int_{\mathbf{z}} G_0(x^+, \mathbf{x} - \mathbf{z}; p^+) U_{\mathbf{z}}^\dagger G_0(-y^+, \mathbf{z} - \mathbf{y}; p^+), \end{aligned} \quad (3.2)$$

where G_0 is the free propagator (B.8), $U_{\mathbf{z}}^\dagger$ is the adjoint Wilson line introduced in Eq. (2.1), and $\int_{\mathbf{z}} \equiv \int d^2 \mathbf{z}$. The physical interpretation of Eq. (3.2) is quite transparent: when x^+ and y^+ are

⁹Strictly speaking, this statement is gauge–dependent, but it is indeed correct in the gauge $a^+ = 0$ that we currently use; see e.g. the discussion in [55].

both positive, or both negative, the gluon does not cross the SW, so it propagates freely; when x^+ and y^+ are on opposite sides of the SW, the gluon propagates freely from the initial point up to the SW, then it crosses the latter at some transverse position \mathbf{z} , thus accumulating a color precession represented by the Wilson line $U_{\mathbf{z}}^\dagger$, then it moves freely again, up to the final point.

Furthermore, since gluons cannot be emitted or absorbed inside the SW, the action of the functional derivative $J_{\mathbf{x}}^a(t)$ on the Wilson lines is piecewise independent of time. Indeed for any negative value of the time argument, one has (compare to Eq. (2.6))

$$J_{\mathbf{x}}^a(t < 0)U_{\mathbf{z}}^\dagger = ig\delta_{\mathbf{z}\mathbf{x}} U_{\mathbf{z}}^\dagger(\infty, t)T^a U_{\mathbf{z}}^\dagger(t, -\infty) = ig\delta_{\mathbf{z}\mathbf{x}} U_{\mathbf{z}}^\dagger T^a \equiv R_{\mathbf{x}}^a U_{\mathbf{z}}^\dagger, \quad (3.3)$$

where we have used $U_{\mathbf{z}}^\dagger(t, -\infty) = 1$ and $U_{\mathbf{z}}^\dagger(\infty, t) = U_{\mathbf{z}}^\dagger(\infty, -\infty) \equiv U_{\mathbf{z}}^\dagger$ for $t < 0$ and a target field localized at $x^+ = 0$. Similarly, for a positive value $t > 0$, one can write

$$J_{\mathbf{x}}^a(t > 0)U_{\mathbf{z}}^\dagger = ig\delta_{\mathbf{z}\mathbf{x}} U_{\mathbf{z}}^\dagger(\infty, t)T^a U_{\mathbf{z}}^\dagger(t, -\infty) = ig\delta_{\mathbf{z}\mathbf{x}} T^a U_{\mathbf{z}}^\dagger \equiv L_{\mathbf{x}}^a U_{\mathbf{z}}^\dagger, \quad (3.4)$$

The above equations have introduced the ‘right’ and ‘left’ functional derivatives, $R_{\mathbf{x}}^a$ and respectively $L_{\mathbf{x}}^a$, which act on the Wilson lines as infinitesimal color rotations of the right, respectively on the left, and measure the color charge density in the projectile prior, respectively after, the collision. They are related by the condition $L_{\mathbf{x}}^a = U_{\mathbf{x}}^{\dagger ab} R_{\mathbf{x}}^b$, which expresses the color rotation acquired by a color current which crosses the shockwave.

The fact that the r.h.s.’s of Eqs. (3.3)–(3.4) are independent of time allows us to perform the time integrations *directly at the level of the evolution Hamiltonian* (2.4), that is, before acting with ΔH on the observable. To that aim, we need to distinguish three regions for the time integrations:

(i) $-\infty < t_1 < 0$ and $0 < t_2 < \infty$: *the evolution gluon crosses the SW*

After using Eqs. (3.3)–(3.4) for the action of the functional derivatives, one sees that the respective contribution to ΔH , denoted as ΔH_{RL} , simplifies to

$$\Delta H_{RL} = \int_{\mathbf{x}, \mathbf{y}} L_{\mathbf{x}}^a R_{\mathbf{y}}^b \int_{x\Lambda}^{\Lambda} \frac{dp^+}{2\pi} \frac{1}{(p^+)^2} \int_{-\infty}^0 dt_1 \int_0^{\infty} dt_2 \partial_{\mathbf{x}}^i \partial_{\mathbf{y}}^i G_{ab}(t_2, \mathbf{x}; t_1, \mathbf{y}; p^+), \quad (3.5)$$

where the adiabatic prescriptions are implicit (they will be exhibited when needed) and, cf. Eq. (3.2),

$$\partial_{\mathbf{x}}^i \partial_{\mathbf{y}}^i G_{ab}(t_2, \mathbf{x}; t_1, \mathbf{y}; p^+) = 2p^+ \int_{\mathbf{z}} \partial_{\mathbf{x}}^i G_0(t_2, \mathbf{x} - \mathbf{z}; p^+) (U_{\mathbf{z}}^\dagger)_{ab} \partial_{\mathbf{y}}^i G_0(-t_1, \mathbf{z} - \mathbf{y}; p^+). \quad (3.6)$$

Due to the factorized structure of the background field propagator (3.6), the two time integrations are independent of each other. To be specific, consider the integral over t_2 . This involves

$$\begin{aligned} \int_0^{\infty} dt_2 \partial_{\mathbf{x}}^i G_0(t_2, \mathbf{x} - \mathbf{z}; p^+) &= \frac{-i}{2p^+} \int \frac{d^2 \mathbf{p}}{(2\pi)^2} p^i e^{i\mathbf{p} \cdot (\mathbf{x} - \mathbf{z})} \int_0^{\infty} dt_2 e^{-i\frac{p_{\perp}^2}{2p^+} t_2} e^{-\epsilon t_2} \\ &= - \int \frac{d^2 \mathbf{p}}{(2\pi)^2} \frac{p^i}{p_{\perp}^2} e^{i\mathbf{p} \cdot (\mathbf{x} - \mathbf{z})} = \frac{i}{2\pi} \frac{x^i - z^i}{(\mathbf{x} - \mathbf{z})^2}. \end{aligned} \quad (3.7)$$

The final result is recognized as the Weizsäcker–Williams field created at \mathbf{z} by a point-like source at \mathbf{x} . Note that the complex exponential in the integral over t_2 has restricted the respective phase-space to an interval of order $\tau_{coh} = 2p^+ / p_{\perp}^2$ after the SW. A similar conclusion holds for the emission

time t_1 , which is restricted to an interval $\sim \tau_{coh}$ before the SW. The respective integral yields

$$\int_{-\infty}^0 dt_1 \partial_{\mathbf{y}}^i G_0(-t_1, \mathbf{z} - \mathbf{y}; p^+) = \frac{i}{2\pi} \frac{y^i - z^i}{(\mathbf{y} - \mathbf{z})^2}. \quad (3.8)$$

Importantly, the final results in Eqs. (3.7)–(3.8) are independent of p^+ . In both cases, this is due to a cancellation between the factor $1/p^+$ implicit in the free propagator G_0 and the phase-space factor $2p^+/p_{\perp}^2$ produced by the time integral. As a consequence, the ensuing integral over p^+ in Eq. (3.5) is *logarithmic*: $\int (dp^+/p^+) = \ln(1/x)$. Putting all together, one finds

$$\Delta H_{RL} = -\ln \frac{1}{x} \frac{1}{(2\pi)^3} \int_{\mathbf{x}\mathbf{y}\mathbf{z}} \mathcal{K}_{\mathbf{x}\mathbf{y}\mathbf{z}} (2L_{\mathbf{x}}^a U_{\mathbf{z}}^{\dagger ab} R_{\mathbf{y}}^b), \quad (3.9)$$

with the following notations:

$$\mathcal{K}_{\mathbf{x}\mathbf{y}\mathbf{z}} \equiv \mathcal{K}_{\mathbf{x}\mathbf{z}}^i \mathcal{K}_{\mathbf{y}\mathbf{z}}^i, \quad \mathcal{K}_{\mathbf{x}\mathbf{z}}^i \equiv \frac{(\mathbf{x} - \mathbf{z})^i}{(\mathbf{x} - \mathbf{z})^2}. \quad (3.10)$$

(ii) $-\infty < t_1 \leq t_2 < 0$: *the evolution gluon is emitted and reabsorbed prior to the SW*

In this case, both functional derivatives within ΔH act as ‘right’ derivatives, cf. Eq. (3.3). Also, the gluon propagator reduces to the free propagator G_0^- , as shown in Eq. (B.7). Consider first the ‘radiation’ piece of this propagator, which gives

$$\Delta H_{RR}^{rad} = \int_{\mathbf{x}, \mathbf{y}} R_{\mathbf{x}}^a R_{\mathbf{y}}^a \int_{x\Lambda}^{\Lambda} \frac{dp^+}{2\pi} \frac{1}{(p^+)^2} \int_{-\infty}^0 dt_2 \int_{-\infty}^{t_2} dt_1 \partial_{\mathbf{x}}^i \partial_{\mathbf{y}}^i G_0(t_2 - t_1, \mathbf{x} - \mathbf{y}; p^+). \quad (3.11)$$

The time integrations involve (with the shorthand notation $p^- \equiv p_{\perp}^2/2p^+$)

$$\begin{aligned} \int_{-\infty}^0 dt_2 \int_{-\infty}^{t_2} dt_1 e^{-ip^-(t_2-t_1)} e^{\epsilon(t_1+t_2)} &= \int_{-\infty}^0 dt_2 e^{-ip^-t_2+\epsilon t_2} \frac{e^{ip^-t_2+\epsilon t_2}}{ip^- + \epsilon} \\ &= \frac{1}{2\epsilon} \frac{1}{ip^- + \epsilon} = \frac{1}{2\epsilon} \frac{1}{ip^-} + \frac{1}{2(p^-)^2} + \mathcal{O}(\epsilon). \end{aligned} \quad (3.12)$$

The use of the adiabatic prescription has been essential in obtaining the above result, as we now explain. The time separation $t_2 - t_1$ is restricted by the oscillatory phase $e^{-ip^-(t_2-t_1)}$ to values of order $\tau_{coh} = 2p^+/p_{\perp}^2$, but the central value $(t_2 + t_1)/2$ is only restricted by the adiabatic switch-off, so the corresponding integral yields an ‘infrared’ divergence proportional to $1/\epsilon$. By itself, this divergence is pretty harmless, since ultimately cancelled by a similar contribution due to the Coulomb piece, as we shall see. What is more subtle though, is the obtention of the finite term accompanying the divergence (namely, the term $\propto 1/(p^-)^2$ in Eq. (3.12)) : this term is correctly computed when using the adiabatic prescription, as above, but it would be mistreated by other regularizations, like a sharp cutoff on $|t_2 + t_1|$ [13, 54]. Importantly, this finite contribution, which is the actual physical result, has been generated by values t_1 and t_2 which both lie in the vicinity of the interaction time $x^+ = 0$, within a distance of order τ_{coh} .

By using Eq. (3.12) together with simple manipulations, one finds

$$\Delta H_{RR}^{rad} = \int_{\mathbf{x}, \mathbf{y}} R_{\mathbf{x}}^a R_{\mathbf{y}}^a \int_{x\Lambda}^{\Lambda} \frac{dp^+}{2\pi} \frac{1}{(p^+)^2} \left\{ -\frac{i}{2\epsilon} \delta_{\mathbf{x}\mathbf{y}} + p^+ \int \frac{d^2\mathbf{p}}{(2\pi)^2} \frac{e^{i\mathbf{p}\cdot(\mathbf{x}-\mathbf{y})}}{p_{\perp}^2} \right\}. \quad (3.13)$$

The first term within the braces exhibits all types of divergences previously identified in relation with the Coulomb piece, cf. Eq. (2.21). As demonstrated by the above calculation (and anticipated in Sect. 2.2), such divergences are also generated by the ‘radiation’ piece after performing the time integrations. We shall shortly check that this singular term is cancelled by the respective ‘Coulomb’ contribution, in agreement with the discussion in Sect. 2.2. Keeping only the second term in Eq. (3.13), one finds that the respective integral over p^+ is again logarithmic and yields

$$\Delta H_{RR} = \ln \frac{1}{x} \frac{1}{(2\pi)^3} \int_{\mathbf{xyz}} \mathcal{K}_{\mathbf{xyz}} R_{\mathbf{x}}^a R_{\mathbf{y}}^a, \quad (3.14)$$

where we have also used the identity

$$\int \frac{d^2 \mathbf{p}}{(2\pi)^2} \frac{e^{i\mathbf{p} \cdot (\mathbf{x} - \mathbf{y})}}{p_{\perp}^2} = \frac{1}{(2\pi)^2} \int_{\mathbf{z}} \mathcal{K}_{\mathbf{xyz}}. \quad (3.15)$$

The above integral over p_{\perp} develops a logarithmic infrared ($p_{\perp} \rightarrow 0$) divergence, which is however harmless, as it disappears in the evolution of gauge-invariant quantities (see e.g. Sect. 3.2 below).

For completeness, let us also consider the respective Coulomb contribution:

$$\begin{aligned} \Delta H_{RR}^{Coul} &= i \int_{\mathbf{x}, \mathbf{y}} R_{\mathbf{x}}^a R_{\mathbf{y}}^a \int_{x\Lambda}^{\Lambda} \frac{dp^+}{2\pi} \frac{1}{(p^+)^2} \int_{-\infty}^0 dt_2 \int_{-\infty}^0 dt_1 \delta(t_2 - t_1) e^{\epsilon(t_1 + t_2)} \delta_{\mathbf{xy}} \\ &= \frac{i}{2\epsilon} \int_{\mathbf{x}} R_{\mathbf{x}}^a R_{\mathbf{x}}^a \int_{x\Lambda}^{\Lambda} \frac{dp^+}{2\pi} \frac{1}{(p^+)^2}. \end{aligned} \quad (3.16)$$

This precisely cancels the divergent piece in Eq. (3.13), as anticipated. This cancellation illustrates a general argument developed in Sect. 2.2, namely the fact that emissions which occur at large distances $\gg \tau_{coh}$ from the interaction region cannot affect the scattering amplitude.

(iii) $0 < t_1 \leq t_2 < \infty$: *the evolution gluon is emitted and reabsorbed after the SW*

The calculation is entirely similar to that in the previous case, so we can write the final result without further discussion:

$$\Delta H_{LL} = \ln \frac{1}{x} \frac{1}{(2\pi)^3} \int_{\mathbf{xyz}} \mathcal{K}_{\mathbf{xyz}} L_{\mathbf{x}}^a L_{\mathbf{y}}^a, \quad (3.17)$$

By combining the previous results (3.9), (3.14), and (3.17), one finds $\Delta H = \ln(1/x) H_{\text{JIMWLK}}$, with the JIMWLK Hamiltonian [19–27] (see also [56–59] for more recent derivations).

$$H_{\text{JIMWLK}} = \frac{1}{(2\pi)^3} \int_{\mathbf{xyz}} \mathcal{K}_{\mathbf{xyz}} [R_{\mathbf{x}}^a R_{\mathbf{y}}^a + L_{\mathbf{x}}^a L_{\mathbf{y}}^a - 2L_{\mathbf{x}}^a U_{\mathbf{z}}^{\dagger ab} R_{\mathbf{y}}^b]. \quad (3.18)$$

By using the unitarity of the Wilson lines together with the condition $L_{\mathbf{x}}^a = U_{\mathbf{x}}^{\dagger ab} R_{\mathbf{x}}^b$, one can rewrite the color structure in Eq. (3.18) in the following form

$$\begin{aligned} R_{\mathbf{x}}^a R_{\mathbf{y}}^a + L_{\mathbf{x}}^a L_{\mathbf{y}}^a - 2L_{\mathbf{x}}^a U_{\mathbf{z}}^{\dagger ab} R_{\mathbf{y}}^b &= [L_{\mathbf{x}}^a - U_{\mathbf{z}}^{\dagger ab} R_{\mathbf{x}}^b] [L_{\mathbf{y}}^a - U_{\mathbf{z}}^{\dagger ac} R_{\mathbf{y}}^c] \\ &= [U_{\mathbf{x}}^{\dagger ab} - U_{\mathbf{z}}^{\dagger ab}] R_{\mathbf{x}}^b [U_{\mathbf{y}}^{\dagger ac} - U_{\mathbf{z}}^{\dagger ac}] R_{\mathbf{y}}^c. \end{aligned} \quad (3.19)$$

This makes it obvious that H_{JIMWLK} vanishes when $A^- = 0$, in agreement with Eq. (2.14).

3.2 The Balitsky–Kovchegov equation

The simplest among the evolution equations generated by the JIMWLK Hamiltonian is the Balitsky–Kovchegov (BK) equation [17, 18], that is, the equation obeyed by the average S -matrix for a $q\bar{q}$ dipole. In what follow we shall present two different derivations for this equation: the standard one in the literature, where one directly acts with H_{JIMWLK} on the dipole operator $\hat{S}_{\mathbf{x}\mathbf{y}}$, and the alternative one based on Eq. (2.18), which distinguishes between ‘real’ and ‘virtual’ corrections. Clearly, the final result will be the same, but the comparison between these two methods will shed more light on the reorganization of the perturbation theory performed by the sum–rule (2.13) and also on the origin of the virtual terms in the B–JIMWLK equations.

(i) *The standard approach*

Consider the dipole–nucleus scattering in a Lorentz frame where the nuclear target carries most of the rapidity separation Y , so that the projectile is a *bare* dipole — a quark–antiquark pair without additional gluons. In this frame, the average S -matrix is computed as [32, 33]

$$\langle \hat{S}_{\mathbf{x}\mathbf{y}} \rangle_Y = \int [DA^-] W_Y[A^-] \frac{1}{N_c} \text{tr}(V_{\mathbf{x}}^\dagger V_{\mathbf{y}}), \quad (3.20)$$

where the ‘CGC weight function’ $W_Y[A^-]$ is a functional probability density describing the distribution of the color fields in the target (including its evolution up to rapidity Y). Let us now increase the rapidity separation, $Y \rightarrow Y + \Delta Y$, by giving an additional boost ΔY to the projectile. Then the dipole evolves by emitting a soft gluon (from either the quark, or the antiquark), with longitudinal momentum fraction x_1 within the range $x < x_1 < 1$, where $\Delta Y = \ln 1/x$. The ensuing evolution of the S -matrix is obtained by acting with the JIMWLK Hamiltonian on the bare scattering operator:

$$\Delta \langle \hat{S}_{\mathbf{x}\mathbf{y}} \rangle_Y = \Delta Y \langle H_{\text{JIMWLK}} \hat{S}_{\mathbf{x}\mathbf{y}} \rangle \equiv \int [DA^-] W_Y[A^-] H_{\text{JIMWLK}} \hat{S}_{\mathbf{x}\mathbf{y}}. \quad (3.21)$$

Using Eq. (3.18) together with the differentiation rules in Eqs. (3.3)–(3.4), one can easily deduce

$$(H_{RR} + H_{LL}) \hat{S}_{\mathbf{x}\mathbf{y}} = -\frac{\bar{\alpha}}{2\pi} \left(1 - \frac{1}{N_c^2}\right) \int_{\mathbf{z}} \mathcal{M}_{\mathbf{x}\mathbf{y}\mathbf{z}} \hat{S}_{\mathbf{x}\mathbf{y}}. \quad (3.22)$$

for the contribution of the ‘non–crossing’ terms and, respectively,

$$\begin{aligned} H_{RL} \hat{S}_{\mathbf{x}\mathbf{y}} &= \frac{\alpha_s}{\pi^2} \int_{\mathbf{z}} \mathcal{M}_{\mathbf{x}\mathbf{y}\mathbf{z}} U_z^{\dagger ab} \frac{1}{N_c} \text{tr}(V_{\mathbf{x}}^\dagger t^b V_{\mathbf{y}} t^a) \\ &= \frac{\bar{\alpha}}{2\pi} \int_{\mathbf{z}} \mathcal{M}_{\mathbf{x}\mathbf{y}\mathbf{z}} \left(\hat{S}_{\mathbf{x}\mathbf{z}} \hat{S}_{\mathbf{z}\mathbf{y}} - \frac{1}{N_c^2} \hat{S}_{\mathbf{x}\mathbf{y}} \right), \end{aligned} \quad (3.23)$$

for that of the ‘crossing’ one. In these equations, $\mathcal{M}_{\mathbf{x}\mathbf{y}\mathbf{z}}$ is the ‘dipole kernel’,

$$\mathcal{M}_{\mathbf{x}\mathbf{y}\mathbf{z}} \equiv \mathcal{K}_{\mathbf{x}\mathbf{x}\mathbf{z}} + \mathcal{K}_{\mathbf{y}\mathbf{y}\mathbf{z}} - 2\mathcal{K}_{\mathbf{x}\mathbf{y}\mathbf{z}} = \frac{(\mathbf{x} - \mathbf{y})^2}{(\mathbf{x} - \mathbf{z})^2 (\mathbf{z} - \mathbf{y})^2}. \quad (3.24)$$

In the linear combination above, the positive terms $\mathcal{K}_{\mathbf{x}\mathbf{x}\mathbf{z}}$ and $\mathcal{K}_{\mathbf{y}\mathbf{y}\mathbf{z}}$ correspond to self–energy corrections, i.e. graphs where both emissions are attached to a same fermion (the quark at \mathbf{x} or the antiquark at \mathbf{y}), whereas the negative term $-2\mathcal{K}_{\mathbf{x}\mathbf{y}\mathbf{z}}$ summarizes the two exchange graphs, where

the gluon is emitted by the quark and absorbed by the antiquark, or vice-versa (see also Fig. 1 for similar graphs). Note that the leading behavior at large z_\perp , which is proportional to $1/z_\perp^2$ for each of these individual graphs, has cancelled in their linear combination, with the result that $\mathcal{M}_{\mathbf{x}\mathbf{y}\mathbf{z}} \sim 1/z_\perp^4$ when $z_\perp \rightarrow \infty$. This decay is sufficiently fast to guarantee that the integral over \mathbf{z} is convergent in this limit. Similar cancellations occur for any projectile which is a color singlet and ensure that the respective evolution equation is free of infrared problems [60].

The second line in Eq. (3.23) follows after reexpressing the adjoint Wilson line in terms of fundamental ones, according to $U_z^{\dagger ab} t^b = V_z t^a V_z^\dagger$, and then using the Fierz identity

$$\text{tr}(t^a A t^a B) = \frac{1}{2} \text{tr} A \text{tr} B - \frac{1}{2N_c} \text{tr}(AB). \quad (3.25)$$

By adding together the above results, one sees that the terms proportional to $1/N_c^2$ exactly cancel between ‘crossing’ and ‘non-crossing’ contributions¹⁰, so the net result reads

$$\frac{\partial \langle \hat{S}_{\mathbf{x}\mathbf{y}} \rangle_Y}{\partial Y} = \frac{\bar{\alpha}}{2\pi} \int_{\mathbf{z}} \mathcal{M}_{\mathbf{x}\mathbf{y}\mathbf{z}} \langle \hat{S}_{\mathbf{x}\mathbf{z}} \hat{S}_{\mathbf{z}\mathbf{y}} - \hat{S}_{\mathbf{x}\mathbf{y}} \rangle_Y, \quad (3.26)$$

where we have also taken the average over the target. Formally, this equation depicts the evolution as the splitting of the original dipole (\mathbf{x}, \mathbf{y}) into a system of two dipoles, (\mathbf{x}, \mathbf{z}) and (\mathbf{z}, \mathbf{y}) , which have a common leg at \mathbf{z} . This would be the actual physical picture at large N_c , but it formally holds also for finite N_c , due to the ‘accidental’ cancellation of the terms suppressed by $1/N_c^2$.

In deriving Eq. (3.26) as above, it has been convenient to work in a frame where the projectile was a bare dipole prior to the evolution step under consideration. But the ensuing equation is valid in any frame (so long as the projectile remains dilute, of course). In a generic frame, where the projectile also includes an arbitrary number of soft gluons, the quantity $\langle \hat{S}_{\mathbf{x}\mathbf{y}} \rangle_Y$ describes the scattering of that complicated partonic system, for a given rapidity separation Y between the projectile and the target. Similarly, the quantity $\langle \hat{S}_{\mathbf{x}\mathbf{z}} \hat{S}_{\mathbf{z}\mathbf{y}} \rangle_Y$ describes the scattering of a projectile which at low energy consists in only two dipoles, but in general also involves additional soft gluons, as produced by the evolution of the ‘valence’ dipoles.

(ii) *The manifestly probabilistic approach*

In applying Eq. (2.18) to a SW target, one must perform manipulations similar to those in Sect. 3.1 — that is, distinguish between ‘crossing’ and ‘non-crossing’ contributions and then compute the respective time integrals. In doing that, it is essential to keep together the ‘real’ and ‘virtual’ pieces in Eq. (2.18), for each of the three integration ranges. Then the calculations simplify since (a) there are no divergences in the intermediate stages, and (b) the full result comes from the ‘crossing’ pieces (‘real’ plus ‘virtual’) alone. Moreover, the associated manipulations have a clear probabilistic interpretation, in agreement with the discussion in Sect. 2.2.

To demonstrate this, notice the following identities for the action of the functional derivative on the dipole S -matrix:

$$\begin{aligned} R_{\mathbf{r}_1}^a R_{\mathbf{r}_2}^a \hat{S}_{\mathbf{x}\mathbf{y}} &= L_{\mathbf{r}_1}^a L_{\mathbf{r}_2}^a \hat{S}_{\mathbf{x}\mathbf{y}} = \left[-g^2 C_F (\delta_{\mathbf{r}_1 \mathbf{x}} - \delta_{\mathbf{r}_1 \mathbf{y}}) (\delta_{\mathbf{r}_2 \mathbf{x}} - \delta_{\mathbf{r}_2 \mathbf{y}}) \right] \hat{S}_{\mathbf{x}\mathbf{y}} \\ &= \left(J^a(t_2, \mathbf{r}_2) J^a(t_1, \mathbf{r}_1) \hat{S}_{\mathbf{x}\mathbf{y}} \Big|_{A^- = 0} \right) \hat{S}_{\mathbf{x}\mathbf{y}}, \end{aligned} \quad (3.27)$$

¹⁰This cancellation too can be recognized as a consequence of the identity (2.13).

where the equality in the second line holds for any t_1 and t_2 . These identities imply that the ‘virtual’ and ‘real’ contributions mutually cancel within the ‘non-crossing’ terms, as anticipated.

Consider now the respective ‘crossing’ contributions. For the ‘real’ term, this has been already computed in Eq. (3.23). For the ‘virtual’ term, we also need the following integral

$$\int_{-\infty}^0 dt_1 \int_0^{\infty} dt_2 \partial_{r_1}^i \partial_{r_2}^i G_0(t_2 - t_1, \mathbf{r}_2 - \mathbf{r}_1; p^+) = -\frac{2}{p^+} \int \frac{d^2 \mathbf{p}}{(2\pi)^2} \frac{e^{i\mathbf{p} \cdot (\mathbf{r}_2 - \mathbf{r}_1)}}{p_{\perp}^2}. \quad (3.28)$$

By using this, together with Eqs. (3.27), (3.15), and (3.24), one finds the following ‘virtual-crossing’ contribution:

$$-\left(\Delta H_{rad} \hat{S}_{\mathbf{x}\mathbf{y}} \Big|_{A^- = 0}\right) \hat{S}_{\mathbf{x}\mathbf{y}} = -\frac{\alpha_s C_F}{\pi^2} \int_{\mathbf{z}} \mathcal{M}_{\mathbf{x}\mathbf{y}\mathbf{z}} \hat{S}_{\mathbf{x}\mathbf{y}}. \quad (3.29)$$

This is the same as the contribution (3.22) of the ‘non-crossing’ terms in the JIMWLK Hamiltonian. By adding this to the ‘real-crossing’ piece in Eq. (3.23), one finally recovers the BK equation (3.26).

The probabilistic interpretation is now manifest. The quantity $(\bar{\alpha}/2\pi)\mathcal{M}_{\mathbf{x}\mathbf{y}\mathbf{z}}dYd^2\mathbf{z}$ is the differential probability for emitting a gluon at transverse coordinate \mathbf{z} out of the quark-antiquark dipole (\mathbf{x}, \mathbf{y}) . The ‘real-crossing’ piece represents the process where the evolved partonic system (quark, antiquark, and gluon) exists at the time of scattering $x^+ = 0$. The ‘virtual-crossing’ piece measures the decrease in the probability to find the original $q\bar{q}$ dipole at $x^+ = 0$. This decrease is associated with evolution processes which occur either before ($x^+ < 0$), or after ($x^+ > 0$), the scattering. So, the ‘virtual-crossing’ contribution must be equal to that of such genuinely ‘non-crossing’ processes. This is indeed what we have found in Eq. (3.29).

The validity of this interpretation is also comforted by the fact the ‘real’ and ‘virtual’ terms in the BK equation separately develop logarithmic ‘ultraviolet’ divergences, which precisely cancel in their sum. These divergences, coming from the poles of the dipole kernel at $\mathbf{z} = \mathbf{x}$ and $\mathbf{z} = \mathbf{y}$, correspond to self-energy corrections where the gluon lies arbitrarily close to its parent quark in the transverse plane. But such short-distance emissions should not affect the S -matrix since the scattering cannot distinguish between a bare quark and a bare quark accompanied by its radiation gluon, so long as the two partons are very close to each other. And indeed, by inspection of (3.26) one sees that the pole of $\mathcal{M}_{\mathbf{x}\mathbf{y}\mathbf{z}}$ at, say, $\mathbf{z} = \mathbf{x}$ is compensated by the linear combination of Wilson line correlators, due to ‘color transparency’ ($\hat{S}_{\mathbf{x}\mathbf{z}} \rightarrow 1$ as $\mathbf{z} \rightarrow \mathbf{x}$).

Notice that, in order for such cancellations to work, it has been essential to have the right relative coefficient between the ‘virtual’ term and the ‘real’ one (or, equivalently, between ‘crossing’ and ‘non-crossing’ contributions). In turn, this emphasizes the importance of using the adiabatic prescription when computing the time integrals in Sect. 3.1 (cf. the discussion after Eq. (3.12)).

Note finally that Eq. (3.26) is not a closed equation — its r.h.s. also involves the S -matrix $\langle \hat{S}_{\mathbf{x}\mathbf{z}} \hat{S}_{\mathbf{z}\mathbf{y}} \rangle_Y$ for a system of two dipoles —, so it cannot be solved as it stands. This is truly the first equation from an infinite hierarchy, the B-JIMWLK hierarchy, which describes the coupled evolution of scattering amplitudes for dilute systems with increasing complexity in terms of partonic structure. This hierarchy simplifies in the large N_c limit, where expectation values of gauge invariant operators can be factorized from each other. In particular, for $N_c \rightarrow \infty$, Eq. (3.26) reduces to a closed equation for the dipole S -matrix, as originally derived by Kovchegov [18]:

$$\frac{\partial \langle \hat{S}_{\mathbf{x}\mathbf{y}} \rangle_Y}{\partial Y} = \frac{\bar{\alpha}}{2\pi} \int_{\mathbf{z}} \mathcal{M}_{\mathbf{x}\mathbf{y}\mathbf{z}} \left\{ \langle \hat{S}_{\mathbf{x}\mathbf{z}} \rangle_Y \langle \hat{S}_{\mathbf{z}\mathbf{y}} \rangle_Y - \langle \hat{S}_{\mathbf{x}\mathbf{y}} \rangle_Y \right\}, \quad (3.30)$$

In the next section, we shall generalize this equation to the case of an extended target.

4 The high-energy evolution of transverse momentum broadening

Starting with this section, we address the main physical problem of interest for us here, namely the high energy evolution of a ‘hard probe’ (energetic parton) which crosses a dense QCD medium, like a weakly-coupled quark-gluon plasma (QGP). The distinguished feature of the ‘medium’ for the present purposes is the fact that its longitudinal extent in x^+ , to be denoted as L , is much larger than the coherence time $\tau_{coh} = 2p^+/p_{\perp}^2$ of the soft gluons generated by the evolution. This is the source of several complications that we here anticipate.

First, the eikonal approximation for the emitted gluon is not appropriate anymore. Rather one has to use the general, but formal, expression of the gluon propagator as a path integral, cf. Eq. (2.10). Accordingly, the Wilson lines attached to the gluon fluctuations become *functionals* of the gluon trajectories, which are themselves random.

Second, the time integrations in Eq. (2.4) cannot be performed *directly at the level of the Hamiltonian*, i.e. before acting with ΔH on the relevant scattering operator. This can be understood by inspection of Eq. (2.6) : if the time argument t of the functional derivative $J^a(t, \mathbf{r})$ lies inside the medium, then the Wilson lines in the r.h.s. of Eq. (2.6) are explicitly time-dependent, in contrast to what happened for a shockwave (compare to Eqs. (3.3)–(3.4)). So one cannot disentangle the integrations over the emission times t_1 and t_2 from the Wilson lines. This also implies that, in order to make progress, one needs to specify the projectile.

Third, even after choosing a projectile and using ΔH to construct the associated evolution equation, this equation is still too complicated to be dealt with in full generality. Not only this is not a closed equation (a feature that we are already familiar with from the example of the B-JIMWLK hierarchy), but this equation is also *functional* (the unknown correlators enter under the path integral representing the trajectory of the fluctuation) and *non-local in time* (the correlators depend upon the integration variables t_1 and t_2). Our strategy to render such equations tractable in practice will be to perform additional simplifications, notably concerning the structure of the medium correlations, and also to study limiting cases which are simpler but still interesting.

For simplicity, we shall focus on the evolution of a color dipole. This is pertinent indeed, since the corresponding scattering amplitude enters the calculation of two important observables — the transverse momentum broadening and the energy loss by an energetic parton — that we shall discuss in this and the next coming sections. Also, we shall use a similar set-up as in the previous section : the quark is approaching the medium from very far away and its interactions are adiabatically switched off at large times, $|x^+| \rightarrow \infty$. This is not necessarily the actual situation in a nucleus-nucleus collision, where the quark can also be created inside the medium, via some hard process. This would lead to additional radiation which could mix with the quantum fluctuations triggered by the interactions in the medium. The simplest way to avoid such a mixing is to assume that the quark was on-shell prior to the collision.

But even though the general set-up looks similar to the shockwave set-up discussed in Sect. 3, the physical problem that we shall consider from now on is fundamentally different, because of the different kinematics. In Sect. 3, we have assumed that the energy $E \equiv p_0^+$ of the incoming projectile is much higher than the characteristic target scale ω_c , cf. Eq. (3.1), in such a way to ensure a large phase-space, at $\omega_c \ll p^+ \ll E$, for long-lived fluctuations to which the target looks like a shockwave. Here, we are instead interested in the complimentary situation, where E and ω_c are comparable with each other. This is indeed the interesting situation for jet production in AA

collisions at the LHC, where the measured jets have energies of the order of 100 GeV, whereas the medium scale ω_c is in the ballpark of 50 GeV. Then the soft quantum fluctuations of the projectile, with energies $p^+ \ll \omega_c$, have relatively short lifetimes, which are typically much smaller than the medium size L . In what follows, we shall describe the evolution encompassing these fluctuations.

4.1 The tree-level approximation

In preparation for the quantum evolution to be discussed in the next sections, we shall first briefly review the tree-level calculation of the transverse momentum broadening. This will give us the opportunity to introduce the relevant scales and notations and, moreover, it will inspire some of the approximations to be performed later on.

At tree-level, the problem of transverse momentum broadening for an energetic quark which enters the medium is formally similar to that of quark production in pA collisions at forward rapidities. In both cases, the cross-section $dN/d^2\mathbf{p}$ for finding the quark in a state with transverse momentum \mathbf{p} after the collision can be computed, within the limits of the eikonal approximation, as the Fourier transform of a dipole forward amplitude (below, $\mathbf{r} \equiv \mathbf{x} - \mathbf{y}$) :

$$\frac{dN}{d^2\mathbf{p}} = \frac{1}{(2\pi)^2} \int_{\mathbf{r}} e^{-i\mathbf{p}\cdot\mathbf{r}} \langle \hat{S}_{\mathbf{x}\mathbf{y}} \rangle. \quad (4.1)$$

The ‘dipole’ here is merely a mathematical construction: the ‘quark leg at \mathbf{x} ’ represents the physical quark in the direct amplitude, whereas the ‘antiquark leg at \mathbf{y} ’ is the physical quark in the complex conjugate amplitude. As usual, the brackets within $\langle \hat{S}_{\mathbf{x}\mathbf{y}} \rangle$ denotes the target average over the configurations of the color field $A_a^-(x)$. The target is a weakly-coupled QCD medium with longitudinal support at $0 < x^+ < L$. For simplicity, we assume this medium to be homogeneous (on the average) in the transverse plane. Accordingly, the average S -matrix depends only upon the dipole size $\mathbf{r} = \mathbf{x} - \mathbf{y}$ and we can write $\langle \hat{S}_{\mathbf{x}\mathbf{y}} \rangle \equiv \mathcal{S}(\mathbf{r})$. Using $\mathcal{S}(0) = 1$ (‘color transparency’), one sees that the cross-section (4.1) is properly normalized: $\int d^2\mathbf{p} (dN/d^2\mathbf{p}) = 1$.

A weakly-coupled medium, such as a QGP with sufficiently high temperature T , can be described as an incoherent collection of independent color charges, ‘quarks’ and ‘gluons’. These charges will be assumed to be point-like and to have no other mutual interactions, except for those responsible for the screening of the color interactions over a (transverse) distance $r \sim 1/m_D$, with m_D the ‘Debye mass’. Under these assumptions, the only non-trivial correlator of the target field A^- is the respective 2-point function, which has the following structure

$$\langle A_a^-(x^+, x^-, \mathbf{x}) A_b^-(y^+, y^-, \mathbf{y}) \rangle_0 = \delta_{ab} \delta(x^+ - y^+) n(x^+) \gamma(\mathbf{x} - \mathbf{y}), \quad (4.2)$$

where n is the number density of the medium constituents (more precisely, a linear combination of the respective densities for quarks and gluons, weighted with appropriate color factors). As indicated in Eq. (4.2), this density can generally depend upon x^+ (e.g. for an expanding medium), but here we shall mostly work with a medium which is uniform in x^+ (within its longitudinal support at $0 < x^+ < L$, of course). Also

$$\gamma(\mathbf{k}) \equiv \int d^2\mathbf{r} e^{i\mathbf{k}\cdot\mathbf{r}} \gamma(\mathbf{r}) \simeq \frac{g^2}{\mathbf{k}^4}, \quad (4.3)$$

with the approximate equality holding for $k_\perp \gg m_D$, is the square of the 2-dimensional Coulomb propagator. It is understood that Eq. (4.3) must be used with an infrared cutoff $k_\perp \simeq m_D$.

The correlator (4.2) is local in the color indices, by gauge symmetry. It is furthermore independent of the light-cone variables x^- and y^- , and it is local in x^+ , because of the high energy kinematics. These properties can be best understood in a frame where the medium is a ultrarelativistic left mover: then, the dynamics in x^- (the light-cone ‘time’ for a left mover) is frozen by Lorentz time dilation, whereas the correlation length in x^+ gets squeezed by Lorentz longitudinal contraction. The locality in x^+ is clearly an idealization, whose limitations will be discussed in Sect. 4.3.3. The shockwave counterpart of Eq. (4.2) is the description of a large nucleus in the McLerran–Venugopalan (MV) model, which employs a Gaussian CGC weight function [61, 62].

For the Gaussian field distribution in Eq. (4.2), it is a straightforward exercise to compute the average S -matrix for a quark–antiquark dipole. One finds

$$\mathcal{S}_0(\mathbf{r}) = \exp \left\{ -g^2 C_F \int_0^L dx^+ n(x^+) \int \frac{d^2 \mathbf{k}}{(2\pi)^2} \gamma(\mathbf{k}) \left(1 - e^{i\mathbf{k} \cdot \mathbf{r}} \right) \right\}. \quad (4.4)$$

The quantity within the braces is (minus) the amplitude for a single scattering between the dipole and the medium. The fact that the multiple scattering series exponentiates reflects the lack of non-trivial medium correlations: successive collisions proceed independently from each other.

Using Eq. (4.3), one sees that the integral over \mathbf{k} in Eq. (4.4) is logarithmically sensitive to the IR cutoff m_D . We shall be mostly interested in small dipole sizes $r \equiv |\mathbf{r}| \ll 1/m_D$. Then, there is a large logarithmic phase-space, at $m_D \ll k_\perp \ll 1/r$. To leading logarithmic accuracy, the integral can be evaluated by expanding the complex exponential $e^{i\mathbf{k} \cdot \mathbf{r}}$ to second order (the linear term vanishes after angular integration). One thus finds (with $n(x^+) = n_0$ from now on)

$$\mathcal{S}_0(\mathbf{r}) \simeq \exp \left\{ -\frac{1}{4} L \hat{q}(1/r^2) \mathbf{r}^2 \right\}, \quad (4.5)$$

where \hat{q} is the *jet quenching parameter* for an incoming quark :

$$\hat{q}(Q^2) \equiv g^2 C_F n_0 \int^{Q^2} \frac{d^2 \mathbf{k}}{(2\pi)^2} \mathbf{k}^2 \gamma(\mathbf{k}) \simeq 4\pi \alpha_s^2 C_F n_0 \ln \frac{Q^2}{m_D^2}. \quad (4.6)$$

In the above integral, the differential cross-section $g^2 C_F \gamma(\mathbf{k})$ for the scattering between the quark and the medium is weighted by the transverse momentum squared k_\perp^2 transferred in the collision. Accordingly, $\hat{q}(Q^2)$ is proportional to a *transport* cross-section — the total cross-section for collisions which are accompanied by a relatively hard transfer of transverse momentum, within the range $m_D^2 \ll k_\perp^2 \ll Q^2$. For a weakly coupled QGP, one has, parametrically, $n_0 \sim T^3$, $m_D^2 \sim \alpha_s T^2$, and hence $\hat{q} \sim \alpha_s^2 N_c T^3 \ln(1/\alpha_s)$. (See Refs. [6, 7, 63] for detailed calculations.)

The dipole scattering becomes strong when the exponent in Eq. (4.5) is of order one, or larger. This happens when $r \gtrsim 1/Q_s$, with Q_s a characteristic transverse momentum scale, defined as

$$Q_s^2 = L \hat{q}(Q_s^2) = 4\pi \alpha_s^2 C_F n_0 L \ln \frac{Q_s^2}{m_D^2}. \quad (4.7)$$

(We implicitly assume that Q_s is much larger than m_D , which in turn requires the medium size L to be large enough; see Sect. 4.3.3 for details.) This scale Q_s is generally referred to as the ‘target saturation momentum’, because the physics responsible for the unitarization of the dipole amplitude — the multiple scattering between the dipole and the color charges in the target — can

also be viewed, in a suitable frame where the target is highly boosted, as the result of non-linear phenomena in the gluon distribution in the target, leading to gluon saturation [12, 32, 33]. In Sect. 4.4, we shall argue that this profound relation between jet quenching and gluon saturation, which here has been observed at tree-level, is also preserved by the high-energy evolution.

Using Eq. (4.5), one can now estimate the Fourier transform in Eq. (4.1) for $p_\perp \gg m_D$. Consider first the case $p_\perp \lesssim Q_s$; then, the integral in Eq. (4.1) is cut off by the dipole S -matrix at a value $r \simeq 1/Q_s$. To the accuracy of interest, one can ignore the slow dependence of the jet quenching parameter upon r , and thus deduce

$$\frac{dN}{d^2\mathbf{p}} \simeq \frac{1}{\pi Q_s^2} e^{-\mathbf{p}^2/Q_s^2}. \quad (4.8)$$

This Gaussian distribution is the hallmark of a diffusive process — a random walk in the transverse momentum space, leading to a momentum broadening $\langle p_\perp^2 \rangle \simeq Q_s^2$ —, which is induced by a succession of independent collisions in the medium.

Consider also the high-momentum limit $p_\perp \gg Q_s$; then, the integral in Eq. (4.1) is cut off by the complex exponential at a value $r \sim 1/p_\perp \ll 1/Q_s$, so it is appropriate to expand the dipole S -matrix to linear order in its exponent. This gives

$$\begin{aligned} \frac{dN}{d^2\mathbf{p}} &\simeq \frac{\alpha_s^2 C_F}{4\pi} n_0 L \int_r e^{-i\mathbf{p}\cdot\mathbf{r}} (-r^2) \ln \frac{1}{r^2 m_D^2} = \frac{4\alpha_s^2 C_F n_0 L}{p_\perp^4} \\ &= \frac{1}{\pi Q_s^2 \ln(Q_s^2/m_D^2)} \frac{Q_s^4}{p_\perp^4}. \end{aligned} \quad (4.9)$$

The logarithmic scale dependence of $\hat{q}(1/r^2)$ has been essential in deriving this result. As clear from its above derivation, the $1/p_\perp^4$ tail in the spectrum at high p_\perp is produced via a single, hard, scattering. This represents a rather rare event, as visible from the fact that the integral of (4.9) over $p_\perp > Q_s$ is suppressed by a large logarithm:

$$\int_{Q_s} d^2\mathbf{p} \frac{dN}{d^2\mathbf{p}} \simeq \frac{1}{\ln(Q_s^2/m_D^2)} \ll 1. \quad (4.10)$$

This is furthermore in agreement with the fact that the probability sum rule $\int d^2\mathbf{p} (dN/d^2\mathbf{p}) = 1$ is already exhausted (to the leading-logarithmic accuracy of interest) by the contribution (4.8) of relatively soft ($k_\perp \lesssim Q_s$) multiple scattering.

In what follows, we shall be mostly interested in typical events, in which the final spectrum is the result of multiple soft scattering and has the Gaussian form in Eq. (4.8). Accordingly, we shall focus on a quark-antiquark dipole with transverse size $r \sim 1/Q_s$. This in turn implies that the exponent in Eq. (4.5) for the dipole S -matrix is of $\mathcal{O}(1)$: on the average, the dipole undergoes *one inelastic scattering* while crossing the medium. This more precisely means that the dipole may undergo a single hard collision, with a transferred momentum $k_\perp \sim Q_s$, or a large number of softer collisions, but in such a way that the total transferred momentum squared is again of order Q_s^2 . The present calculation cannot distinguish between such scenarios, so in that sense the jet quenching parameter $\hat{q}(Q_s^2)$ is not really a *local* transport coefficient, but rather a measure of the average properties of the medium coarse-grained over a longitudinal distance of order L . (This is also visible in the fact that the quantity $\hat{q}(Q_s^2)$ ‘knows’ about the overall size L of the medium, via its logarithmic dependence upon $Q_s^2 \propto L$.) This should be kept in mind when interpreting the radiative corrections to be computed in what follows.

4.2 The dipole evolution equation

The relation (4.1) between the cross-section for p_\perp -broadening and the forward dipole amplitude is known to be preserved by the high-energy evolution up to the next-to-leading logarithmic accuracy (in the sense of large energy logarithms, like $\ln(\omega_c/p^+)$ in the present context) [13, 64]. Here, we shall merely work at leading logarithmic accuracy, so we can safely use this dipole picture for the purpose of understanding the high energy evolution of the momentum broadening. As before, we shall construct an evolution equation for the average dipole S -matrix by first acting with the evolution Hamiltonian ΔH on the dipole operator $\hat{S}_{\mathbf{x}\mathbf{y}}$ and then taking the average over the target. As explained in Sect. 3.2, this procedure assumes that the projectile is a ‘bare’ dipole prior to the evolution step under consideration, which implicitly means that the effects of the earlier steps have been incorporated in the distribution of the color fields in the target (the CGC weight function $W_Y[A^-]$). Hence, in general, this distribution can be more complicated than the Gaussian introduced in the previous subsection and which applies at tree-level.

In the present context, it becomes advantageous to use the alternative form (2.18) for the action of ΔH , since this permits to avoid spurious divergences already before integrating over the emission times t_1 and t_2 (an operation that we shall not be able to perform in general). In particular, the ‘virtual’ term required by probability conservation is automatically built in. Let us first compute the coefficient of this ‘virtual’ term, which is independent of the background field and thus immediately follows from Eqs. (2.20) and (3.27) :

$$-\Delta H_{rad} \hat{S}_{\mathbf{x}\mathbf{y}} \Big|_{A^-=0} = \frac{g^2 C_F}{2\pi} \int_{\omega}^{\omega_c} \frac{dp^+}{(p^+)^2} \int_{-\infty}^{\infty} dt_2 \int_{-\infty}^{t_2} dt_1 \left[\partial_{\mathbf{r}_2}^i \partial_{\mathbf{r}_1}^i G_0(t_2 - t_1, \mathbf{r}_2 - \mathbf{r}_1; p^+) \right] \Big|_{\substack{\mathbf{r}_2=\mathbf{x} \\ \mathbf{r}_1=\mathbf{y}}}^{\substack{\mathbf{r}_1=\mathbf{x} \\ \mathbf{r}_1=\mathbf{y}}}. \quad (4.11)$$

As compared to Eq. (2.4), we have changed the integration limits for p^+ , to emphasize that the maximum energy of the gluon fluctuations is now of the order of the medium scale ω_c , which reads

$$\omega_c = Q_s^2 L = \hat{q}(Q_s^2) L^2. \quad (4.12)$$

We assume here that the energy E of the incoming quark is larger than ω_c , albeit not *much* larger. The minimal energy ω is at this stage generic, but it is understood that it is small enough, $\omega \ll \omega_c$, to leave a sufficiently large phase-space for the high energy evolution (see Sect. 4.3.3).

Consider now the ‘real’ term in Eq. (2.18), which involves the radiation piece of the background field propagator, cf. Eq. (2.19). By repeatedly using Eq. (2.6), one finds

$$\begin{aligned} \Delta H_{rad} \hat{S}_{\mathbf{x}\mathbf{y}} = & -g^2 \int_{\omega}^{\omega_c} \frac{dp^+}{2\pi} \frac{1}{(p^+)^2} \int_{-\infty}^{\infty} dt_2 \int_{-\infty}^{t_2} dt_1 \partial_{\mathbf{r}_1}^i \partial_{\mathbf{r}_2}^i G_{ab}(t_2, \mathbf{r}_2; t_1, \mathbf{r}_1; p^+) \\ & \left\{ \delta_{\mathbf{r}_1\mathbf{x}} \delta_{\mathbf{r}_2\mathbf{x}} \frac{\text{tr}}{N_c} \left[\left(V_{\infty, t_2}^\dagger t^a V_{t_2 t_1}^\dagger t^b V_{t_1, -\infty}^\dagger \right)_{\mathbf{x}} V_{\mathbf{y}} \right] \right. \\ & + \delta_{\mathbf{r}_1\mathbf{y}} \delta_{\mathbf{r}_2\mathbf{y}} \frac{\text{tr}}{N_c} \left[V_{\mathbf{x}}^\dagger \left(V_{t_1, -\infty} t^b V_{t_2 t_1} t^a V_{\infty, t_2} \right)_{\mathbf{y}} \right] \\ & - \delta_{\mathbf{r}_1\mathbf{y}} \delta_{\mathbf{r}_2\mathbf{x}} \frac{\text{tr}}{N_c} \left[\left(V_{\infty, t_2}^\dagger t^a V_{t_2, -\infty}^\dagger \right)_{\mathbf{x}} \left(V_{t_1, -\infty} t^b V_{\infty, t_1} \right)_{\mathbf{y}} \right] \\ & \left. - \delta_{\mathbf{r}_1\mathbf{x}} \delta_{\mathbf{r}_2\mathbf{y}} \frac{\text{tr}}{N_c} \left[\left(V_{\infty, t_1}^\dagger t^b V_{t_1, -\infty}^\dagger \right)_{\mathbf{x}} \left(V_{t_2, -\infty} t^a V_{\infty, t_2} \right)_{\mathbf{y}} \right] \right\}. \quad (4.13) \end{aligned}$$

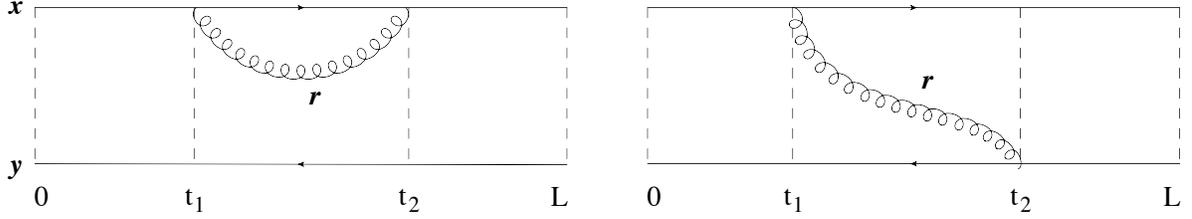


Figure 1. Two diagrams illustrating the dipole evolution described by Eq. (4.13) (they correspond to the first and respectively the fourth term in the r.h.s. of Eq. (4.13)). It is understood that all the partonic lines (quark, antiquark, and gluon) are accompanied by Wilson lines describing scattering off the medium.

Note that $V_{t_2 t_1} \equiv (V_{t_2 t_1}^\dagger)^\dagger$ truly describes backward propagation in time, from t_2 to t_1 (recall that $t_2 > t_1$). The physical interpretation of the four terms within the braces in the r.h.s. of Eq. (4.13) is quite transparent (see also Fig. 1): the first two terms describes processes in which the soft gluon is emitted and then reabsorbed by a same leg of the dipole (either the quark, or the antiquark); the last two terms, which have the opposite sign, correspond to exchange processes where the gluon is emitted by the quark and then absorbed by the antiquark, or vice-versa.

To obtain an evolution equation, one needs to average Eq. (4.13) over the target field distribution and also perform the integrations over the emission times t_1 and t_2 . (Note that the target average should also include the adjoint Wilson line implicit in the structure of the gluon propagator, cf. Eq. (2.10).) We here meet with one of the difficulties anticipated at the beginning of this section: unlike in the corresponding discussion for a shockwave, the support of the Wilson lines in Eq. (4.13) is now truly dependent upon the emission times t_1 and t_2 . Accordingly, the time integrations cannot be disentangled from the target correlations anymore: the Wilson line correlators which enter $\langle \Delta H \hat{S}_{\mathbf{x}\mathbf{y}} \rangle$ are explicitly time dependent. So, it seems impossible to make further progress *in full generality* — i.e., without additional assumptions about the medium correlations.

Inspired by the situation at tree-level and also by the mean field approximation to the B-JIMWLK equations [32, 34–40], which appears to be remarkably successful [40, 41], we shall from now on assume that the background field distribution remains approximatively Gaussian after including the effects of the high energy evolution. That is, the only non-trivial background field correlator is the respective 2-point function, which has the general structure (compare to Eq. (4.2))

$$\langle A_a^-(x^+, x^-, \mathbf{x}) A_b^-(y^+, y^-, \mathbf{y}) \rangle_\omega = \delta_{ab} \delta(x^+ - y^+) \bar{\Gamma}_\omega(x^+, \mathbf{x} - \mathbf{y}). \quad (4.14)$$

This depends upon the energy scale ω down to which one has integrated out the soft gluons, since this fixes the longitudinal resolution on which one probes the medium correlations. The x^+ -dependence of the correlator $\bar{\Gamma}_\omega(x^+, \mathbf{x} - \mathbf{y})$ reflects the evolution of the time inhomogeneity introduced at tree-level by the charged particles density $n(x^+)$, cf. Eq. (4.2). Vice-versa, if the latter is independent of time, $n(x^+) = n_0$, then so is also the function $\bar{\Gamma}_\omega$ — except, of course, for the fact that its longitudinal support is restricted¹¹ to $0 < x^+ < L$.

The main characteristic of the 2-point function (4.14) is to be *local in time*. This was an approximation already at tree-level and it is even more so after including the effects of the radiative

¹¹This restriction is not affected by the evolution since one can neglect the fluctuations occurring near the edges of the medium; see the discussion below.

corrections associated with soft gluon emissions, which are delocalized over a time interval $t_2 - t_1 \sim \tau_{coh}$. If this approximation makes nevertheless sense, it is because, as we shall see, the most interesting emissions have very short lifetimes, which are much shorter than the medium length L . The locality of Eq. (4.14) in x^+ allows one to factorize the Wilson correlations within $\langle \Delta H \hat{S}_{\mathbf{x}\mathbf{y}} \rangle$ according to their time arguments. To be specific, consider the first among the four terms within the braces in Eq. (4.13). After also including the adjoint Wilson line from the gluon propagator, cf. Eq. (2.10), we are led to the following medium correlation function:

$$\begin{aligned}
& \left\langle U_{t_2 t_1}^{\dagger ab}[\mathbf{r}] \frac{\text{tr}}{N_c} \left[\left(V_{\infty, t_2}^{\dagger} t^a V_{t_2 t_1}^{\dagger} t^b V_{t_1, -\infty}^{\dagger} \right)_{\mathbf{x}} V_{\mathbf{y}} \right] \right\rangle = \\
& = \left\langle \frac{\text{tr}}{N_c} \left(V_{\infty, t_2}^{\dagger}(\mathbf{x}) V_{\infty, t_2}(\mathbf{y}) \right) \right\rangle \left\langle U_{t_2 t_1}^{\dagger ab}[\mathbf{r}] \frac{\text{tr}}{N_c} \left(t^a V_{t_2 t_1}^{\dagger}(\mathbf{x}) t^b V_{t_2 t_1}(\mathbf{y}) \right) \right\rangle \left\langle \frac{\text{tr}}{N_c} \left(V_{t_1, -\infty}^{\dagger}(\mathbf{x}) V_{t_1, -\infty}(\mathbf{y}) \right) \right\rangle \\
& = \frac{N_c}{2} \left\{ \langle \hat{S}_{\infty, t_2}(\mathbf{x}, \mathbf{y}) \rangle \langle \hat{S}_{t_2, t_1}(\mathbf{x}, \mathbf{r}) \hat{S}_{t_2, t_1}(\mathbf{r}, \mathbf{y}) \rangle \langle \hat{S}_{t_1, -\infty}(\mathbf{x}, \mathbf{y}) \rangle - \frac{1}{N_c^2} \langle \hat{S}(\mathbf{x}, \mathbf{y}) \rangle \right\}, \quad (4.15)
\end{aligned}$$

where the first equality is obtained by using the Gaussian Ansatz (4.14) for the medium averages and the second one follows via the Fierz identity (3.25). We have defined the time-dependent dipole operator $\hat{S}_{t_2, t_1}(\mathbf{x}, \mathbf{y})$ via the obvious generalization of Eq. (2.2). To simplify writing, we keep implicit the dependence of the various correlations upon the renormalization scale ω . Also, in the very last term we have reconstructed the average of the global S -matrix according to

$$\langle \hat{S}(\mathbf{x}, \mathbf{y}) \rangle = \langle \hat{S}_{\infty, t_2}(\mathbf{x}, \mathbf{y}) \rangle \langle \hat{S}_{t_2, t_1}(\mathbf{x}, \mathbf{y}) \rangle \langle \hat{S}_{t_1, -\infty}(\mathbf{x}, \mathbf{y}) \rangle. \quad (4.16)$$

This last term, which is explicitly suppressed at large N_c , vanishes against the respective contribution of the ‘virtual’ term. A similar cancellation has been noticed in Sect. 3.2 at the level of the BK equation. As in that case though, it is nevertheless convenient to consider the large- N_c limit, which allows us to factorize the two-dipoles S -matrix during the lifetime of the fluctuation:

$$\langle \hat{S}_{t_2, t_1}(\mathbf{x}, \mathbf{r}) \hat{S}_{t_2, t_1}(\mathbf{r}, \mathbf{y}) \rangle \simeq \langle \hat{S}_{t_2, t_1}(\mathbf{x}, \mathbf{r}) \rangle \langle \hat{S}_{t_2, t_1}(\mathbf{r}, \mathbf{y}) \rangle \quad \text{at large } N_c. \quad (4.17)$$

One should keep in mind that $\hat{S}_{t_2, t_1}(\mathbf{x}, \mathbf{r}) \equiv \hat{S}_{t_2, t_1}(\mathbf{x}, [\mathbf{r}(t)]; \omega)$ is truly a *functional* of the path $\mathbf{r}(t)$, with $t_1 < t < t_2$, and also a function of ω , although such features are kept implicit, to simplify the notations. In what follows, we shall often use the more compact notations

$$\mathcal{S}_{t_2, t_1}(\mathbf{x}, \mathbf{y}) \equiv \langle \hat{S}_{t_2, t_1}(\mathbf{x}, \mathbf{y}) \rangle, \quad \mathcal{S}(\mathbf{x}, \mathbf{y}) \equiv \mathcal{S}_{\infty, -\infty}(\mathbf{x}, \mathbf{y}). \quad (4.18)$$

Before we proceed, let us open here a parenthesis on the generalization of the present results to finite N_c : within the Gaussian approximation at hand, it is in fact possible to also evaluate the finite- N_c corrections. (See e.g. Refs. [34, 36–38, 40, 41] for corresponding discussions in the framework of the CGC.) To keep the presentation as simple as possible, we shall stick to the large- N_c limit in all the intermediate steps, but indicate the generalization of the final results to finite N_c . Some formulæ which are useful to that purpose are summarized in Appendix D.

We now close the parenthesis and return to the evaluation of Eq. (4.13) in the Gaussian approximation and at large N_c . The first term in the r.h.s. has been already discussed in Eqs. (4.15)–(4.17). The remaining three terms can be similarly manipulated. Under the present assumptions, they all involve the same product of Wilson line correlators, as written down in the last line of Eq. (4.15). Thus, they differ from each other (and from the first term) only via the actual values taken by the

endpoints \mathbf{r}_1 and \mathbf{r}_2 of the emitted gluon. By putting together the previous results and adding the contribution of the ‘virtual’ piece (i.e. Eq. (4.11) times $\mathcal{S}(\mathbf{x}, \mathbf{y})$), one obtains

$$\begin{aligned} \langle \Delta H \hat{\mathcal{S}}_{\mathbf{x}\mathbf{y}} \rangle &= -\frac{\alpha_s N_c}{2} \int_{\omega}^{\omega_c} \frac{dp^+}{(p^+)^3} \int_{-\infty}^{\infty} dt_2 \int_{-\infty}^{t_2} dt_1 \partial_{\mathbf{r}_1}^i \partial_{\mathbf{r}_2}^i \left\{ \int [\mathcal{D}\mathbf{r}(t)] e^{i \frac{p^+}{2} \int_{t_1}^{t_2} dt \dot{\mathbf{r}}^2(t)} \right. \\ &\quad \left. \times \mathcal{S}_{\infty, t_2}(\mathbf{x}, \mathbf{y}) \left[\mathcal{S}_{t_2, t_1}(\mathbf{x}, \mathbf{r}) \mathcal{S}_{t_2, t_1}(\mathbf{r}, \mathbf{y}) - \mathcal{S}_{t_2, t_1}(\mathbf{x}, \mathbf{y}) \right] \mathcal{S}_{t_1, -\infty}(\mathbf{x}, \mathbf{y}) \right\} \Bigg|_{\substack{\mathbf{r}_2=\mathbf{x} \\ \mathbf{r}_2=\mathbf{y}}}^{\substack{\mathbf{r}_1=\mathbf{x} \\ \mathbf{r}_1=\mathbf{y}}}. \end{aligned} \quad (4.19)$$

This equation can be recognized as a generalization of the BK equation (3.30), to which it reduces in the limit where the target is a shockwave. Namely, for a target localized near $x^+ = 0$, the BK equation is obtained from Eq. (4.19) by integrating over positive values for t_2 and negative values for t_1 . (When both t_1 and t_2 have the same sign, one has $\mathcal{S}_{t_2, t_1} = 1$ for a SW target and then the r.h.s. of Eq. (4.19) simply vanishes.) In that case, $\mathcal{S}_{\infty, t_2} = \mathcal{S}_{t_1, -\infty} = 1$, whereas $\mathcal{S}_{t_2, t_1}(\mathbf{x}, \mathbf{y}) = \mathcal{S}(\mathbf{x}, \mathbf{y})$ is independent of time. Moreover, the S -matrices for the two daughter dipoles, $\mathcal{S}(\mathbf{x}, \mathbf{r})$ and $\mathcal{S}(\mathbf{r}, \mathbf{y})$, do not depend upon the detailed trajectory $\mathbf{r}(t)$ of the soft gluon, but only upon its position $\mathbf{r}(0)$ at the interaction time $t = 0$. Hence one can write (compare to Eq. (B.9))

$$\mathcal{S}(\mathbf{x}, [\mathbf{r}(t)]) \simeq \mathcal{S}(\mathbf{x}, \mathbf{r}(0)) = \int d^2\mathbf{z} \delta^{(2)}(\mathbf{z} - \mathbf{r}(0)) \mathcal{S}(\mathbf{x}, \mathbf{z}). \quad (4.20)$$

After also using the factorization property (B.10) for the free path integral, one can perform the time integrations as in Eqs. (3.7), (3.8) and (3.28), then recognize the logarithmic enhancement of the ensuing integral over p^+ , and finally reconstruct the BK equation (3.30), as anticipated.

Returning to the case of an extended target, we notice that the time integrations can still not be done in full generality at the level of Eq. (4.19), although the latter looks both simpler and physically more transparent than the original expression in Eq. (4.13). Yet, as we shall shortly see, Eq. (4.19) is a convenient starting point for further studies: it allows for explicit calculations in limiting situations of interest and also for general physics conclusions. Before we proceed with more specific studies, it is convenient to recast this expression in a more suggestive form.

First, one can interpret Eq. (4.19) as an equation for the evolution w.r.t. the longitudinal momentum (‘energy’) $p^+ \equiv \omega$ of the emitted gluon. To that aim, we shall write

$$\langle \Delta H \hat{\mathcal{S}}_{\mathbf{x}\mathbf{y}} \rangle = \Delta \mathcal{S}(\mathbf{x}, \mathbf{y}) \equiv \int_{\omega}^{\omega_c} d\omega_1 \frac{\partial \mathcal{S}(\mathbf{x}, \mathbf{y})}{\partial \omega_1}, \quad (4.21)$$

which by comparison with Eq. (4.19) allows us to deduce the following evolution equation

$$\begin{aligned} -\frac{\partial \ln \mathcal{S}(\mathbf{x}, \mathbf{y})}{\partial \omega} &= \frac{\alpha_s N_c}{2} \frac{1}{\omega^3} \int_{-\infty}^{\infty} dt_2 \int_{-\infty}^{t_2} dt_1 \partial_{\mathbf{r}_1}^i \partial_{\mathbf{r}_2}^i \left\{ \int [\mathcal{D}\mathbf{r}(t)] e^{i \frac{\omega}{2} \int_{t_1}^{t_2} dt \dot{\mathbf{r}}^2(t)} \right. \\ &\quad \left. \times \left[\mathcal{S}_{t_2, t_1}(\mathbf{x}, \mathbf{r}) \mathcal{S}_{t_2, t_1}(\mathbf{r}, \mathbf{y}) \mathcal{S}_{t_2, t_1}^{-1}(\mathbf{x}, \mathbf{y}) - 1 \right] \right\} \Bigg|_{\substack{\mathbf{r}_2=\mathbf{x} \\ \mathbf{r}_2=\mathbf{y}}}^{\substack{\mathbf{r}_1=\mathbf{x} \\ \mathbf{r}_1=\mathbf{y}}}. \end{aligned} \quad (4.22)$$

(Recall that $0 < \mathcal{S} \leq 1$, so $\ln \mathcal{S} < 0$.) Eq. (4.22) is somewhat formal because, so far, we have not demonstrated the logarithmic enhancement $\int (d\omega/\omega)$ of the soft gluon emission for the case of an

extended target. Yet, as we shall see starting with Sect. 4.3, such enhancement shows up indeed in all the cases where we will be able to perform the time integrations.

Furthermore, we anticipate that the dominant corrections in the regime of interest are associated with very soft gluons, with energies $p^+ \ll \omega_c$. Such gluons have small lifetimes $\tau_{coh} \ll L$, hence they are typically emitted and absorbed *deeply inside the medium*: boundary effects, i.e. emissions which occur within a distance $\sim \tau_{coh}$ from the medium edges at $x^+ = 0$ or $x^+ = L$, are comparatively suppressed by a factor $\tau_{coh}/L \ll 1$. Accordingly, it is justified to restrict the time integrations in Eq. (4.22) to $0 < t_1 < t_2 < L$. In this range, one can exploit the Gaussian nature of the medium correlations, cf. Eq. (4.14), to express the dipole S -matrix as (compare to Eq. (4.5))

$$\mathcal{S}_{t_2, t_1}(\mathbf{x}, \mathbf{y}; \omega) = \exp \left\{ -g^2 C_F \int_{t_1}^{t_2} dt \Gamma_\omega(t, \mathbf{x} - \mathbf{y}) \right\} = \exp \left\{ -g^2 C_F (t_2 - t_1) \Gamma_\omega(\mathbf{x} - \mathbf{y}) \right\} \quad (4.23)$$

where $\Gamma_\omega(t, \mathbf{x} - \mathbf{y}) \equiv \bar{\Gamma}_\omega(t, \mathbf{0}) - \bar{\Gamma}_\omega(t, \mathbf{x} - \mathbf{y})$. The second equality in Eq. (4.23) holds for a medium which is homogeneous in time, a case to which we shall restrict ourselves in what follows. In particular, $\mathcal{S}(\mathbf{x}, \mathbf{y})$ is obtained by replacing $t_2 - t_1 \rightarrow L$ in Eq. (4.23).

After using Eq. (4.23) and restricting the time integrations to the support of the target, Eq. (4.22) can be rewritten as an equation for $\Gamma_\omega(\mathbf{x} - \mathbf{y})$:

$$L \frac{\partial \Gamma_\omega(\mathbf{x}, \mathbf{y})}{\partial \omega} = \frac{1}{4\pi\omega^3} \int_0^L dt_2 \int_0^{t_2} dt_1 \partial_{r_1}^i \partial_{r_2}^i \left\{ \int [\mathcal{D}\mathbf{r}] e^{i \frac{\omega}{2} \int_{t_1}^{t_2} dt' \dot{\mathbf{r}}^2(t')} \times \left[\exp \left(-\frac{g^2 N_c}{2} \int_{t_1}^{t_2} dt [\Gamma_\omega(\mathbf{x}, \mathbf{r}(t)) + \Gamma_\omega(\mathbf{r}(t), \mathbf{y}) - \Gamma_\omega(\mathbf{x}, \mathbf{y})] \right) - 1 \right] \right\} \Bigg|_{\substack{\mathbf{r}_2=\mathbf{x} \\ \mathbf{r}_1=\mathbf{y}}}^{\substack{\mathbf{r}_2=\mathbf{x} \\ \mathbf{r}_1=\mathbf{x}}} \quad (4.24)$$

We have also used $C_F \simeq N_c/2$, as appropriate at large N_c .

It is in fact easy to generalize the above results to *finite* N_c and also to a *generic representation* R for the original color dipole (see Appendix D for details): within the limits of the Gaussian approximation (4.14), the average S -matrix for an $R\bar{R}$ -dipole and for finite N_c is given by Eq. (4.23) with $C_F \rightarrow C_R$ (the second Casimir for the respective representation) and with the function $\Gamma_\omega(\mathbf{x} - \mathbf{y})$ obeying *exactly the same equation* as above, i.e. Eq. (4.24). Such a simplification has been previously noticed in Ref. [37], where the analog of Eq. (4.24) has been proposed in the context of a shockwave target (that is, as a mean field approximation to JIMWLK evolution at finite N_c).

Note finally that Eq. (4.24) can be viewed as a generalization (and also a corrected version) of a corresponding result in Ref. [9], as shown in Eqs. (11–12) there¹². Eq. (4.24) is more general because it is an *evolution equation*, whose solution (say, as obtained via successive iterations) would resum an infinite series of radiative corrections of arbitrary loop order (within the high-energy approximations at hand). By comparison, Eq. (12) in [9] is a one-loop result, which can be viewed as the first iteration of our Eq. (4.24) — the limit in which the r.h.s. of the latter is evaluated in the tree-level approximation (i.e., by using the expression (4.5) for the average S -matrix). Moreover,

¹²For the sake of this comparison, note that the quantities denoted as $S(x_\perp)$ and $N(x_\perp, \omega)$ in [9] correspond to our present quantities $\Delta\mathcal{S}(\mathbf{x}, \mathbf{y})$ and respectively $\omega(\partial\mathcal{S}/\partial\omega)$, cf. Eq. (4.21). Hence, Eq. (12) in [9] must be compared to the equation obtained by multiplying both sides of our Eq. (4.24) by a factor $[-\omega(g^2 N_c/2)\mathcal{S}(\mathbf{x}, \mathbf{y})]$.

even at one-loop order, Eq. (12) in [9] mistreats the ‘virtual’ corrections: instead of subtracting a term proportional to $\mathcal{S}(\mathbf{x}, \mathbf{y})$, as required by the correct prescription in Eq. (2.18), the authors of Ref. [9] have merely subtracted the vacuum limit ($A^- \rightarrow 0$) of the corresponding ‘real’ term¹³. This imprecision has consequences to leading logarithmic accuracy, as we shall see in the next subsection. (In Ref. [9], the proper virtual term has been heuristically added in the calculation of the single-logarithmic corrections, where it was indeed needed.)

4.3 The single scattering approximation

In this section, we shall discuss two approximate versions of Eq. (4.24), the BFKL equation and the DLA equation, which, besides being simple enough to allow for explicit solutions, have also the virtue to capture the most interesting physical regime for the high energy evolution of jet quenching.

4.3.1 The BFKL equation

We first recall our basic working assumptions: the transverse size $r \equiv |\mathbf{x} - \mathbf{y}|$ of the original dipole is parametrically of order $1/Q_s$, with $Q_s^2 = \hat{q}L$, and the typical energies of the emitted gluons obey $\omega \ll \omega_c$, with $\omega_c = \hat{q}L^2$. Under these assumptions, we shall focus on the regime where the quark-gluon (‘two-dipole’) fluctuation living during the time interval $\Delta t = t_2 - t_1$ undergoes a single collision with the medium, as illustrated in Fig. 2. We shall refer to this regime as the ‘single scattering approximation’, but one should keep in mind that multiple scattering is still allowed prior to, and after, the fluctuation, that is, during the comparatively large time intervals between 0 and t_1 and, respectively, between t_2 and L . Roughly speaking, this approximation is justified provided the transverse separation between the soft gluon and the parent dipole (or, equivalently, the transverse sizes of the two daughter dipoles) is small enough (see Eq. (4.32) below).

Within this ‘single scattering’ regime, one can expand the exponential within the square brackets in Eq. (4.24) to linear order in its exponent. This gives

$$L \frac{\partial \Gamma_\omega(\mathbf{x}, \mathbf{y})}{\partial \omega} = -\frac{\alpha_s N_c}{2} \frac{1}{\omega^3} \int_0^L dt_2 \int_0^{t_2} dt_1 \partial_{\mathbf{r}_1}^i \partial_{\mathbf{r}_2}^i \left\{ \int [D\mathbf{r}] e^{i \frac{\omega}{2} \int_{t_1}^{t_2} dt' \dot{\mathbf{r}}^2(t')} \right. \\ \left. \times \int_{t_1}^{t_2} dt \left[\Gamma_\omega(\mathbf{x}, \mathbf{r}(t)) + \Gamma_\omega(\mathbf{r}(t), \mathbf{y}) - \Gamma_\omega(\mathbf{x}, \mathbf{y}) \right] \right\} \Bigg|_{\substack{\mathbf{r}_2=\mathbf{x} \\ \mathbf{r}_2=\mathbf{y}}}^{\substack{\mathbf{r}_1=\mathbf{x} \\ \mathbf{r}_1=\mathbf{y}}}. \quad (4.25)$$

Once the solution to this linear equation is known, it can be also used to compute the effects of *multiple* scattering, via Eq. (4.23) which holds for generic values of its exponent. A main virtue of Eq. (4.25) is that the time integrals over t_1 , t_2 , and t , can be explicitly performed, as we now explain. To that aim, it is convenient to reverse the order of these integrations, as follows:

$$\int_0^L dt_2 \int_0^{t_2} dt_1 \int_{t_1}^{t_2} dt = \int_0^L dt \int_0^t dt_1 \int_t^L dt_2. \quad (4.26)$$

¹³In our present set-up, the procedure of Ref. [9] would amount to subtracting just the *coefficient* (4.11) of the virtual term, and not the product between that coefficient and the average S -matrix $\mathcal{S}(\mathbf{x}, \mathbf{y})$ of the unevolved dipole.

After introducing the identity in the form $1 = \int d^2\mathbf{z} \delta^{(2)}(\mathbf{z} - \mathbf{r}(t))$ and using Eq. (B.10) with $\mathbf{r}(0) \rightarrow \mathbf{r}(t)$, Eq. (4.25) becomes

$$L \frac{\partial \Gamma_\omega(\mathbf{x}, \mathbf{y})}{\partial \omega} = -\frac{\alpha_s N_c}{2} \frac{1}{\omega^3} \int d^2\mathbf{z} \left[\Gamma_\omega(\mathbf{x}, \mathbf{z}) + \Gamma_\omega(\mathbf{z}, \mathbf{y}) - \Gamma_\omega(\mathbf{x}, \mathbf{y}) \right] \\ \times \int_0^L dt \int_0^t dt_1 \int_t^L dt_2 \partial_{\mathbf{r}_1}^i \partial_{\mathbf{r}_2}^i \left\{ \mathcal{G}_0(t_2 - t, \mathbf{r}_2 - \mathbf{z}; \omega) \mathcal{G}_0(t - t_1, \mathbf{z} - \mathbf{r}_1; \omega) \right\} \Bigg|_{\substack{\mathbf{r}_2 = \mathbf{x} \\ \mathbf{r}_2 = \mathbf{y}}} \Bigg|_{\substack{\mathbf{r}_1 = \mathbf{x} \\ \mathbf{r}_1 = \mathbf{y}}}. \quad (4.27)$$

The time integrations can now be performed as in Eqs. (3.7)–(3.8). For instance,

$$\frac{1}{2\omega} \int_t^L dt_2 \partial_{\mathbf{r}_2}^i \mathcal{G}_0(t_2 - t, \mathbf{r}_2 - \mathbf{z}; \omega) = \frac{-i}{2\omega} \int \frac{d^2\mathbf{p}}{(2\pi)^2} p^i e^{i\mathbf{p} \cdot (\mathbf{r}_2 - \mathbf{z})} \int_t^L dt_2 e^{-i\frac{p_\perp^2}{2\omega}(t_2 - t)} \\ = - \int \frac{d^2\mathbf{p}}{(2\pi)^2} \frac{p^i}{p_\perp^2} e^{i\mathbf{p} \cdot (\mathbf{r}_2 - \mathbf{z})} \left[1 - e^{-i\frac{p_\perp^2}{2\omega}(L-t)} \right] \\ \simeq - \int \frac{d^2\mathbf{p}}{(2\pi)^2} \frac{p^i}{p_\perp^2} e^{i\mathbf{p} \cdot (\mathbf{r}_2 - \mathbf{z})} = \frac{i}{2\pi} \frac{r_2^i - z^i}{(\mathbf{r}_2 - \mathbf{z})^2}. \quad (4.28)$$

The crucial approximation that has been performed here, was to neglect the rapidly-oscillating complex exponential in the second line. This is indeed justified for the problem at hand (even beyond the single scattering approximation), because the lifetime $\tau_{coh} = 2\omega/p_\perp^2$ of the interesting gluon fluctuations is much smaller than L , as we shall see. Accordingly, the final result in Eq. (4.28) is independent of t . A similar reasoning applies to the integral over t_1 , whose result can be read off Eq. (3.8). The final integral over t then simply yields a factor of L , which cancels the similar factor in the l.h.s. of Eq. (4.25). Note that the dominant contributions come from times t_1 and t_2 which are distributed within a distance $\sim \tau_{coh}$ around the interaction time t ; accordingly, one has $\Delta t \equiv t_2 - t_1 \sim \tau_{coh}$, as expected from the uncertainty principle.

We are thus lead to the following, relatively simple, equation for Γ_ω ,

$$\omega \frac{\partial \Gamma_\omega(\mathbf{x}, \mathbf{y})}{\partial \omega} = \frac{\bar{\alpha}}{2\pi} \int_{\mathbf{z}} \mathcal{M}_{\mathbf{x}\mathbf{y}\mathbf{z}} \left[\Gamma_\omega(\mathbf{x}, \mathbf{z}) + \Gamma_\omega(\mathbf{z}, \mathbf{y}) - \Gamma_\omega(\mathbf{x}, \mathbf{y}) \right], \quad (4.29)$$

where $\bar{\alpha} = \alpha_s N_c / \pi$ and the ‘dipole’ kernel $\mathcal{M}_{\mathbf{x}\mathbf{y}\mathbf{z}}$ has been defined in Eq. (3.24). Eq. (4.29) is recognized as the BFKL equation [65–67] (up to issues related to the integration limits, to be shortly discussed). In particular, the differential operator in its l.h.s. is $\omega(\partial/\partial\omega) = \partial/\partial Y$, which demonstrates the logarithmic enhancement of the respective radiative corrections.

Let us now clarify the validity limits for Eq. (4.29). From its above derivation, it is clear that this equation holds so long as the argument of the exponential within the square brackets in Eq. (4.24) — the amplitude for having a single scattering during Δt for any of the two daughter dipoles — remains much smaller than one. This condition can be written as

$$2g^2 C_F \Delta t \Gamma_\omega(B_\perp) \ll 1, \quad (4.30)$$

where B_\perp is the maximal size of any of the daughter dipoles during Δt — that is, the largest among the distances $|\mathbf{x} - \mathbf{r}(t)|$ and $|\mathbf{r}(t) - \mathbf{y}|$ for $t_1 < t < t_2$ — and the overall factor of 2 stands for the two daughter dipoles (see also Fig. 2). As we shall shortly check, this B_\perp is typically much larger

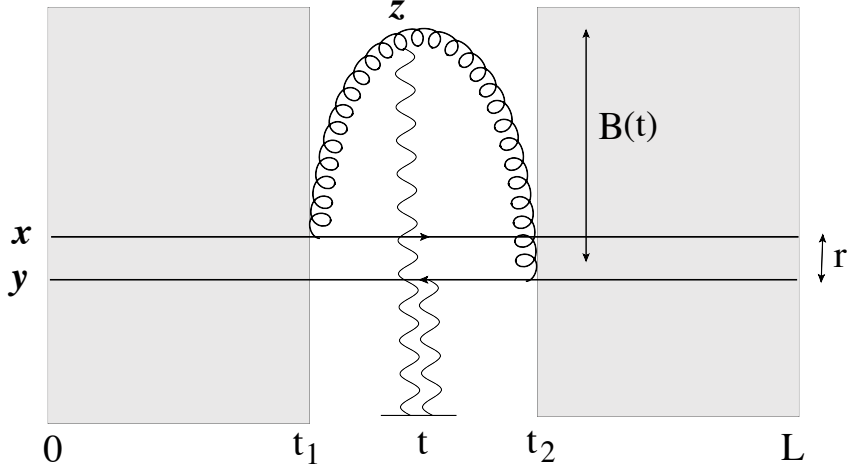


Figure 2. A diagram for dipole evolution in the single scattering approximation, cf. Eqs. (4.27) and (4.29). The grey areas prior and after the fluctuation are regions of multiple scattering. During the fluctuation, the 3-parton ($q\bar{q}g$) system scatters only once, at some intermediate time t . The lifetime $\Delta t = t_2 - t_1$ of the fluctuation is considerably smaller than L ; its transverse size B_\perp is typically much larger than the size r of the original dipole, but much smaller than the ‘saturation’ size $2/k_{\text{br}}(\omega)$ introduced by multiple scattering.

than the size $r \sim 1/Q_s$ of the original dipole, hence it is indeed justified to indistinguishably treat the two daughter dipoles.

To be more specific, let us estimate the fluctuation time via the uncertainty principle, $\Delta t \simeq 2\omega/p_\perp^2 \simeq \omega B_\perp^2/2$, and use the tree-level estimate for Γ in Eq. (4.5): $g^2 C_F \Gamma(B_\perp) \simeq \hat{q}(1/B_\perp^2) B_\perp^2/4$. Then the condition (4.30) can be rewritten as an energy-dependent upper limit on B_\perp^2 :

$$B_\perp^2 \ll \frac{4}{2\sqrt{\omega\hat{q}}} \equiv \frac{4}{k_{\text{br}}^2(\omega)}, \quad (4.31)$$

with \hat{q} itself evaluated on the scale set by this limit: $\hat{q} = \hat{q}(k_{\text{br}}^2)$. This constraint will be confirmed by the analysis in Sect. 4.5, which also shows that the very large fluctuations, with sizes $B_\perp \gtrsim 2/k_{\text{br}}$, are efficiently suppressed by multiple scattering. On the other hand, the very small fluctuations, with transverse sizes much smaller than $r \sim 2/Q_s$, do not contribute to the evolution, since their effects cancel between the ‘real’ and ‘virtual’ terms in Eq. (4.29). To conclude, the phase-space for the single scattering approximation reads

$$r \simeq \frac{2}{Q_s} \lesssim |\mathbf{x} - \mathbf{z}|, |\mathbf{z} - \mathbf{y}| \ll \frac{2}{k_{\text{br}}(\omega)}. \quad (4.32)$$

Via the uncertainty principle, Eq. (4.32) implies that the transverse momentum p_\perp of the emitted gluons lies within the range $k_{\text{br}}(\omega) \ll p_\perp \lesssim Q_s$. This phase-space depends upon the energy ω of the emitted gluons, so it is important to recall that the interesting fluctuations have $\omega \ll \omega_c$. When ω approaches the upper limit ω_c , one has $k_{\text{br}}(\omega_c) \sim Q_s$ and then the phase-space in Eq. (4.32) shrinks to zero. Vice-versa, for the soft gluons with $\omega \ll \omega_c$, one has $k_{\text{br}}^2(\omega) \ll Q_s^2$ and the transverse phase-space for linear evolution is significantly large.

The previous discussion also explains why the present BFKL approximation is fundamentally different from that emerging in the context of the BK–JIMWLK evolution. In that case, the

single scattering approximation is obtained by linearizing the BK equation (3.26) w.r.t. the dipole amplitude $\mathcal{T}_Y(\mathbf{x}, \mathbf{y}) \equiv 1 - \langle \hat{S}_{\mathbf{x}\mathbf{y}} \rangle_Y$. The ensuing equation for $\mathcal{T}_Y(\mathbf{x}, \mathbf{y})$, which is formally similar to our Eq. (4.29) above, is valid so long as the scattering amplitude remains small, $\mathcal{T}_Y \ll 1$. In our present notations, this condition is tantamount to $g^2 C_F L \Gamma_\omega(B_\perp) \ll 1$, or, equivalently, $B_\perp^2 \ll 1/Q_s^2$, with $Q_s^2 = \hat{q}L$. This condition is independent of the energy ω of the fluctuation (up to high-order effects introduced by the evolution) and implies that the transverse phase-space for the evolution is roughly independent of the respective longitudinal phase-space. As a consequence, the high-energy evolution is almost exclusively controlled by the longitudinal phase-space (which increases with Y) and it is faithfully described, so long as $B_\perp^2 \lesssim 1/Q_s^2$, by the BFKL equation supplemented with the saturation boundary $\mathcal{T}_Y < 1$ [28–30]. But for the present problem, the longitudinal and transverse phase-spaces are equally important and the ensuing evolution is qualitatively different, as we shall shortly see.

4.3.2 The double logarithmic approximation

The discussion around Eq. (4.32) shows that, when increasing the *longitudinal* phase-space for the evolution by decreasing ω below ω_c , one simultaneously increases the corresponding *transverse* phase-space, by decreasing the lower limit $k_{\text{br}}(\omega)$ on the transverse momentum p_\perp of the fluctuations (or, equivalently, increasing the upper limit on their transverse size, cf. Eq. (4.32)). In view of this and of the well-known fact that the BFKL evolution admits a double-logarithmic regime [16], it is clear that the radiative corrections can be enhanced not just by the large energy logarithm $\ln(\omega_c/\omega)$, but also by the even larger *double logarithm* $\ln(\omega_c/\omega) \ln(Q_s^2/k_{\text{br}}^2(\omega)) = (1/2) \ln^2(\omega_c/\omega)$. This enhancement has been previously recognized in Ref. [9], where the respective correction to the transverse momentum broadening has been first computed (see also [14, 68]).

In what follows, we will use Eq. (4.29) to identify, compute, and resum the corrections enhanced by a double logarithm. To that aim, we need to focus on the relatively large fluctuations with $|\mathbf{x} - \mathbf{z}| \simeq |\mathbf{z} - \mathbf{y}| \gg r$. Since the dipole scattering amplitude $\Gamma_\omega(\mathbf{x}, \mathbf{z})$ is a rapidly growing function of the dipole size $|\mathbf{x} - \mathbf{z}|$ (see below), it is quite clear that, in this regime, one can neglect the ‘virtual’ term $\propto \Gamma_\omega(\mathbf{x}, \mathbf{y})$ in Eq. (4.29). Then this equation simplifies to

$$\omega \frac{\partial \Gamma_\omega(r)}{\partial \omega} \simeq \bar{\alpha} \int dB_\perp^2 \frac{r^2}{B_\perp^4} \Gamma_\omega(B_\perp), \quad (4.33)$$

where we have used B_\perp to denote the size of any of the two daughter dipoles. The initial condition for this equation at $\omega \simeq \omega_c$, i.e. the tree-level result in Eq. (4.5), is roughly proportional to the dipole size squared. Remarkably, Eq. (4.33) shows that this property is preserved by the evolution under the approximations of interest. Hence, we can write

$$g^2 C_F \Gamma_\omega(B_\perp) \equiv \frac{1}{4} \hat{q}_\omega(1/B_\perp^2) B_\perp^2, \quad (4.34)$$

where the function $\hat{q}_\omega(1/B_\perp^2)$ has only a weak dependence upon B_\perp^2 (for $\omega \simeq \omega_c$, it reduces to the zeroth order result in Eq. (4.6)). Then Eq. (4.33) implies the following equation for \hat{q}_ω :

$$\omega \frac{\partial \hat{q}_\omega(1/r^2)}{\partial \omega} \simeq \bar{\alpha} \int_{r^2}^{4/k_{\text{br}}^2(\omega)} \frac{dB_\perp^2}{B_\perp^2} \hat{q}_\omega(1/B_\perp^2), \quad (4.35)$$

where the limits in the integral over B_\perp^2 follow from the previous discussion. Eq. (4.35) looks similar to the familiar ‘double-logarithmic approximation’ (DLA) to the BFKL equation (see e.g. [16]).

But one should keep in mind that the upper limit in the above integral, which is energy–dependent, is specific to the problem at hand and reflects the non–linear physics of multiple scattering. For this particular problem, and unlike in more standard applications of the BFKL equation to high–energy scattering [16, 28–30], the DLA encompasses the *dominant* radiative corrections in the high–energy limit $\omega_c/\omega \gg 1$: its solution is equivalent to the resummation of the double–logarithmic corrections singled out in [9] (see below).

Importantly, the approximation (4.34) for the dipole amplitude automatically implies that the radiative corrections that we are about to compute can be absorbed into a redefinition of \hat{q} . Indeed, with this approximation for Γ_ω , the evolved dipole S –matrix in Eq. (4.23) has the same formal structure as at tree–level, that is (compare to Eq. (4.5))

$$\mathcal{S}_\omega(\mathbf{r}) \simeq \exp \left\{ -\frac{1}{4} L \hat{q}_\omega (1/r^2) \mathbf{r}^2 \right\}. \quad (4.36)$$

In turn, this implies that the quark spectrum has the Gaussian form in Eq. (4.8), but with a *renormalized*, energy–dependent, saturation momentum, defined by $Q_s^2 = \hat{q}_\omega(Q_s^2)L$.

Consider now the first iteration to Eq. (4.35) and assume for simplicity that the respective zeroth order result (to be denoted as $\hat{q}^{(0)}$ in what follows) is scale–independent. The first order correction implied by Eq. (4.35) reads¹⁴

$$\begin{aligned} \delta \hat{q}_\omega^{(1)}(Q_s^2) &= \bar{\alpha} \hat{q}^{(0)} \int_\omega^{\omega_c} \frac{d\omega_1}{\omega_1} \int_{k_{\text{br}}^2(\omega_1)}^{Q_s^2} \frac{dp_\perp^2}{p_\perp^2} = \bar{\alpha} \hat{q}^{(0)} \int_\omega^{\omega_c} \frac{d\omega_1}{\omega_1} \ln \frac{Q_s^2}{k_{\text{br}}^2(\omega_1)} \\ &\simeq \frac{\bar{\alpha}}{2} \hat{q}^{(0)} \int_\omega^{\omega_c} \frac{d\omega_1}{\omega_1} \ln \frac{\omega_c}{\omega_1} = \frac{\bar{\alpha}}{4} \hat{q}^{(0)} \ln^2 \frac{\omega_c}{\omega}, \end{aligned} \quad (4.37)$$

where the approximate equality sign refers to the double–logarithmic accuracy and we preferred to use the transverse momentum variable $p_\perp^2 \equiv 4/B_\perp^2$ as an integration variable, instead of B_\perp^2 . As expected, this correction is of order $\bar{\alpha}$, but it is enhanced by the potentially large double logarithm $\ln^2(\omega_c/\omega)$. To understand how large can this actually be, one needs to know what is the minimal value for ω which is allowed on physical grounds. This issue has been previously addressed in Ref. [9], where one has argued that this minimal value is controlled by a lower limit λ on the lifetime $\tau_{\text{coh}} = 2\omega/p_\perp^2$ of the fluctuations, which is independent of L . In the next subsection, we shall revisit and complete the arguments in Ref. [9] and thus clarify the physical origin and the value of λ . But for the time being, it suffices to know that such a cutoff exists and examine its consequences. As we now explain, this implies the existence of a large phase–space for double–logarithmic evolution in the regime where $L \gg \lambda$.

Specifically, the condition $\tau_{\text{coh}} > \lambda$ implies a lower limit on the gluon energy, $\omega > \lambda p_\perp^2/2$, which also depends upon its transverse momentum p_\perp . This last feature forces us to modify our previous analysis leading to Eq. (4.44). Indeed, in the integral over p_\perp^2 within that equation, we have assumed that the maximal limit is equal to Q_s^2 , but in reality this cannot exceed a value $p_{\perp\text{max}}^2 = 2\omega_1/\lambda$ which also depends upon ω_1 (the other integration variable there). That is, the proper integration range in p_\perp^2 for a given value of ω is

$$k_{\text{br}}^2(\omega) \ll p_\perp^2 \ll \min \left(\frac{2\omega}{\lambda}, Q_s^2 \right). \quad (4.38)$$

¹⁴To the accuracy of interest, one can replace $\hat{q} \simeq \hat{q}^{(0)}$ within the argument of the logarithm.

The upper limit introduces two constraints. First, it implies the necessary condition $2\omega/\lambda \gg k_{\text{br}}^2(\omega)$, or equivalently $\omega \gg \omega_0 \equiv \hat{q}\lambda^2$, showing that ω_0 is the absolute lower limit on the energy ω of the fluctuation. Second, it means that, when performing the integrals over the phase-space, one must distinguish between two different ranges in ω , namely $\omega_0 < \omega < \omega_*$ and $\omega_* < \omega < \omega_c$, where $\omega_* \equiv Q_s^2\lambda/2$ is the energy for which Q_s^2 becomes equal to $2\omega/\lambda$ and obeys $\omega_* \gg \omega_0$ for $L \gg \lambda$.

To summarize, the DLA phase-space is defined as the range (4.38) in p_{\perp}^2 together with the energy range at $\omega_0 \ll \omega \ll \omega_c$. The whole analysis becomes more transparent if, instead of the original variables ω and p_{\perp}^2 , one uses the variables $\tau \equiv 2\omega/p_{\perp}^2$ (the lifetime of the fluctuation) and p_{\perp}^2 . As an intermediate step, notice that Eq. (4.38) is tantamount to

$$\max\left(\lambda, \frac{2\omega}{Q_s^2}\right) \ll \tau \ll \tau_{\text{br}}(\omega) \equiv \frac{2\omega}{k_{\text{br}}^2(\omega)} = \sqrt{\frac{\omega}{\hat{q}}}. \quad (4.39)$$

Then it is easy to see that, in terms of the new variables τ and p_{\perp}^2 , the DLA phase-space can be simply characterized as (see also Fig. 3 for an illustration)

$$\lambda \ll \tau \ll L, \quad 2\hat{q}\tau \ll p_{\perp}^2 \ll Q_s^2. \quad (4.40)$$

Then the first order correction is computed as (compare to Eq. (4.44))

$$\delta\hat{q}^{(1)} = \bar{\alpha}\hat{q}^{(0)} \int_{\lambda}^L \frac{d\tau}{\tau} \int_{2\hat{q}\tau}^{Q_s^2} \frac{dp_{\perp}^2}{p_{\perp}^2} = \bar{\alpha}\hat{q}^{(0)} \int_{\lambda}^L \frac{d\tau}{\tau} \ln \frac{L}{2\tau} \simeq \hat{q}^{(0)} \frac{\bar{\alpha}}{2} \ln^2 \frac{L}{\lambda}, \quad (4.41)$$

where we have used $Q_s^2 = \hat{q}L$. (As before, we ignore the difference between \hat{q} and $\hat{q}^{(0)}$, or the factors of 2, in the argument of the logarithm.) The above result, which is in agreement with Refs. [9, 68], is not the same as the result of evaluating Eq. (4.44) at the minimal value of the energy $\omega = \omega_0$. The last calculation would be naive, in that it would incorrectly treat the contribution of the low energy region at $\omega_0 < \omega < \omega_*$.

More generally, it is preferable to use the new variables τ and p_{\perp}^2 also within the DLA equation (4.35) and to replace the latter by an integral equation, where all the integration limits are explicit. This equation reads

$$\hat{q}_L(Q_s^2) = \hat{q}^{(0)} + \bar{\alpha} \int_{\lambda}^L \frac{d\tau}{\tau} \int_{\hat{q}\tau}^{Q_s^2} \frac{dp_{\perp}^2}{p_{\perp}^2} \hat{q}_{\tau}(p_{\perp}^2). \quad (4.42)$$

Eq. (4.42) shows that the physical quantity $\hat{q}_L(Q_s^2)$ of interest — the renormalized jet quenching parameter as obtained after including the radiative corrections to DLA accuracy — is obtained as the value of a function of two variables, $\hat{q}_{\tau}(p_{\perp}^2)$, at the physical point $\tau = L$ and $p_{\perp}^2 = Q_s^2(L)$ in the phase-space. (As it will be explained in Sect. 4.4, this physical point lies on the saturation line for the gluon distribution of the medium; see also Fig. 3.) In turn, the function $\hat{q}_{\tau}(p_{\perp}^2)$ has support at $p_{\perp}^2 > \hat{q}\tau$ and is obtained as the solution to the following integral equation:

$$\hat{q}_{\tau}(p_{\perp}^2) = \hat{q}^{(0)} + \bar{\alpha} \int_{\lambda}^{\tau} \frac{d\tau_1}{\tau_1} \int_{\hat{q}\tau_1}^{p_{\perp}^2} \frac{dk_{\perp}^2}{k_{\perp}^2} \hat{q}_{\tau_1}(k_{\perp}^2). \quad (4.43)$$

As already stressed after Eq. (4.35), the above equation differs from the standard DLA equation which appears e.g. in studies of the jet evolution in the vacuum [15, 16] via the τ -dependence of the lower limit in the integral over p_{\perp}^2 , which comes from the restriction to single scattering.

Eq. (4.43) can be easily solved via iterations. The first iteration (with $\hat{q}^{(0)}$ assumed to be scale-independent, once again) gives

$$\delta\hat{q}_\tau^{(1)}(p_\perp^2) = \hat{q}^{(0)} \frac{\bar{\alpha}}{2} \left(\ln^2 \frac{p_\perp^2}{\hat{q}\lambda} - \ln^2 \frac{p_\perp^2}{\hat{q}\tau} \right), \quad (4.44)$$

which on the physical point $\tau = L$ and $p_\perp^2 = \hat{q}L$ reduces to Eq. (4.41), as it should. The second iteration yields (we only show its result at the physical point)

$$\delta\hat{q}^{(2)} = \hat{q}^{(0)} \frac{\bar{\alpha}^2}{2!3!} \ln^4 \frac{L}{\lambda}. \quad (4.45)$$

These and the subsequent terms in this iterative procedure are recognized as the Taylor expansion of the modified Bessel function¹⁵ $I_1(x)$:

$$\hat{q}_L(Q_s^2) = \hat{q}^{(0)} \frac{1}{\sqrt{\bar{\alpha}} \ln(L/\lambda)} I_1 \left(2\sqrt{\bar{\alpha}} \ln \frac{L}{\lambda} \right). \quad (4.46)$$

The same result has been obtained in Ref. [9] via a resummation of the relevant Feynman graphs. This resummation becomes pertinent when the medium is large enough, such that $\bar{\alpha} \ln^2(L/\lambda) \gtrsim 1$. In such a case, the radiative corrections enhance the medium-size dependence of the (renormalized) jet quenching parameter, which thus becomes even more non-local than it was at tree-level.

We conclude this subsection with a few comments on the physical meaning of the radiative corrections displayed in Eqs. (4.41) or (4.46). As obvious from the previous calculations, these corrections are generated by the emission of soft gluons with energies ω deeply within the range between $\omega_0 = \hat{q}\lambda^2$ and $\omega_c = \hat{q}L^2$ and with transverse momenta p_\perp deeply between $k_{\text{br}}(\omega)$ and Q_s . Such gluons have lifetimes considerably smaller than the medium longitudinal size L and transverse sizes which are considerably larger than the size $r \sim 1/Q_s$ of the original dipole. This hierarchy is furthermore respected by the successive emissions which are summed up by Eq. (4.46) and whose energies are softer and softer with increasing generation. Because of this hierarchy, the corrections appear to be quasi-local on the longitudinal scale relevant for measuring the transverse momentum broadening, which is L . Similarly, they do not affect the transverse resolution on which we scrutinize the medium properties, which is set by Q_s . This ultimately explains why such corrections can be simply accounted for by a renormalization of the jet quenching parameter $\hat{q}_L(Q_s^2)$.

4.3.3 The phase-space for the high-energy evolution

In the previous section, we have argued that the phase-space for the double-logarithmic approximation is given by Eq. (4.40), where the lower limit λ has not yet been specified. In this subsection, we shall first explain the physical origin and the value of λ , thus following a discussion in Ref. [9]. Then we shall critically revisit the original arguments in Ref. [9] and demonstrate that, in general, the structure of the DLA phase-space is more complicated than suggested there (and shown in Eq. (4.40)). The differences are unessential in the limit where the medium size L is arbitrarily large, but they become important for realistic values of L , in which case they limit the validity of the DLA. Based on such considerations, we shall derive the constraint (4.52) for the applicability of the DLA (and, more generally, of the present high-energy approximations) in the case where the target is a weakly coupled QGP.

¹⁵This should be contrasted to the standard DLA solution, which involves the Bessel function $I_0(x)$ [16].

As discussed in Ref. [9], the existence of a lower limit λ on the lifetime τ of the fluctuations follows from energy–momentum conservation. In the high–energy approximation of interest, the gluon fluctuation is nearly on–shell, so it carries a ‘minus’ momentum $p^- = p_\perp^2/2\omega$ (recall that $\omega \equiv p^+$). This component cannot be inherited from the parent quark, which is a right mover, so it must be acquired via interactions with the medium. Since moreover we assume that there is only one scattering during the fluctuation, it is clear that either the virtual gluon, or its parent quark, must have absorbed a quanta having this momentum p^- . This quanta is a (generally off–shell) gluon exchanged between the projectile and some constituent of the medium — say, a thermal quark or gluon, in the case where the medium is a finite temperature plasma. Let us denote by k^- the respective 4–momentum component of that particular constituent and introduce the *longitudinal momentum fraction* $x \equiv p^-/k^-$, with $x \leq 1$ of course. (This is ‘longitudinal’ since the medium is a left mover.) We have

$$x = \frac{p_\perp^2}{2\omega k^-} = \frac{p_\perp^2}{2p \cdot k}, \quad (4.47)$$

where the second equality, which confirms that x is boost invariant, follows from the high energy kinematics. Indeed, in whatever frame we use, at least one of the two subsequent statements is correct: (I) p^+ is the large component of the 4–momentum of the gluon fluctuation, and (II) k^- is the large component of the 4–momentum of the medium constituent.

In particular, in the plasma rest frame, one has $k^- \simeq T$ for a typical plasma particle and Eq. (4.47) becomes

$$x \simeq \frac{p_\perp^2}{2\omega T} = \frac{\lambda}{\tau}, \quad (4.48)$$

where $\tau = 2\omega/p_\perp^2$ and $\lambda \equiv 1/T$ is the typical thermal wavelength. Since $x \leq 1$ and $\tau \leq L$, the above relation implies the following ranges of values for x and τ :

$$\frac{\lambda}{L} \leq x \leq 1, \quad L \geq \tau \geq \lambda. \quad (4.49)$$

This motivated the authors of Ref. [9] to choose $\lambda = 1/T$ as the minimal value for τ in equations like (4.42). This conclusion is essentially correct, but its validity is restricted by an additional kinematical constraint, that has been overlooked in the analysis in Ref. [9] and that we shall now discuss.

The high–energy picture that we have developed so far is based on the assumption that the gluon fluctuations are very energetic in the plasma rest frame, meaning that their ‘energy’ ω is (much) larger than their transverse momentum: $\omega \gg p_\perp$. In particular, this must be true for the hardest allowed fluctuations, with energy $\sim \omega_c$ and transverse momentum $\sim Q_s$. Hence, the inequality $\omega_c \gg Q_s$, or equivalently $\hat{q}L^3 \gg 1$, is a necessary condition for the validity of our approach. This condition has been implicitly assumed throughout our analysis and is indeed well satisfied in practice. Returning to generic values for ω and p_\perp , we observe that the kinematical constraint $\omega \gg p_\perp$ implies the following conditions on the lifetime $\tau = 2\omega/p_\perp^2$ of the fluctuations: $\tau \gg 1/p_\perp \gg 1/\omega$. For a given τ , the transverse momentum cannot be smaller than a value $p_\perp^{\min} \sim \sqrt{\hat{q}\tau}$ introduced by multiple scattering. So, clearly, the kinematical constraint $\tau > 1/p_\perp$ is satisfied for any permitted value of p_\perp provided the following condition is fulfilled:

$$\tau \gtrsim \frac{1}{p_\perp^{\min}} \sim \frac{1}{\sqrt{\hat{q}\tau}} \implies \tau \gtrsim \hat{q}^{-1/3}. \quad (4.50)$$

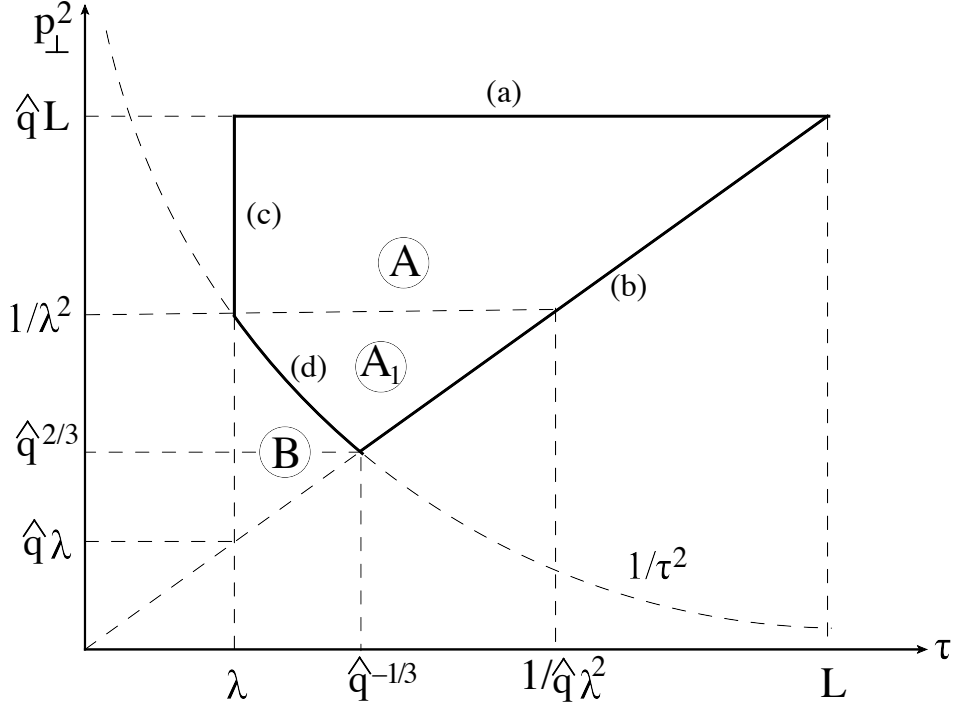


Figure 3. The phase-space for the high-energy evolution of jet quenching, in terms of the variables τ and p_{\perp}^2 (the lifetime and the transverse momentum squared of the gluon fluctuations). We assume $\hat{q}\lambda^3 \ll 1$ and $\hat{q}L\lambda^2 \gg 1$. Line (b) is the ‘saturation line’ $p_{\perp}^2 = \hat{q}\tau$ (see Sect. 4.4). Line (d) reads $p_{\perp}^2 = 1/\tau^2$ and implements the kinematic constraint $p^+ > p_{\perp}$. The phase-space for the double-logarithmic evolution is region A, as delimited by the lines (a), (b), (c), and (d). For discussions of regions B and A_1 , see the main text.

If this condition was satisfied for any τ within the range $\lambda \lesssim \tau < L$, then the kinematical constraint would play no special role for the present analysis (since automatically satisfied throughout the phase-space). But for a weakly coupled QGP and with $\lambda = 1/T$, the condition (4.50) is *not* satisfied for sufficiently small values $\tau \sim \lambda$: one has indeed $\hat{q}^{1/3}\lambda \sim [\alpha_s^2 \ln(1/\alpha_s)]^{1/3} \ll 1$.

The solution to this problem is in fact quite simple¹⁶: it suffices to impose the additional constraint $\tau > 1/p_{\perp}$ on the kinematical domain (4.40) for the double-logarithmic contributions. This leads to the phase-space denoted by the letter A in Fig. 3. Note that, in drawing this figure, we have chosen not only $\hat{q}L^3 \gg 1$ (together with $\hat{q}\lambda^3 \ll 1$, of course), but also the stronger condition $\hat{q}L\lambda^2 \gg 1$. The reason for that should shortly become clear.

The domain A in Fig. 3 differs from the original phase-space in (4.40) by the domain denoted there by the letter B, whose contribution to $\delta\hat{q}$ can be computed as

$$\delta\hat{q}_B = \bar{\alpha}\hat{q}^{(0)} \int_{\lambda}^{\hat{q}^{-1/3}} \frac{d\tau}{\tau} \int_{\hat{q}\tau}^{1/\tau^2} \frac{dp_{\perp}^2}{p_{\perp}^2} = \hat{q}^{(0)} \frac{\bar{\alpha}}{6} \ln^2 \frac{1}{\hat{q}\lambda^3}. \quad (4.51)$$

This contribution is independent of the medium size L , so clearly it becomes negligible compared to the DLA result in Eq. (4.41) — the contribution of the domains $A \cup B$ in Fig. 3 — for sufficiently

¹⁶I am grateful to Al Mueller for clarifying discussions on this point.

large values of L . The precise condition is

$$\frac{L}{\lambda} \gg \frac{1}{\hat{q}\lambda^3} \sim \frac{1}{\alpha_s^2 \ln(1/\alpha_s)}, \quad \text{or, equivalently,} \quad Q_s^2 \gg \frac{1}{\lambda^2} \sim T^2, \quad (4.52)$$

where the parametric estimates refer to the weakly coupled QGP. Vice-versa, these considerations suggest the existence of L -independent radiative corrections of order $\alpha_s \ln^2(1/\alpha_s^2)$, which are quite large and are not properly taken into account by our high-energy approximations.

Note finally that, under the same assumptions as above, cf. Eq. (4.52), the radiative corrections of interest for us here can be fully attributed to the relatively hard fluctuations, with transverse momenta within the range $Q_s \gtrsim p_\perp \gg 1/\lambda = T$. Indeed, the respective contribution of the softer momenta $p_\perp \leq 1/\lambda$ is given by the domain A_1 in Fig. 3 (a subdomain of region A) and can be easily estimated as

$$\delta\hat{q}_{A_1} = \bar{\alpha}\hat{q}^{(0)} \int_{\hat{q}^{2/3}}^{1/\lambda^2} \frac{dp_\perp^2}{p_\perp^2} \int_{1/p_\perp}^{p_\perp^2/\hat{q}} \frac{d\tau}{\tau} = \hat{q}^{(0)} \frac{\bar{\alpha}}{3} \ln^2 \frac{1}{\hat{q}\lambda^3}. \quad (4.53)$$

This contribution is comparable to that in Eq. (4.51) and hence it is negligible under the same conditions. Moreover, these small contributions, from domains B and A_1 , are not even enhanced by a *single* large logarithm $\ln(L/\lambda)$, so they are irrelevant for the high-energy evolution.

To summarize, the gluon fluctuations which control the high-energy evolution of a slice of weakly-coupled QGP which is large enough (in the sense of Eq. (4.52)) are characterized by large lifetimes $\tau \gg 1/T$, large transverse momenta $p_\perp \gg T$, and even larger energies $\omega \gg p_\perp$. In particular, the phase-space for DLA can be restricted to the ‘hard’ region depicted as $A \setminus A_1$ (i.e. the difference between the domains A and A_1) in Fig. 3.

4.4 Gluon evolution and saturation in the medium

In this subsection, we shall develop an alternative physical picture for the high-energy evolution of jet quenching in terms of the gluon distribution in the medium. In particular, we would like to argue that the multiple scattering between the soft fluctuations and the medium can be alternatively interpreted as saturation effects in the gluon distribution at small x . To develop this new picture, we will have to use a different Lorentz frame, namely, an ‘infinite momentum frame’ for the medium, in which the relevant gluon fluctuations appear as ‘partons’ from the plasma. A similar picture has been developed for a strongly coupled plasma described by $\mathcal{N} = 4$ SYM [69–71], but we are not aware of previous, related, discussions at weak coupling, except at tree-level (cf. Sect. 4.1).

Namely, consider the interaction between the projectile (the quark, or the dipole) and the medium (plasma) in a frame where the projectile is quite slow whereas the target is an ultrarelativistic left mover, with a Lorentz boost factor of order¹⁷ $\gamma \simeq \omega_c/Q_s = \sqrt{\hat{q}L^3}$. In this frame, all the fluctuations that we have discussed so far become left movers, so they are more naturally associated with the plasma. They cannot be a part of the thermal distribution, since that was not true in the plasma rest frame and the thermal distribution is boost invariant. Rather, they must be considered as bremsstrahlung (or Weizsäcker–Williams) quanta emitted by the medium

¹⁷In the plasma rest frame, a gluon fluctuation with energy ω and transverse momentum k_\perp has a rapidity η such that $\gamma \equiv \cosh \eta \simeq \omega/k_\perp$. Since $k_\perp^2 \gtrsim k_{\text{br}}^2 = \sqrt{\hat{q}\omega}$, this implies $\gamma \lesssim (\omega^3/\hat{q})^{1/4}$, where the upper limit reaches a maximal value $\gamma_{\text{max}} = \omega_c/Q_s$ corresponding to $\omega = \omega_c$.

constituents (thermal quarks and gluons). Thus, in this boosted frame, the relevant fluctuations are a part of the *medium gluon distribution*.

The typical fluctuations carry small fractions $x \ll 1$ of the longitudinal (k^-) momenta of their parent particles (which are large, $k^- \simeq \gamma T$, in the boosted frame). Accordingly, they have large wavelengths $\Delta x^+ \sim 1/(xk^-) \gg 1/k^-$, meaning that they overlap with many medium constituents. On the other hand, they have very short lifetimes $\Delta x^- = 1/p^+ \ll \gamma/T$, which explain why they cannot thermalize. (Notice that γ/T is the smallest time scale associated with the thermal distribution in this frame.) Furthermore, the high-energy evolution that we had previously associated with the wavefunction of the projectile can be alternatively interpreted as an evolution of the medium gluon distribution with decreasing x . Interestingly, this evolution is somewhat different than it would be in a shockwave : the small- x gluons cannot overlap with all the color sources within a longitudinal tube throughout the target (as they do in a shockwave [12, 32, 33]), but only with those within a longitudinal distance $\Delta x^+ \sim 1/(xk^-)$. This is consistent with the peculiar boundaries on the phase-space for linear evolution, as discussed in the previous sections. It furthermore implies a stronger x -dependence of the respective saturation momentum, as we now explain.

To make contact with the previous developments, let us recall that the ‘unintegrated gluon distribution’ in the target — the number of gluons per unit rapidity $Y \equiv \ln(1/x)$ and per unit transverse phase-space — is closely related to the cross-section (4.1) for transverse momentum broadening. One has indeed (see e.g. the discussion in Ref. [38])

$$x \frac{dN_g}{dx d^2\mathbf{p} d^2\mathbf{b}} = \frac{N_c^2 - 1}{4\pi^3} \frac{p_\perp^2}{g^2 C_F} \int_{\mathbf{r}} e^{-i\mathbf{p}\cdot\mathbf{r}} \mathcal{S}(\mathbf{r}), \quad (4.54)$$

where the subscript g stays for ‘gluon’ and \mathbf{b} denotes the position in transverse space, or ‘impact parameter’. More precisely, Eq. (4.54) is the gluon distribution ‘unintegrated’ in the transverse phase-space, but integrated in the longitudinal (x^+) direction over the whole size L of the target. Since our medium is assumed to be homogeneous in both x^+ and \mathbf{x} , the *occupation number* for gluons with 3-momentum (p^-, \mathbf{p}) is naturally estimated as

$$f(p^-, \mathbf{p}) \equiv \frac{4\pi^3}{N_c^2 - 1} \frac{1}{L} \frac{dN_g}{dp^- d^2\mathbf{p} d^2\mathbf{b}} = \frac{p_\perp^2}{g^2 C_F p^- L} \int_{\mathbf{r}} e^{-i\mathbf{p}\cdot\mathbf{r}} \mathcal{S}(\mathbf{r}). \quad (4.55)$$

As a simple illustration, consider the high-momentum (or low occupancy) regime, where the dipole S -matrix in Eq. (4.54) can be evaluated in the single scattering approximation. At tree-level one obtains, similarly to Eq. (4.9),

$$f_0(p^-, p_\perp) \simeq \frac{4\pi\alpha_s n_0}{p^- p_\perp^2}. \quad (4.56)$$

Although valid in the dilute regime, this result can be used to estimate the borderline of the saturation region. Namely, the non-linear effects in the gluon distribution are expected to become important when $f \sim 1/\bar{\alpha}$ [12, 32, 33]. This occurs for a transverse momentum p_\perp of the order of the *saturation momentum* $Q_s(x)$, which at tree-level is estimated as

$$Q_{s0}^2(x) \sim \frac{\alpha_s^2 N_c n_0}{p^-} \sim \frac{\hat{q}^{(0)} \lambda}{x}, \quad (4.57)$$

where we have used $p^- = xk^-$ and the second equality is written, for convenience, in the plasma rest frame, where $k^- \simeq 1/\lambda$ and, parametrically, $\alpha_s^2 N_c n_0 \sim \hat{q}^{(0)}$. Using $\tau = \lambda/x$, the above equation

can also be written as $Q_{s0}^2(\tau) = \hat{q}^{(0)}\tau$, which is recognized as the line (b) in Fig. 3 (the borderline of the multiple scattering region).

What is remarkable about the saturation momentum in Eq. (4.57) is that it exhibits a strong x -dependence already at tree-level (unlike the corresponding scale for a shockwave, which is independent of x). Clearly, this is the consequence of the fact that the longitudinal phase-space for gluon overlapping is now the longitudinal wavelength $\Delta x^+ \propto 1/x$ of a gluon fluctuation, and not the width L of the target as a whole. This quantity $Q_{s0}^2(x)$ reaches its maximal value $Q_{s0}^2 = \hat{q}^{(0)}L$ for $x_{\min} = \lambda/L$. Thus, the quantity that we had conventionally dubbed ‘the saturation momentum’ in our previous discussion (e.g. in Eq. (4.7)) is in fact the *proper* saturation scale for the *softest*¹⁸ fluctuations allowed by the size of the medium. This quantity is boost invariant, but its physical interpretation as a saturation scale holds only in a frame where the target is highly boosted.

Going beyond tree-level, it is clear that the evolution of the dipole scattering amplitude in the linear approximation, Eq. (4.29), can be interpreted as the BFKL evolution of the gluon occupation number in the medium. Indeed, in the single scattering approximation, Eqs. (4.55) and (4.23) imply

$$f_\omega(p^-, \mathbf{p}) \simeq -\frac{p_\perp^2}{p^-} \int_{\mathbf{r}} e^{-i\mathbf{p}\cdot\mathbf{r}} \Gamma_\omega(\mathbf{r}) \sim \frac{1}{\bar{\alpha}} \frac{\hat{q}_\omega(p_\perp^2)}{p^- p_\perp^2}, \quad (4.58)$$

where the second, parametric, estimate holds to double-logarithmic accuracy, cf. Eq. (4.34). Moreover, the effects of multiple scattering, i.e. the non-linear terms in Eq. (4.24), can be interpreted as gluon saturation in the medium, as we now explain. Indeed, such effects become important when the exponent in Eq. (4.24) becomes of $\mathcal{O}(1)$. Using the DLA estimate (4.58) for $f_\omega(p^-, \mathbf{p})$, this condition can be recognized as the saturation condition for the gluon occupation number:

$$1 \sim \hat{q}_\omega(1/B_\perp^2) B_\perp^2 \Delta t \sim \frac{\hat{q}_\omega(p_\perp^2)}{p_\perp^2} \frac{\lambda}{x} \sim \bar{\alpha} f_\omega(x, \mathbf{p}). \quad (4.59)$$

Solving this condition for p_\perp^2 , one finds the saturation momentum in the presence of radiative corrections (to double-logarithmic accuracy):

$$Q_s^2(x) \sim \frac{\hat{q}(x)\lambda}{x}, \quad (4.60)$$

where $\hat{q}(x) \equiv \hat{q}_\tau(p_\perp^2)$ with $\tau = \lambda/x$ and $p_\perp^2 = Q_s^2(x)$. That is, $\hat{q}(x)$ is the function $\hat{q}_\tau(p_\perp^2)$ evaluated along the saturation line. (In particular, for $x = x_{\min} = \lambda/L$, this is the physical jet quenching parameter.) In view of Eq. (4.43), this can be given by the following integral representation

$$\hat{q}(x) = \hat{q}^{(0)} + \bar{\alpha} \int_x^1 \frac{dx_1}{x_1} \int_{Q_s^2(x_1)}^{Q_s^2(x)} \frac{dp_\perp^2}{p_\perp^2} \hat{q}_{x_1}(p_\perp^2). \quad (4.61)$$

Within the integration limits above, one can use the zeroth order estimate $Q_s^2(x) \simeq \hat{q}^{(0)}\lambda/x$. Note that, with decreasing x , both the longitudinal phase-space and the transverse phase-space in Eq. (4.61) increase equally fast — that is, the both increase like $\ln(1/x)$ — due to the rapid increase $Q_s^2(x) \sim 1/x$ of the saturation scale. Accordingly, the above DLA calculation correctly captures the dominant radiative corrections to the evolution of $Q_s^2(x)$, unlike what happens in

¹⁸By ‘softest’ we here mean the smallest value of x , as appropriate from the viewpoint of the left-moving target; from the viewpoint of the right-moving projectile, these are rather the *hardest* fluctuations, with ‘energy’ $p^+ = \omega_c$.

the case of a shockwave. (For the latter, the longitudinal phase-space increases faster than the transverse one in the approach towards saturation, hence the correct calculation of $Q_s^2(x)$ requires the full BFKL equation, and not just its DLA limit [28, 29].)

In particular, if one treats the zeroth order result $\hat{q}^{(0)}$ as a constant, one finds (cf. Eq. (4.46))

$$\hat{q}(x) = \hat{q}^{(0)} \frac{1}{\sqrt{\bar{\alpha}} \ln(1/x)} I_1 \left(2\sqrt{\bar{\alpha}} \ln \frac{1}{x} \right). \quad (4.62)$$

In the extreme limit where $2\sqrt{\bar{\alpha}} \ln(1/x) \gg 1$, one can use the asymptotic behavior of the modified Bessel function to deduce

$$Q_s^2(x) \simeq \frac{Q_0^2}{x^{1+\gamma_s}}, \quad (4.63)$$

with $Q_0^2 \equiv \hat{q}^{(0)}\lambda$ and the ‘anomalous dimension’ $\gamma_s = 2\sqrt{\bar{\alpha}}$. The overall power $\lambda_s \equiv 1 + \gamma_s$ in Eq. (4.63) is the medium saturation exponent within the present approximation. This is independent of the precise nature of the medium, as it is fully determined by the high-energy evolution. The radiative correction γ_s looks like a strong effect since $2\sqrt{\bar{\alpha}} \sim 1$ for $\alpha_s \approx 0.3$ and $N_c = 3$. But one should keep in mind that the present approximation is strictly valid only when $\bar{\alpha} \ll 1$.

This being said, it is also interesting to notice that this perturbative result appears as a reasonable interpolation towards the corresponding result in $\mathcal{N} = 4$ SYM at infinitely strong coupling ($g^2 N_c \rightarrow \infty$), as obtained in [69]. Namely, Ref. [69] reported a saturation momentum $Q_s^2(x) \sim T^2/x^2$, where the ‘saturation exponent’ $\lambda_s = 2$ can be recognized as the sum of a kinematical contribution $\lambda_{s0} = 1$, the same as in Eq. (4.57), and a large ‘anomalous dimension’ $\gamma_s = 1$, which is the intercept of the graviton. (At strong coupling, the unitarization occurs via multiple graviton exchanges [72].) Together, the present results and the previous ones in Ref. [69] suggest a rather smooth and fast transition from a weak coupling-like behavior to a strong coupling-like with increasing $\bar{\alpha}$ (at least, in the absence of running coupling effects).

4.5 Comments on the effects of multiple scattering

So far, we have not attempted to explicitly evaluate the non-linear terms in Eq. (4.24), which encode the effects of multiple scattering. Rather, we have used them within semi-quantitative considerations allowing us to restrict the phase-space for the linear approximation and to develop a physical picture in terms of gluon saturation. But, clearly, it would be interesting to have a more quantitative control on these effects, e.g. in order to understand the systematics of the high-energy resummation. Ideally, one would like to isolate all the radiative corrections which are enhanced by a large energy logarithm $\ln(1/x) \sim \ln(L/\lambda)$ and thus obtain a non-linear equation which is explicitly valid to leading logarithmic accuracy. Unfortunately, this turns out to be very hard since the non-linear effects enter Eq. (4.24) via a path-integral, in which the unknown function $\Gamma_\omega(\mathbf{r})$ plays the role of the effective potential. That is, Eq. (4.24) is truly a *functional* integro-differential equation and very little is known about how to deal with such equations in practice.

In this section, we shall perform a limited study of the non-linear terms in Eq. (4.24), with two main objectives: to elucidate the systematics of the logarithmically-enhanced radiative corrections (which turns out to be very different from the case where the target is a shockwave) and to better justify the arguments in the previous sections concerning the kinematics of the fluctuations and the borderlines of the single scattering regime.

Concerning the first objective above, we would like to demonstrate the following point : for the case of an extended target, and unlike for a shockwave, the individual terms beyond the first one in the multiple scattering series — i.e. the terms describing double scattering, triple scattering etc — are not *separately* enhanced by a large energy logarithm. This is so because the longitudinal phase-space for multiple scattering is the lifetime of the soft gluon fluctuations, which is itself energy-dependent. This being said, the effects of multiple scattering are nevertheless important for a complete calculation at leading logarithmic accuracy, in that they provide the physical cutoff for the respective contribution of the single scattering (which otherwise would be infrared divergent).

To be specific, let us first recall the way how the energy logarithm has occurred for the single-scattering contribution. This arises via the phase-space for the three time integrations in Eq. (4.27) : over the emission times t_1 and t_2 , with $0 < t_1 < t_2 < L$, and over the interaction time t . Namely, the integral over t between t_1 and t_2 scales like $\Delta t = t_2 - t_1$, that over Δt scales like $\tau_{coh} = 2\omega/p_\perp^2$, and the final integral over say t_2 scales like L . Altogether, there is a longitudinal phase-space $L\tau_{coh}^2 \propto \omega^2$ which, when combined with the overall factor $1/\omega^3$ in Eq. (4.27), produces the logarithmic phase-space $\int(d\omega/\omega)$ for the ensuing energy integration. Now, let us similarly consider the contribution of a double scattering. As compared to the previous case, there are now two interaction times to be integrated over between t_1 and t_2 . This introduces an additional factor Δt , so the global result scales like $L\tau_{coh}^3 \propto \omega^3$, which spoils the logarithmic integration over ω . A similar conclusion holds for the contribution of n successive collisions, which scales like $L\tau_{coh}^{n+1} \propto \omega^{n+1}$.

It is further instructive to compare with the respective situation for a shockwave target, as discussed in Sect. 3.1. In that case, the two integrals over t_1 and t_2 separately restrict each of the emission times to values of order τ_{coh} around $t = 0$ (the position of the shockwave). Also each scattering with the target occurs within the longitudinal extent L of the latter (with $L \ll \tau_{coh}$ in this context), so the corresponding time integral brings in a factor of L . Hence, an individual n -scattering contribution with $n \geq 1$ scales like $\tau_{coh}^2 L^n \propto \omega^2$, and thus it is by itself accompanied by a large energy logarithm.

Returning to the case of an extended target, one should observe that the previous power-counting argument was a bit formal, in that it is plagued with infrared divergences: each additional scattering brings in a factor $\tau_{coh} = 2\omega/p_\perp^2$, which becomes singular when $p_\perp \rightarrow 0$. This leads to a logarithmic divergence in the single-scattering contribution, as manifest on Eq. (4.35), and to even stronger, power-like, divergences in the terms with two or more scatterings. We expect such divergences to be cured by the resummation of the multiple scattering series to all orders, but in order to verify this, one needs a non-perturbative calculation of this series.

To illustrate these considerations, let us consider the first iteration of Eq. (4.24). That is, we shall evaluate the r.h.s. of this equation using the tree-level approximation for the dipole S -matrix, Eq. (4.5), together with the ‘harmonic approximation’ for the jet quenching parameter — meaning that we ignore the scale dependence of the latter : $\hat{q} \simeq \text{const}$ (throughout this subsection, one has $\hat{q} \equiv \hat{q}^{(0)}$). The harmonic approximation is indeed important for the present purposes, since it allows us to explicitly perform the path integral in Eq. (4.24), which becomes

$$\mathcal{I}(\mathbf{r}_2, \mathbf{r}_1, \Delta t) \equiv \int [\mathcal{D}\mathbf{r}] e^{i\frac{\omega}{2} \int_{t_1}^{t_2} dt' \dot{\mathbf{r}}^2(t')} \exp \left\{ -\frac{\hat{q}}{4} \int_{t_1}^{t_2} dt \left[(\mathbf{x} - \mathbf{r}(t))^2 + (\mathbf{r}(t) - \mathbf{y})^2 - (\mathbf{x} - \mathbf{y})^2 \right] \right\} \quad (4.64)$$

with boundary conditions $\mathbf{r}(t_1) = \mathbf{r}_1$ and $\mathbf{r}(t_2) = \mathbf{r}_2$. (\mathcal{I} is also a function of \mathbf{x} and \mathbf{y} , but the respective arguments are kept implicit.) A standard calculation yields

$$\begin{aligned} \mathcal{I}(\mathbf{r}_2, \mathbf{r}_1, \Delta t) &= \frac{-i}{2\pi} \frac{\omega\Omega}{\sinh \Omega\Delta t} e^{\frac{i}{2}\Omega\Delta t(\mathbf{x}-\mathbf{y})^2} \\ &\quad \times \exp \left\{ \frac{i}{2} \frac{\omega\Omega}{\sinh \Omega\Delta t} \left[\cosh \Omega\Delta t \left((\mathbf{r}_2 - \mathbf{R})^2 + (\mathbf{r}_1 - \mathbf{R})^2 \right) - 2(\mathbf{r}_2 - \mathbf{R}) \cdot (\mathbf{r}_1 - \mathbf{R}) \right] \right\}, \end{aligned} \quad (4.65)$$

where $\mathbf{R} \equiv (\mathbf{x} + \mathbf{y})/2$ and

$$\Omega = \frac{1+i}{\sqrt{2}} \sqrt{\frac{\hat{q}}{\omega}} = \frac{1+i}{\sqrt{2}} \frac{1}{\tau_{\text{br}}(\omega)}. \quad (4.66)$$

In the limit $\hat{q} \rightarrow 0$ (no scattering), this reduces to the ‘non-relativistic’ propagator in the vacuum, as it should (cf. Eq. (2.10)): $\mathcal{I} \rightarrow \mathcal{G}_0$ with

$$\mathcal{G}_0(\mathbf{r}_2 - \mathbf{r}_1, \Delta t) = \frac{-i}{2\pi} \frac{\omega}{\Delta t} \exp \left\{ \frac{i\omega(\mathbf{r}_2 - \mathbf{r}_1)^2}{2\Delta t} \right\}. \quad (4.67)$$

The perturbative (‘small \hat{q} ’) expansion of Eq. (4.65), which would reconstruct the multiple scattering series, turns out to be quite tedious. However, by inspection of this equation, it is clear that such an expansion makes sense only for sufficiently small times $\Delta t \ll \tau_{\text{br}}(\omega)$. In this perturbative regime at early times, the convergence in Δt is controlled by the free propagator (4.67), which implies that the transverse size of the gluon fluctuation grows via quantum diffusion: $|\mathbf{r}_2 - \mathbf{r}_1| \simeq \sqrt{2\Delta t/\omega}$. However, when Δt approaches $\tau_{\text{br}}(\omega)$, the effects of the interactions become non-perturbative. Via the Gaussian in Eq. (4.65), they restrict the further growth of the transverse separation $B_\perp \equiv \max(|\mathbf{r}_2 - \mathbf{R}|, |\mathbf{r}_1 - \mathbf{R}|)$ to values $B_\perp \lesssim 2/k_{\text{br}}(\omega)$, in agreement with Eq. (4.32). For even larger time separations $\Delta t \gtrsim \tau_{\text{br}}(\omega)$, we can use

$$\frac{1}{2\sinh \Omega\Delta t} \simeq e^{-\Omega\Delta t} \propto e^{-\Delta t/\sqrt{2}\tau_{\text{br}}}, \quad (4.68)$$

showing that the long-lived gluon fluctuations are exponentially suppressed. Note that this behaviour at large Δt is non-analytic in \hat{q} , so it indeed arises from resumming the perturbative series to all orders.

To summarize, the effect of multiple scattering is to limit the lifetime and the transverse size of a gluon fluctuation with energy ω to values $\Delta t \lesssim \tau_{\text{br}}(\omega)$ and respectively $B_\perp \lesssim 2/k_{\text{br}}(\omega)$. Moreover, since the perturbative expansion of Eq. (4.65) is truly an expansion in powers of $\Delta t/\tau_{\text{br}}(\omega)$ and $B_\perp k_{\text{br}}(\omega)$, it is clear that the single scattering approximation — which corresponds to the first non-trivial term in this expansion — is valid only for fluctuations which are hard enough (in the sense of having a sufficiently large transverse momentum) for $\Delta t \ll \tau_{\text{br}}(\omega)$ and $B_\perp \ll 1/k_{\text{br}}(\omega)$. These conditions have been often used in the previous discussion in this section.

Using the explicit expression for the path integral in Eq. (4.65), it is in principle possible the fully evaluate the r.h.s. of Eq. (4.24) and thus compute the leading-order radiative correction to the dipole amplitude beyond the double-logarithmic approximation. In general this calculation is hindered by the complexity of the time integrations. In Ref. [9], this calculation has been pushed to *single* logarithmic accuracy — that is, one has explicitly evaluated the subleading correction to \hat{q} of order $\bar{\alpha} \ln(L/\lambda)$. Note that Eq. (4.65) explicitly includes the ‘virtual’ term that has been added by hand in the respective calculation in Ref. [9].

5 The high-energy evolution of the radiative energy loss

In the previous section, we have studied the high-energy evolution of the transverse momentum broadening for an energetic quark propagating through a dense QCD medium. As well known, this physical problem is closely related to another one: the energy loss by an energetic parton via *medium-induced radiation*, that is, gluon emissions which are triggered by the interactions between the parent parton or the radiated gluon and the constituents of the medium. Within the high-energy kinematics of interest, the differential cross-section for such an emission involves Wilson line correlators which measure the color coherence between the emitter and its radiation. This coherence is progressively washed out via rescattering in the medium and thus is sensible to the physics of collisions, as encoded in \hat{q} . This relation is manifest at tree level, where any Wilson line correlator — the medium average of a gauge-invariant product of Wilson lines — can be expressed in terms of the ‘dipole cross-section’ (the exponent in Eq. (4.4)) and hence in terms of $\hat{q}^{(0)}$ (as defined in Eq. (4.6)). In what follows, we would like to demonstrate that this relation remains valid after including the effects of the high-energy evolution within the double-logarithmic approximation. That is, to compute the radiative energy loss in the presence of radiative corrections and to DLA accuracy, one can use the same formulæ as at tree level, but with $\hat{q}^{(0)}$ replaced by the solution $\hat{q}_L(Q_s^2)$ to Eq. (4.42). A similar conclusion has been independently obtained in Ref. [53].

5.1 The tree-level approximation: the BDMPSZ formalism

To start with, let us briefly review the relevant formalism at tree-level, namely the BDMPSZ calculation of medium-induced gluon radiation [42–52].

We consider the emission of a single gluon by an asymptotic quark and assume, for simplicity, that the incoming quark is energetic enough to be treated in the eikonal approximation. On the other hand, the eikonal approximation cannot be used for the emitted gluon, because the transverse diffusion plays an essential role for the gluon formation. The energy lost by the quark is the energy taken away by the emitted gluon and can be computed from the respective spectrum as

$$\Delta E = \int_0^{\omega_c} dk^+ k^+ \frac{dN_g}{dk^+} = \int_0^{\omega_c} dk^+ \int d^2\mathbf{k} k^+ \frac{dN_g}{dk^+ d^2\mathbf{k}}. \quad (5.1)$$

The upper cutoff ω_c stems from the fact that only gluons with energies $k^+ < \omega_c$ can be emitted via the mechanism at hand (see below). Moreover, the spectrum $k^+(dN_g/dk^+)$ of the radiated gluons is such that the integral over k^+ in Eq. (5.1) is dominated by this upper cutoff. Accordingly, in what follows we shall focus on the emission of relatively hard gluons, with $k^+ \sim \omega_c$.

As before, we assume that the medium correlations at tree-level are Gaussian and local in x^+ . Under these assumptions, one can deduce the following formula for the spectrum of the medium-induced gluon radiation [48] (see also Refs. [1, 4, 5, 73, 74] for pedagogical discussions)

$$k^+ \frac{dN_g}{dk^+ d^2\mathbf{k}} = \frac{\alpha_s C_F}{2\pi^2} \frac{1}{(k^+)^2} \text{Re} \int_{-\infty}^{\infty} dx^+ \int_{-\infty}^{x^+} dy^+ \times \int d^2\mathbf{x} e^{-i\mathbf{k}\cdot\mathbf{x}} \mathcal{S}_{L,x^+}^{\text{adj}}(\mathbf{x}) \partial_{\mathbf{x}}^i \partial_{\mathbf{y}}^j \mathcal{K}(x^+, \mathbf{x}; y^+, \mathbf{y}; k^+) \Big|_{\mathbf{y}=0}. \quad (5.2)$$

As announced, we consider an on-shell (or ‘asymptotic’) quark which enters the medium coming from far away¹⁹. Eq. (5.2) is a cross-section, so it is obtained by multiplying the direct amplitude (DA) times the complex conjugate amplitude (CCA), as illustrated in Fig. 4. The time variables y^+ and x^+ are the emission times in the DA and respectively the CCA, so their difference $\Delta x^+ = x^+ - y^+$ is indicative of the formation time. We have chosen $x^+ > y^+$ and multiplied the result by 2 to account for the opposite time ordering. Also, $\mathbf{x}_0 = 0$ is the transverse position of the quark, which remains unchanged during the process (eikonal approximation) and is the same in the DA and the CCA (since we do not measure the transverse momentum broadening of the quark). In writing Eq. (5.2), we have already set $\mathbf{x}_0 = 0$, but in the subsequent discussion we shall keep the notation \mathbf{x}_0 at intermediate stages, for more clarity. On the other hand, the transverse momentum of the emitted gluon *is* measured, so the respective transverse coordinates are different in the DA and the CCA. Their difference is denoted as \mathbf{x} in Eq. (5.2) and it is conjugated to the transverse momentum \mathbf{k} via the Fourier transform. With these differences in mind, Eq. (5.2) is quite similar to Eq. (4.22) for the emission of a *virtual* gluon and can be read by analogy with the latter.

Once again, the locality of the medium correlations in x^+ has allowed us to factorize the process into three stages, like in Eq. (4.15), and thus express the cross-section for gluon radiation in terms of scattering amplitudes for effective dipoles (see Fig. 5 for an illustration of this representation) :

(i) *Prior to the first gluon emission, i.e. for time values smaller than y^+* : The Wilson lines describing the color precession of the quark mutually cancel between the DA and the CCA, by unitarity. Accordingly, there is no imprint of this first stage on the cross-section in Eq. (5.2).

(ii) *During the formation time, i.e. for time values between y^+ and x^+* : The partonic system consists in a quark-gluon pair in the DA and the original quark in the CCA. The relevant Wilson line correlator reads

$$\begin{aligned} \left\langle U_{x^+y^+}^{\dagger ab}[\mathbf{u}] \frac{\text{tr}}{N_c} \left(t^a V_{x^+y^+}^{\dagger}(\mathbf{x}_0) t^b V_{x^+y^+}(\mathbf{x}_0) \right) \right\rangle &= \frac{1}{2N_c} \left\langle \text{Tr} U_{x^+y^+}^{\dagger}[\mathbf{u}] U_{x^+y^+}(\mathbf{x}_0) \right\rangle \\ &= C_F \mathcal{S}_{x^+,y^+}^{\text{adj}}([\mathbf{u}], \mathbf{x}_0), \end{aligned} \quad (5.3)$$

where t^a and t^b are color matrices at the emission vertices, $\mathbf{u}(t)$ represents the trajectory of the gluon in the DA for times $y^+ \leq t \leq x^+$, and \mathcal{S}^{adj} is the average S -matrix for a color dipole in the adjoint representation,

$$\mathcal{S}_{x^+,y^+}^{\text{adj}}(\mathbf{x}, \mathbf{y}) \equiv \frac{1}{N_c^2 - 1} \left\langle \text{Tr} U_{x^+y^+}^{\dagger}(\mathbf{x}) U_{x^+y^+}(\mathbf{y}) \right\rangle. \quad (5.4)$$

The dipole in Eq. (5.3) is built with one adjoint Wilson line for the emitted gluon and another one for the precession of the color current of the quark (a color vector in the adjoint representation). The ‘dipole propagator’ $\mathcal{K}(x^+, \mathbf{x}; y^+, \mathbf{y}; k^+)$ which enters Eq. (5.2) represents the functional average of the Wilson line correlator (5.3) over the quantum trajectories of the gluon:

$$\mathcal{K}(x^+, \mathbf{x}; y^+, \mathbf{y}; k^+) = \int [\mathcal{D}\mathbf{u}] e^{i \frac{k^+}{2} \int_{y^+}^{x^+} dt \mathbf{u}^2(t)} \mathcal{S}_{x^+,y^+}^{\text{adj}}([\mathbf{u}(t)], \mathbf{x}_0), \quad (5.5)$$

with boundary conditions $\mathbf{u}(y^+) = \mathbf{y}$ and $\mathbf{u}(x^+) = \mathbf{x}$.

¹⁹The case of an off-shell quark which is produced by a hard process occurring at some finite time x_0^+ can be obtained by replacing $-\infty \rightarrow x_0^+$ in the lower limits of the time integrations in Eq. (5.2).

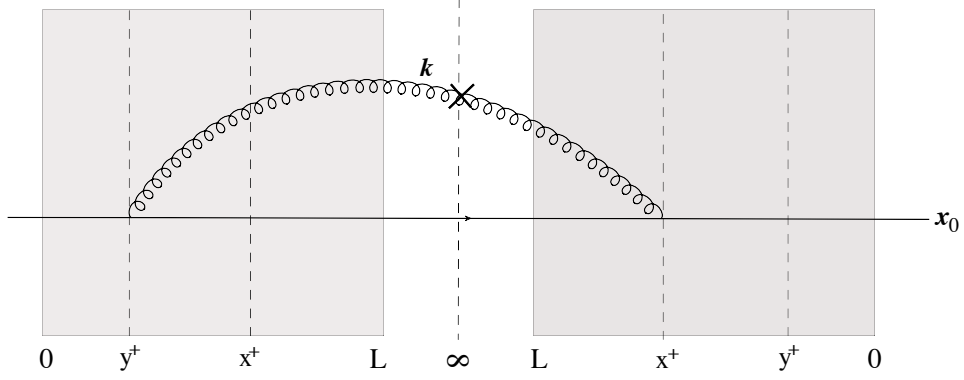


Figure 4. Feynman graph contributing to the cross-section for producing a gluon with 3-momentum $k = (k^+, \mathbf{k})$, as computed in Eq. (5.2). The l.h.s. corresponds to the DA and the r.h.s. to the CCA. Both emissions times y^+ and x^+ are chosen inside the medium, $0 < y^+ < x^+ < L$, since this is the most interesting configuration for our present purposes.

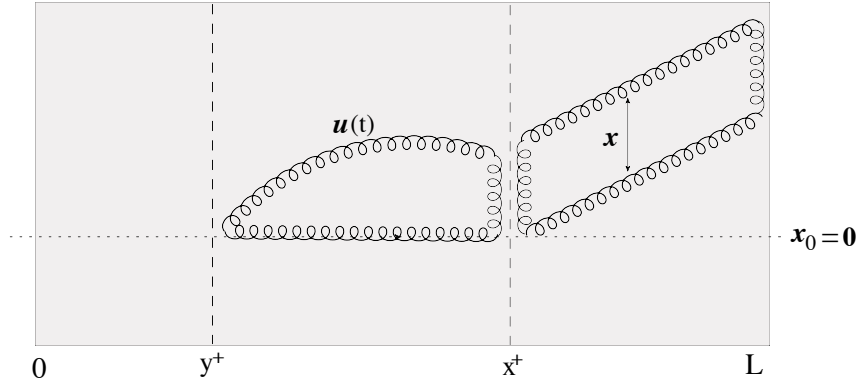


Figure 5. Alternative representation for the cross-section in Fig. 4, in terms of dipole amplitudes, which is obtained after performing the medium average in the Gaussian approximation. The ‘vertical’ lines closing the two dipoles represent the sum over the color indices.

(iii) *After the gluon formation, i.e. for time values larger than x^+* : In this case too, the quark Wilson lines from the DA and the CCA mutually cancel, so we are left with two adjoint Wilson lines, which both refer to the emitted gluon (one for the DA, the other one for the CCA). These Wilson lines combine in the adjoint dipole $\mathcal{S}_{L,x^+}^{\text{adj}}(\mathbf{x} - \mathbf{x}_0)$, which describes the transverse momentum broadening acquired by the gluon after formation (so long as $x^+ < L$, of course). The *average* transverse size of this dipole is constant, due to the medium homogeneity in the transverse plane, and hence it is equal to its original value at time x^+ , which is $\mathbf{x} - \mathbf{x}_0 = \mathbf{x}$.

If one is not interested in the k_{\perp} -spectrum of the produced gluon, but only in the energy lost by the quark, then one can integrate Eq. (5.2) over \mathbf{k} and use $\mathcal{S}_{L,x^+}^{\text{adj}}(0) = 1$, to deduce

$$k^+ \frac{dN_g}{dk^+} = \frac{2\alpha_s C_F}{(k^+)^2} \text{Re} \int_{-\infty}^{\infty} dx^+ \int_{-\infty}^{x^+} dy^+ \partial_x^i \partial_y^i \mathcal{K}(x^+, \mathbf{x}; y^+, \mathbf{y}; k^+) \Big|_{\mathbf{x}=\mathbf{y}=0}. \quad (5.6)$$

To be more specific, consider the situation where the emission occurs within the medium in

both the DA and the CCA: $0 < y^+ < x^+ < L$. This situation yields the dominant contribution for sufficiently small energies $k^+ \ll \omega_c$, but the corresponding result can also be used when $k^+ \sim \omega_c$, at least for parametric estimates. Then the average dipole S -matrix in Eq. (5.3) can be computed as in Eqs. (4.4)–(4.6) and reads (we set $\mathbf{x}_0 = 0$ from now on)

$$\mathcal{S}_{x^+, y^+}^{\text{adj}}[\mathbf{u}] \simeq \exp \left\{ -\frac{1}{4} \int_{y^+}^{x^+} dt \hat{q}_g(1/u^2) \mathbf{u}^2(t) \right\}, \quad \hat{q}_g(Q^2) \equiv \frac{N_c}{C_F} \hat{q}(Q^2), \quad (5.7)$$

where the subscript ‘g’ in \hat{q}_g refers to ‘gluon’. (The quantity $\hat{q}(Q^2)$ without any subscript refers to a quark in the fundamental representation and has been introduced in Eq. (4.6).)

To compute the path integral in Eq. (5.5), we perform the ‘harmonic approximation’ in Eq. (5.7), that is, we replace $\hat{q}_g(1/u^2)$ with the constant quantity $\hat{q}_g(k_{\text{br}}^2)$, where $k_{\text{br}}^2(k^+) \equiv \sqrt{2k^+ \hat{q}_g}$ is the transverse momentum acquired by the gluon during formation. This approximation is appropriate for gluon emissions triggered by multiple soft scattering in the medium. Then the path integral yields

$$\mathcal{K}(x^+, \mathbf{x}; y^+, \mathbf{y}; k^+) = \frac{-i}{2\pi} \frac{k^+ \Omega}{\sinh \Omega \Delta \tau} \exp \left\{ \frac{i}{2} \frac{k^+ \Omega}{\sinh \Omega \Delta \tau} [(\mathbf{x}^2 + \mathbf{y}^2) \cosh \Omega \Delta \tau - 2 \mathbf{x} \cdot \mathbf{y}] \right\}, \quad (5.8)$$

where $\Delta \tau = x^+ - y^+$ and²⁰

$$\Omega = \frac{1+i}{\sqrt{2}} \frac{1}{\tau_{\text{br}}(k^+)}, \quad \tau_{\text{br}}(k^+) = \sqrt{\frac{2k^+}{\hat{q}_g}}. \quad (5.9)$$

It is now straightforward to evaluate the transverse derivatives in Eq. (5.6) and then perform the time integrals within the range $0 < y^+ < x^+ < L$. In this process, one must subtract the vacuum piece of Eq. (5.8), this is, its limit when $\hat{q}_g \rightarrow 0$: this would give a spurious contribution, which is moreover divergent. This procedure yields the BDMPSZ spectrum for soft energies $k^+ \ll \omega_c$:

$$k^+ \frac{dN_g}{dk^+} \simeq \frac{2\alpha_s C_F}{\pi} \sqrt{\frac{\omega_c}{2k^+}} \quad \text{with} \quad \omega_c = \frac{1}{2} \hat{q}_g L^2. \quad (5.10)$$

This result can be used to check that the integral in Eq. (5.1) is indeed dominated by its upper limit. The general result valid for any k^+ can be found in Refs. [44, 45, 47].

Concerning the k_{\perp} -spectrum, notice that the dominant dependence upon \mathbf{x} within the integrand of Eq. (5.2) is contained in the following product of two Gaussians:

$$\exp \left\{ \frac{i}{2} k^+ \Omega \coth \Omega \Delta \tau \mathbf{x}^2 \right\} \exp \left\{ -\frac{\hat{q}_g}{4} (L - x^+) \mathbf{x}^2 \right\}. \quad (5.11)$$

The first factor arises after letting $\mathbf{y} = 0$ in Eq. (5.8), while the second one is the two-gluon dipole $\mathcal{S}_{L, x^+}^{\text{adj}}(\mathbf{x})$ with \hat{q}_g evaluated at a momentum scale $\sim Q_s^2$. The transverse momentum spectrum obtained via the Fourier transform of the above is clearly Gaussian and peaked at a typical value

$$\langle k_{\perp}^2 \rangle \simeq \sqrt{2k^+ \hat{q}_g} + \hat{q}_g (L - x^+) \sim Q_s^2 \equiv \hat{q}_g L, \quad (5.12)$$

²⁰The current expressions for $\tau_{\text{br}}(k^+)$ and $k_{\text{br}}(k^+)$ are consistent with their respective definitions in Sect. 4 in view of the relation $\hat{q}_g \simeq 2\hat{q}$ valid at large N_c . (Recall that the discussion in Sect. 4 was carried mostly at large N_c .)

where Q_s^2 now denotes the *gluon* saturation momentum. In Eq. (5.12) we recognize the sum of the momentum broadening acquired via collisions during the formation time and that acquired after the formation. For $k^+ \sim \omega_c$, both contributions are parametrically of $\mathcal{O}(Q_s^2)$. More details on the k_\perp -spectrum can be found in Refs. [48, 49, 75].

Returning to Eq. (5.8), this can be used to read the characteristic scales for gluon formation. The r.h.s. of Eq. (5.8) is exponentially suppressed for time separations $\Delta\tau \gg \tau_{\text{br}}$ and for transverse separations $(\mathbf{x} - \mathbf{x}_0)^2 \gg 1/k_{\text{br}}^2$ (recall that we set $\mathbf{x}_0 = 0$). Accordingly, the emission of a gluon with energy k^+ via the present mechanism takes a time of order $\tau_{\text{br}}(k^+)$. Also, the maximal transverse separation between the emitted gluon and its parent parton is of order $1/k_{\text{br}}(k^+)$. When $k^+ \sim \omega_c$, as relevant for the calculation of the energy loss, these scales become $\tau_{\text{br}} \sim L$ and $1/k_{\text{br}} \sim 1/Q_s$ — that is, they are parametrically similar to those underlying the physics of transverse momentum broadening, as discussed in Sect. 4. Hence, no surprisingly, the respective discussions of the radiative corrections will be quite similar as well.

5.2 The dominant radiative corrections

Without loss of generality, we can restrict our discussion of the evolution to the case where the gluon with longitudinal momentum $k^+ \sim \omega_c$ (the one which is responsible for the energy loss) is emitted inside the medium, in both the direct and the complex conjugate amplitudes. (Indeed this case is the most complicated one, in terms of medium interactions.) We keep the same conventions as before: the gluon is first emitted in the DA, at time y^+ , and then in the CCA, at time x^+ .

As in Sect. 4, we assume that the high-energy evolution preserves the Gaussian nature of the medium correlations, cf. Eq. (4.14). It is then quite clear that this evolution will also preserve the factorization of the cross-section into the three stages discussed in Sect. 5.1. This is so because the relevant quantum fluctuations are short-lived: their coherence time $\tau_{\text{coh}} = 2\omega/p_\perp^2$ is much shorter than the typical duration of any of these three stages. As before, in Sect. 4, the variables ω and p_\perp denote the ‘energy’ (in the sense of p^+) and the transverse momentum of the evolution gluon, and the most interesting situation is such that $\omega \ll k^+$ and $p_\perp \ll Q_s$. In this situation, the quantum fluctuations which overlap with two different stages (and thus could break down the factorization) are suppressed by the smallness of their longitudinal phase-space.

Consider e.g. a fluctuation where the soft gluon is emitted by the quark at some time $t_1 < y^+$ and then absorbed by either the quark or the nascent gluon at some time t_2 during the ‘formation’ stage ($y^+ < t_2 < x^+$). This fluctuation has a lifetime $t_2 - t_1 \sim \tau_{\text{coh}}$, so both t_1 and t_2 must lie within an interval $\sim \tau_{\text{coh}}$ around y^+ . Accordingly, the respective longitudinal phase-space is of order τ_{coh}^2 and thus is much smaller than that, of order $(x^+ - y^+)\tau_{\text{coh}}$, corresponding to fluctuations which fully develop during the formation time ($y^+ < t_1 < t_2 < x^+$). We have indeed $x^+ - y^+ \sim \tau_{\text{br}}(k^+) \gg \tau_{\text{coh}}(\omega)$ for $\omega \ll k^+$. This discussion implies that the cross-section for medium-induced radiation can still be given the factorized structure in Eq. (5.2), but with the individual factors generally modified by radiative corrections.

With reference to Eq. (5.2), it is quite obvious that the evolution has no influence on the first stage at $t < y^+$, i.e. prior to the emission of the nascent gluon in the DA. During that stage, the quarks in the DA and the CCA make up a zero-size ‘dipole’, which does not interact, so its high-energy evolution cannot be measured. It is furthermore clear that the main effect of the evolution during the last stage at $t > x^+$ (after gluon formation) is to renormalize the jet quenching parameter within the two-gluon dipole amplitude $\mathcal{S}_{L,x^+}^{\text{adj}}(\mathbf{x})$, in the way explained in Sect. 4.3.2 :

to double-logarithmic accuracy, the renormalized adjoint dipole S -matrix reads

$$\mathcal{S}_{L,x^+}^{\text{adj}}(\mathbf{x}) \simeq \exp \left\{ -\frac{1}{4} \hat{q}_g(L, Q_s^2)(L - x^+) \mathbf{x}^2 \right\}, \quad (5.13)$$

with $\hat{q}_g(L, Q_s^2)$ the solution to Eq. (4.42) for $Q_s^2 = \hat{q}_g L$. This differs from the corresponding quark transport coefficient merely by a color factor: $\hat{q}_g(L, Q_s^2) = (N_c/C_F)\hat{q}_L(Q_s^2)$. In choosing the scales for \hat{q}_g above, we have used the fact that, parametrically, $L - x^+ \sim L$ and $x_\perp^2 \sim 1/Q_s^2$.

As compared to Sect. 4, the only situation which is somewhat new is when the fluctuation lives during the formation time of the radiated gluon. This is new since, unlike in Sect. 4, we do not assume anymore the eikonal approximation for the evolving dipole : the trajectory $\mathbf{u}(t)$ of the nascent gluon, which is the same as the size of the effective dipole (since the quark is fixed at $\mathbf{x}_0 = 0$), is randomly varying via transverse diffusion. Yet, this transverse motion looks relatively slow on the typical time scale for quantum fluctuations (since the respective ‘transverse mass’ k^+ is comparatively hard), so we expect some kind of ‘adiabatic approximation’ to be applicable for the fluctuations. This will be detailed in what follows.

The respective evolution equation is obtained as in Sect. 4.2, that is, by first acting with the Hamiltonian ΔH on the (adjoint) dipole scattering operator $\hat{S}_{x^+,y^+}^{\text{adj}}[\mathbf{u}]$ and then performing the medium average within the Gaussian approximation (4.14). This procedure implies

$$\mathcal{S}_{x^+,y^+}^{\text{adj}}([\mathbf{u}]; \omega) = \exp \left\{ -g^2 N_c \int_{y^+}^{x^+} dt \Gamma_\omega(\mathbf{u}(t)) \right\} \quad (5.14)$$

with the function $\Gamma_\omega(\mathbf{r})$ now obeying (compare to Eq. (4.24))

$$\begin{aligned} \int_{y^+}^{x^+} dt \frac{\partial \Gamma_\omega(\mathbf{u}(t))}{\partial \omega} &= \frac{1}{4\pi\omega^3} \int_{y^+}^{x^+} dt_2 \int_{y^+}^{t_2} dt_1 \partial_{\mathbf{r}_1}^i \partial_{\mathbf{r}_2}^i \left\{ \int [\mathcal{D}\mathbf{r}] e^{i\frac{\omega}{2} \int_{t_1}^{t_2} dt' \mathbf{r}^2(t')} \right. \\ &\quad \left. \times \left[e^{-\frac{g^2 N_c}{2} \int_{t_1}^{t_2} dt (\Gamma_\omega(\mathbf{u}(t) - \mathbf{r}(t)) + \Gamma_\omega(\mathbf{r}(t)) - \Gamma_\omega(\mathbf{u}(t)))} - 1 \right] \right\} \Bigg|_{\mathbf{r}_2=0}^{\mathbf{r}_2=\mathbf{u}(t_2)} \Bigg|_{\mathbf{r}_1=0}^{\mathbf{r}_1=\mathbf{u}(t_1)}. \end{aligned} \quad (5.15)$$

Within the present approximations, these equations hold for arbitrary N_c . The main difference w.r.t. Eq. (4.24) is the fact that the endpoints \mathbf{r}_1 and \mathbf{r}_2 of the path integral in Eq. (5.15) (i.e. the transverse positions of the virtual gluon at the emission points) are time-dependent whenever they refer to emissions by the nascent gluon.

Once again, we are mostly interested in the situation where the partonic system created by the fluctuation scatters only once in the medium. This is illustrated in Fig. 6 and is described by the linearized version of Eq. (5.15), as obtained by expanding the exponential. After manipulations similar to those in Sect. 4.3, this can be written as (cf. Eq. (4.27))

$$\begin{aligned} \int_{y^+}^{x^+} dt \frac{\partial \Gamma_\omega(\mathbf{u}(t))}{\partial \omega} &= -\frac{\alpha_s N_c}{2} \frac{1}{\omega^3} \int_{y^+}^{x^+} dt \int d^2\mathbf{z} \left[\Gamma_\omega(\mathbf{u}(t) - \mathbf{z}) + \Gamma_\omega(\mathbf{z}) - \Gamma_\omega(\mathbf{u}(t)) \right] \\ &\quad \times \int_{y^+}^t dt_1 \int_t^{x^+} dt_2 \partial_{\mathbf{r}_1}^i \partial_{\mathbf{r}_2}^i \left\{ \mathcal{G}_0(t_2 - t, \mathbf{r}_2 - \mathbf{z}; \omega) \mathcal{G}_0(t - t_1, \mathbf{z} - \mathbf{r}_1; \omega) \right\} \Bigg|_{\mathbf{r}_2=0}^{\mathbf{r}_2=\mathbf{u}(t_2)} \Bigg|_{\mathbf{r}_1=0}^{\mathbf{r}_1=\mathbf{u}(t_1)}, \end{aligned} \quad (5.16)$$

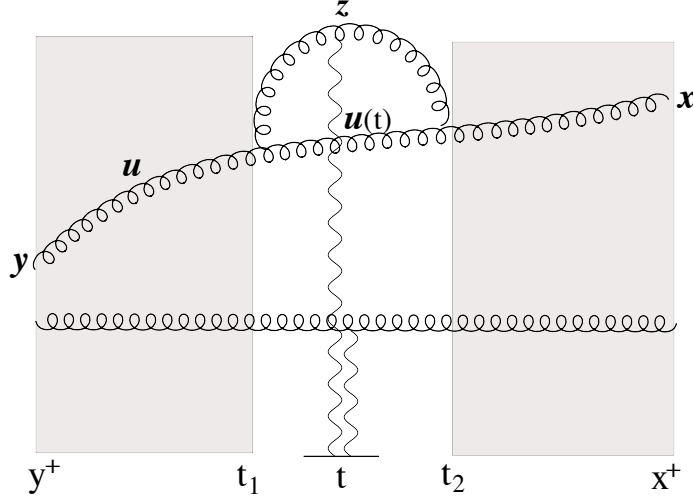


Figure 6. A diagram contributing to the evolution of a non-eikonal dipole, as described by Eq. (5.16). The evolving dipole lives fully inside the medium ($0 < y^+ < x^+ < L$). The grey areas prior and after the fluctuation are regions of multiple scattering. During the lifetime of the fluctuation, between t_1 and t_2 , the partonic system (effectively made with three gluons) scatters only once, at some intermediate time t .

where we recall that \mathbf{z} denotes the position of the virtual gluon at the interaction time t , with $t_1 < t < t_2$. For the corresponding equation in Sect. 4.3, we have been able to explicitly perform the integrals over t_1 and t_2 . Here, however, these integrals are complicated by the time dependence of the endpoints \mathbf{r}_1 and \mathbf{r}_2 . To overcome this difficulty, we shall exploit the separation of time scales between the radiated gluon with energy k^+ and the virtual one with energy $\omega \ll k^+$. During the lifetime $\Delta t \equiv t_2 - t_1 \lesssim \tau_{\text{br}}(\omega)$ of the fluctuation, the transverse position of the hard gluon changes by an amount

$$\Delta u_{\perp}^2 \sim \frac{2\Delta t}{k^+} \lesssim \frac{2\tau_{\text{br}}(\omega)}{k^+}, \quad (5.17)$$

which is small compared to the typical separation $\langle u_{\perp}^2 \rangle \simeq 4/k_{\text{br}}^2 (k^+)$ between the hard gluon and the quark :

$$\frac{\Delta u_{\perp}^2}{\langle u_{\perp}^2 \rangle} \sim \frac{\tau_{\text{br}}(\omega)}{\tau_{\text{br}}(k^+)} \sim \sqrt{\frac{\omega}{k^+}} \ll 1. \quad (5.18)$$

Hence, when evaluating the endpoints \mathbf{r}_1 and \mathbf{r}_2 in Eq. (5.16), one can neglect the small difference between $\mathbf{u}(t_2)$ and $\mathbf{u}(t_1)$ and approximate them both with the intermediate value $\mathbf{u}(t)$ (the transverse size of the parent dipole at the interaction time). Then the integrals over t_1 and t_2 can be done as in Eq. (4.28), and one is led to

$$\int_{y^+}^{x^+} dt \omega \frac{\partial \Gamma_{\omega}(\mathbf{u}(t))}{\partial \omega} = \frac{\bar{\alpha}}{2\pi} \int_{y^+}^{x^+} dt \int_{\mathbf{z}} \frac{\mathbf{u}^2(t)}{(\mathbf{z} - \mathbf{u}(t))^2 z^2} \left[\Gamma_{\omega}(\mathbf{u}(t) - \mathbf{z}) + \Gamma_{\omega}(\mathbf{z}) - \Gamma_{\omega}(\mathbf{u}(t)) \right]. \quad (5.19)$$

This holds for generic values of the integration limits y^+ and x^+ (recall that these variables are themselves integrated over in Eq. (5.2)), hence it must hold *locally* in t :

$$\omega \frac{\partial \Gamma_{\omega}(\mathbf{u}(t))}{\partial \omega} = \frac{\bar{\alpha}}{2\pi} \int_{\mathbf{z}} \frac{\mathbf{u}^2(t)}{(\mathbf{z} - \mathbf{u}(t))^2 z^2} \left[\Gamma_{\omega}(\mathbf{u}(t) - \mathbf{z}) + \Gamma_{\omega}(\mathbf{z}) - \Gamma_{\omega}(\mathbf{u}(t)) \right]. \quad (5.20)$$

This is recognized as the BFKL equation for a dipole with time–dependent transverse size $\mathbf{u}(t)$. As clear from its above derivation, this equation is valid so long as the relative change in $\mathbf{u}(t)$ remains negligible during the lifetime of the typical fluctuations.

In particular, the time–dependence of $\mathbf{u}(t)$ is irrelevant for the double–logarithmic approximation that we are primarily interested in. As explained in Sect. 4.3.2, this is controlled by fluctuations with relatively large transverse sizes, which are only logarithmically sensitive to the parent dipole size. At DLA, Eq. (5.20) reduces to an equation like Eq. (4.42) which describes the evolution of the jet quenching parameter $\hat{q}_g(\tau, Q^2)$ with the longitudinal (τ) and transverse (Q^2) resolution scales. For the problem at hand, the relevant scales are $\tau = \tau_{\text{br}}(k^+)$ (the formation time for the radiated gluon) and $Q^2 = k_{\text{br}}^2(k^+) = \hat{q}_g \tau_{\text{br}}(k^+)$ (the transverse momentum squared acquired by this gluon during formation). Hence, the leading–order radiative correction reads (compare to Eq. (4.41))

$$\delta\hat{q}_g^{(1)} = \hat{q}_g^{(0)} \frac{\bar{\alpha}}{2} \ln^2 \frac{\tau_{\text{br}}(k^+)}{\lambda} = \hat{q}_g^{(0)} \frac{\bar{\alpha}}{8} \ln^2 \frac{k^+}{\omega_0}, \quad (5.21)$$

with $\omega_0 \equiv \hat{q}_g \lambda^2/2$. For the energy–loss problem, $k^+ \sim \omega_c$ and $\tau_{\text{br}}(k^+) \sim L$, hence we return to the original version of the logarithm, as appearing in Eqs. (4.41) or (4.46).

To summarize, the dominant effect of the radiative corrections on the calculation of medium–induced gluon radiation consists in the renormalization of the jet quenching parameter within the corresponding tree–level calculation. In particular, the energy loss by an energetic quark can be estimated as (cf. Eqs. (5.1) and (5.10))

$$\Delta E(L) = \kappa \frac{2\alpha_s C_F}{\pi} \omega_c^{\text{ren}} = \kappa \frac{\alpha_s C_F}{\pi} \hat{q}_g(L, Q_s^2) L^2, \quad (5.22)$$

where κ is a number of $\mathcal{O}(1)$ which is fully determined at tree–level. (Eq. (5.10) would predict $\kappa = \sqrt{2}$ but this value changes after using the correct version of the BDMPSZ spectrum, which remains valid when $k^+ \sim \omega_c$ [44, 45, 47].) We thus see that the radiative corrections have the effect to increase the value of the energy loss (via the corresponding increase in \hat{q}_g) and also to enhance its dependences upon the medium size L and its temperature $T = 1/\lambda$. In particular, if the medium is sufficiently large, one may approach the asymptotic scaling $\Delta E(L) \propto L^{2+\gamma_s}$ with $\gamma_s = 2\sqrt{\bar{\alpha}}$ the ‘saturation exponent’ introduced in Eq. (4.63). A similar observation is made in [53].

6 Conclusions and perspectives

In this paper we have developed the theory for the non–linear evolution of jet quenching and related phenomena to leading order in perturbative QCD at high energy. This theory can be viewed as a generalization of the BK–JIMWLK evolution for ‘dilute–dense’ scattering to the case of a target with an arbitrary longitudinal extent. This generalization is complicated by the need to go beyond the eikonal approximation in the treatment of multiple scattering and also to explicitly take into account the non–locality of the quantum fluctuations in time. Accordingly, the general evolution equations, such as the generalized BK equation (4.22), are extremely complicated and the construction of exact solutions appears to be prohibitive, except perhaps via numerical methods.

Fortunately, this theory allows for a drastic simplification in so far as the dominant radiative corrections are concerned: as originally noticed in Ref. [9], these corrections are enhanced by the double logarithm $\ln^2(L/\lambda)$ and they can be resummed to all orders by solving the relatively simple,

linear, equation (4.42), where the non-linear effects enter only via the restriction on the transverse phase-space for single scattering. This equation, which here emerges via controlled approximations from the generalized BK equation alluded to above, has also been obtained by directly computing the relevant Feynman graphs to DLA accuracy [9, 53].

One of our main results here is to explain the emergence of this remarkable simplification, which is the DLA, from a physical perspective. As we discuss in Sect. 4.4, this is a consequence of the special way how gluon saturation occurs in a medium: the saturation momentum $Q_s^2(x)$ is proportional to the longitudinal wavelength of the gluons and hence it increases very fast with $1/x$ already in the absence of the quantum evolution. This in turn implies that the transverse phase-space grows as fast as the longitudinal one when increasing the medium size L , thus favoring a double-logarithmic evolution.

Within this double-logarithmic approximation, the radiative corrections are sufficiently mild to be absorbed into a renormalization of the jet quenching parameter, which then evolves according to Eq. (4.42). Here, we have demonstrated this property for two particular observables, the transverse momentum broadening and the radiative energy loss, which in the approximations of interest are both related to the scattering amplitude of a color dipole. It would be interesting to understand whether a similar property remains true in more general situations and for more complicated observables, which are also sensitive to other correlations of the Wilson lines, like the quadrupole. Examples in that sense include the calculation of the medium-induced gluon radiation beyond the eikonal approximation (for the parent parton) [45, 47, 52], the study of color (de)coherence for multi-gluon emissions inside a medium [74, 76–78], and the evolution of a jet via successive medium-induced parton branchings [68, 75, 79]. Some generalizations in that sense, notably to the problem of the jet evolution, will be presented in [53].

It would be furthermore interesting to have a deeper understanding of the systematics of the *single-logarithmic* corrections, i.e. the terms of order $\bar{\alpha} \ln(L/\lambda)$, or $\bar{\alpha} \ln(1/x)$, in the evolution equations. As discussed in Sect. 4.5, the situation is quite different in that respect from the BK–JIMWLK evolution: the individual terms in the multiple scattering series are not separately enhanced by a large logarithm $\ln(1/x)$, yet they contribute to leading-logarithmic accuracy in a *non-perturbative* way — their resummation limits the phase-space for the single scattering approximation. It is not clear to us whether, in this context, it is possible or even useful to explicitly isolate the terms enhanced by $\ln(1/x)$ within the evolution equations.

An obviously important, open, problem refers to the inclusion of perturbative corrections of higher loop order, such as the running of the QCD coupling. As noticed in Sect. 4.4, the leading order correction to the saturation exponent is quite large for realistic values of α_s , a situation which generally signals the importance of higher-order corrections. A similar problem occurs for the saturation exponent of a shockwave and in that case we know that the resummation of higher-order effects drastically reduces the leading-order estimate (roughly by a factor of 3) [80, 81]. The calculation of the NLO corrections to the BK–JIMWLK equations has just been completed [82, 83], but the corresponding program for the physics of jet quenching is still awaiting.

Also, it would be important to develop numerical techniques for attacking functional evolution equations like the generalized BK equation (4.22). The original BK equation turned out to be a formidable tool for the phenomenology of particle production in pp , pA , and even AA collisions (especially after being supplemented with running coupling effects) [33, 84], and it would be very useful to dispose of a similar tool for the phenomenology of jet quenching.

Last but not least, it is interesting to notice the convergence between some of the present results at weak coupling, e.g. the saturation exponent for the plasma, or the L -dependence of the renormalized \hat{q} and of the energy loss, and the corresponding results at strong coupling²¹ [69–71, 87–89]. One may view this as merely a coincidence, but we do not believe so: as discussed in Refs. [70, 71], the dominant mechanism for transverse momentum broadening in a strongly coupled plasma is the recoil associated with medium-induced radiation. (That is, at strong coupling, the same mechanism is responsible for both energy loss and momentum broadening.) The perturbative corrections that we have considered here at weak coupling are themselves associated with radiation, so their inclusion naturally interpolates towards the physical scenario expected at strong coupling. And indeed, the present perturbative results, which as we have seen predict a (global) saturation momentum $Q_s^2(L) = \hat{q}(L)L \propto L^{1+\gamma_s}$ and an energy loss $\Delta E(L) \propto L^{2+\gamma_s}$ with $\gamma_s = 2\sqrt{\alpha}$, suggest a relatively smooth approach towards the respective trends at strong coupling, namely $Q_s^2(L) \propto L^2$ [69, 71] and respectively $\Delta E(L) \propto L^3$ [70, 71, 87–89]. It remains to be seen whether such a smooth convergence survives after including higher order perturbative corrections.

Acknowledgments

I am grateful to Al Mueller for many insightful discussions, for repeatedly reading the manuscript, and for helping me clarifying some of the arguments. During the gestation of this work, I have benefited from many inspiring discussions with my colleagues in Saclay, Jean-Paul Blaizot, Fabio Dominguez, Yacine Mehtar-Tani, and Bin Wu. This research is supported by the European Research Council under the Advanced Investigator Grant ERC-AD-267258. All figures were made with Jaxodraw [90].

A A succinct derivation of the evolution Hamiltonian

In this Appendix, we shall explicitly perform one step in the high energy evolution of the projectile S -matrix and show that the result is indeed equivalent to acting with the Hamiltonian (2.4) on the original S -matrix operator.

The precise nature of the projectile is irrelevant for the present purposes. It suffices to say that, in some given frame where the target has rapidity²² Y_T and the projectile has rapidity Y_P , with $Y_T + Y_P = Y$ (the total rapidity separation between the projectile and the target), the S -matrix is represented by some color-singlet operator $\hat{\mathcal{O}}_{Y_P}[A^-]$, which is built with Wilson lines (one for each partonic constituent of the projectile) and thus depends upon the target field A^- . The actual structure of this operator can be quite complicated, as it reflects the evolution of the projectile wavefunction over the rapidity interval Y_P . The *average* S -matrix, which is the physical observable, is obtained by averaging $\hat{\mathcal{O}}_{Y_P}[A^-]$ over all the realizations of the random field A^- , according to the CGC weight function $W_{Y_T}[A^-]$ (see e.g. [32, 33]):

$$\langle \hat{\mathcal{O}} \rangle_Y = \int [DA^-] W_{Y_T}[A^-] \hat{\mathcal{O}}_{Y_P}[A^-]. \quad (\text{A.1})$$

²¹More precisely, we mean here the results concerning the energy loss and momentum broadening of *light* partons, which is the most interesting case in the high-energy limit. For a more general survey of the related AdS/CFT literature, including the important case of a heavy quark, we refer to the review papers [85, 86].

²²Strictly speaking, the rapidity of the target — a left-mover — is negative with our present conventions, but here we shall reserve the notation Y_T for the positive quantity $|Y_T|$.

As indicated by the notations above, the physical S -matrix depends only upon the total rapidity separation Y , by boost invariance. The CGC weight function $W_{Y_T}[A^-]$ is a functional probability density for the target field A^- , which encodes the relevant information about the target wavefunction (including its high-energy evolution up to rapidity Y_T) in the approximations of interest. Eq. (A.1) expresses the CGC factorization of the high-energy evolution between the projectile and the target, for a dense-dilute scattering. Strictly speaking, this factorization has been established [33] only for the case where the target is a large nucleus localized near $x^+ = 0$ (a ‘shockwave’), but the results of this paper demonstrate that it also holds for a target with a finite, possibly large, extent in x^+ . As a matter of facts, a factorization similar to Eq. (A.1), but with $W_{Y_T}[A^-]$ taken to be simply a Gaussian in A^- , has been used in several previous studies of jet quenching and energy loss, which however did not address the problem of the high-energy evolution of the observables.

To study this high-energy evolution, we shall now increase the rapidity difference Y by an amount ΔY , by boosting the projectile: $Y_P \rightarrow Y_P + \Delta Y$. To understand the physical consequences of this boost, let us first remind some general facts about the high-energy evolution:

(i) The wavefunction of the projectile with rapidity Y_P includes quanta — the valence partons and the relatively soft gluons produced via radiation — with longitudinal momenta p^+ within the strip $\Lambda_0 < p^+ < \Lambda_0 e^{Y_P}$. Here, Λ_0 is the infrared cutoff used to properly define the wavefunction (the softest longitudinal momentum that can be measured).

(ii) When the projectile is boosted by an amount ΔY , the already existing partons act as sources for the emission of additional gluons within the range $\Lambda_0 < p^+ < \Lambda_0 e^{\Delta Y}$. The new gluons are much softer than their sources (whose typical p^+ momenta are very large as compared to $\Lambda_0 e^{\Delta Y}$), so their emission can be computed in the eikonal approximation.

(iii) Albeit soft relative to their sources, the ‘evolution’ gluons are still fast enough as compared to the target, so their scattering off the latter can be described by Wilson lines.

(iv) The probability for a soft gluon emission within the range $\Lambda_0 < p^+ < \Lambda_0 e^{\Delta Y}$ is of order $\bar{\alpha} \Delta Y$, with $\bar{\alpha} \equiv \alpha_s N_c / \pi$. Hence, by keeping $\Delta Y \ll 1/\bar{\alpha}$, one can ensure that there is only one additional gluon emission, which can be treated in perturbation theory.

In particular, the above discussion shows that, when $\alpha_s Y_P \ll 1$, the high-energy evolution of the projectile is negligible, so the associated wavefunction reduces to the valence partons. One then speaks about a ‘bare’ projectile, like a $q\bar{q}$ color dipole, whose S -matrix operator is relatively simple (recall Eq. (2.2)). Conversely, a projectile with $Y_P \gtrsim 1/\bar{\alpha}$ has generally a complicated structure, including a large number of soft gluons, which increases exponentially with Y_P .

After such general considerations, let us return to the high-energy evolution of Eq. (A.1) under the boost $Y_P \rightarrow Y_P + \Delta Y$ of the projectile, with $\bar{\alpha} \Delta Y \ll 1$. This is obtained by inserting into Eq. (A.1) a path integral describing the quantum gluons with longitudinal momenta within the range $\Lambda_0 < |p^+| < \Lambda_0 e^{\Delta Y}$, together with their eikonal couplings to their sources (the partons already included in the structure of $\hat{\mathcal{O}}_{Y_P}$) and also to the target :

$$\langle \hat{\mathcal{O}} \rangle_{Y+\Delta Y} = \int [DA^-] W_{Y_T}[A^-] Z_{\Delta Y}^{-1} \int_{\Delta Y} [Da^\mu] \delta(a^+) e^{iS_0[a^\mu; A^-]} \hat{\mathcal{O}}_{Y_P}[A^- + a^-]. \quad (\text{A.2})$$

Here $a_a^\mu(x)$ are the gauge fields describing the soft quantum fluctuations. The path integral is written in the projectile light-cone gauge $a^+ = 0$. The effective action $S_0[a^\mu; A^-]$ is obtained by keeping only the terms quadratic in a^μ in the expansion of the Yang-Mills action $S_{YM}[A^\mu + a^\mu]$

around the background field $A^\mu = \delta^{\mu-} A^-$:

$$S_0[a^\mu; A^-] = \frac{1}{2} \int d^4x \left[a^i (-D^2) a^i + (\partial^+ a^- + \partial_i a^i)^2 \right], \quad (\text{A.3})$$

where $D^2 = 2\partial^+ D^- - \nabla_\perp^2$, with $D^- = \partial^- - igA^-$ (the covariant derivative built with the background field), and we recall that $\partial_i = \partial/\partial x^i = -\partial^i$. The action (A.3) is formally written as a 4-dimensional integral, but the integrand is homogeneous in x^- and it is understood that the integral over the corresponding modes p^+ is restricted to the strip $\Lambda_0 < |p^+| < \Lambda_0 e^{\Delta Y}$. The quadratic action (A.3) generates, as usual, the propagator $G^{\mu\nu}$ of the soft gluons in the background field and in the LC gauge $a^+ = 0$. Namely, Eq. (A.3) is tantamount to

$$iS_0[a^\mu; A^-] = -\frac{1}{2} \int_{\text{strip}} \frac{dp^+}{2\pi} \int_{x^+, y^+} \int_{\mathbf{x}, \mathbf{y}} a_b^\mu(x^+, \mathbf{x}, p^+) G_{\mu\nu}^{-1, bc}(x^+, \mathbf{x}; y^+, \mathbf{y}; p^+) a_c^\nu(y^+, \mathbf{y}, p^+), \quad (\text{A.4})$$

where $G^{\mu\nu}$ is the background-field gluon propagator in the LC gauge, to be constructed in Appendix B. The eikonal approximation for the interactions between the quantum gluons and the target is enforced by keeping within S_0 only the ‘large’ component A^- of the target field. Also, the fact that the soft emissions are treated in the eikonal approximation is manifest in the fact that the quantum gluons are coupled to their sources via a simple shift $A^- \rightarrow A^- + a^-$ of the functional argument of the S -matrix $\hat{\mathcal{O}}_{Y_P}$; that is, the relatively fast partons included in $\hat{\mathcal{O}}_{Y_P}$ couple to both the target field and the soft gluons to be emitted via Wilson lines. Finally, the normalization factor $Z_{\Delta Y}$ is given by a similar path integral, but without the factor $\hat{\mathcal{O}}_{Y_P}$.

In writing the action (A.3) we have ignored the self-interactions of the quantum gluons, which is indeed correct to leading order in α_s . As a bookkeeping, the target field is strong, $gA^- \sim \mathcal{O}(1)$, and must be treated exactly, whereas the quantum fields are weak, $ga^\mu \ll 1$, and should be expanded out in perturbation theory. For consistency, one should also expand the scattering operator $\hat{\mathcal{O}}_{Y_P}[A^- + a^-]$ in powers of a^- , up to quadratic order. (This is tantamount to considering a single gluon emission.) The linear term in this expansion vanishes after performing the path integral, whereas the second order term, proportional to G^{--} , expresses the change in the average S -matrix due to a soft gluon emission, to the accuracy of interest:

$$\langle \hat{\mathcal{O}} \rangle_{Y+\Delta Y} - \langle \hat{\mathcal{O}} \rangle_Y = \int [DA^-] W_{Y_T}[A^-] \Delta H \hat{\mathcal{O}}_{Y_P}[A^-]. \quad (\text{A.5})$$

We have recognized here the evolution ‘Hamiltonian’ ΔH according to its definition, Eq. (2.4), in which we identify $\Lambda \equiv \Lambda_0 e^{\Delta Y}$ and $x \equiv e^{-\Delta Y}$ (so that $x\Lambda = \Lambda_0$). Eq. (A.5), which can be rewritten in operator form as

$$\hat{\mathcal{O}}_{Y_P+\Delta Y}[A^-] - \hat{\mathcal{O}}_{Y_P}[A^-] = \Delta H \hat{\mathcal{O}}_{Y_P}[A^-], \quad (\text{A.6})$$

confirms that ΔH is indeed the right evolution operator.

Returning to Eq. (A.5), note that the functional derivatives implicit in ΔH can be integrated by parts and thus made to act on the CGC weight function $W_{Y_T}[A^-]$. Accordingly, the change in the average S -matrix can be alternatively associated with a *target* evolution, of the form

$$W_{Y_T+\Delta Y}[A^-] - W_{Y_T}[A^-] = \Delta H W_{Y_T}[A^-]. \quad (\text{A.7})$$

This is a consequence of boost invariance: one can increase the rapidity difference Y between the projectile and the target by either boosting the projectile, or by boosting the target in the opposite direction; both procedures should give the same evolution for the S -matrix.

B The background field gluon propagator

In this Appendix, we construct the background field gluon propagator in the light-cone gauge $A^+ = 0$ and collect some related formulæ that were used in the main text. Our presentation will be brief since similar constructions can be found in the literature. (See e.g. Sect. 6 in Ref. [24] for a related discussion.) The propagator is defined as in Appendix A, that is,

$$\begin{aligned} G_{ab}^{\mu\nu}(x, y) &\equiv \langle \text{T } a_a^\mu(x) a_b^\nu(y) \rangle \\ &= Z^{-1} \int [Da^\mu] \delta(a^+) a_a^\mu(x) a_b^\nu(y) e^{iS_0[a^\mu; A^-]}, \end{aligned} \quad (\text{B.1})$$

where the symbol T refers to operator ordering in LC time (x^+) and $x^\mu = (x^+, x^-, \mathbf{x})$. It is implicitly assumed that the longitudinal momentum p^+ of the quantum fluctuations is restricted to the strip (2.5), whereas the background field $A^\mu = \delta^{\mu-} A^-$ carries no p^+ momentum (i.e. it is homogeneous in x^-). The action $S_0[a^\mu; A^-]$ is shown in Eq. (A.3) and is quadratic in the quantum fields a^μ . It is convenient to bring this action to a diagonal form, by replacing $a^- \rightarrow \tilde{a}^-$ with

$$\tilde{a}^-(x) \equiv a^-(x) + \frac{\partial^i}{\partial^+} a^i(x). \quad (\text{B.2})$$

Then the action becomes (we recall that $D^2 = 2\partial^+ D^- - \nabla_\perp^2$ and $D^- = \partial^- - igA^-$)

$$S_0[\tilde{a}^-, a^i; A^-] = \frac{1}{2} \int d^4x \left[a^i (-D^2) a^i + (\partial^+ \tilde{a}^-)^2 \right], \quad (\text{B.3})$$

which implies that the propagator G^{ij} of the transverse fields is the same as the ‘scalar’ propagator: $G^{ij} = \delta^{ij} G$, with $G_{ab}(x, y)$ obeying Eq. (2.9) (after a Fourier transform $x^- - y^- \rightarrow p^+$). Also,

$$\langle \text{T } \tilde{a}_a^-(x) \tilde{a}_b^-(y) \rangle = \delta_{ab} \int \frac{d^4p}{(2\pi)^4} e^{-ip \cdot (x-y)} \frac{i}{(p^+)^2}, \quad \langle \text{T } \tilde{a}_a^-(x) a_b^i(y) \rangle = 0. \quad (\text{B.4})$$

After inverting the transformation in Eq. (B.2), we finally obtain [in the mixed Fourier representation (\vec{x}, p^+) with $\vec{x} \equiv (x^+, \mathbf{x})$ and color indices suppressed]

$$\begin{aligned} G^{-i}(\vec{x}, \vec{y}; p^+) &= \frac{i}{p^+} \partial_{\vec{x}}^i G(\vec{x}, \vec{y}; p^+), & G^{i-}(\vec{x}, \vec{y}; p^+) &= -\frac{i}{p^+} \partial_{\vec{y}}^i G(\vec{x}, \vec{y}; p^+), \\ G^{--}(\vec{x}, \vec{y}; p^+) &= \frac{1}{(p^+)^2} \partial_{\vec{x}}^i \partial_{\vec{y}}^i G(\vec{x}, \vec{y}; p^+) + \frac{i}{(p^+)^2} \delta^{(3)}(\vec{x} - \vec{y}). \end{aligned} \quad (\text{B.5})$$

The propagator is to be considered with the Feynman prescription for the pole at the mass-shell. For instance, the free ($A^- = 0$) scalar propagator reads $G_{0,ab} = \delta_{ab} G_0$, with

$$G_0(p) = \frac{i}{2p^+ p^- - \mathbf{p}^2 + i\epsilon}, \quad (\text{B.6})$$

in momentum space. This implies e.g.

$$G_0^{--}(p) = \frac{\mathbf{p}^2}{(p^+)^2} G_0(p) + \frac{i}{(p^+)^2} = \frac{2p^-}{p^+} \frac{i}{2p^+ p^- - \mathbf{p}^2 + i\epsilon}, \quad (\text{B.7})$$

The ‘axial’ pole at $p^+ = 0$ needs no special prescription, since p^+ cannot vanish within the present context, as manifest on Eq. (2.5). The expression of the free propagator in mixed Fourier representation will also be useful:

$$G_0(t, \mathbf{x}; p^+) = \frac{1}{2p^+} [\theta(t)\theta(p^+) - \theta(-t)\theta(-p^+)] \int \frac{d^2\mathbf{p}}{(2\pi)^2} e^{i\mathbf{p}\cdot\mathbf{x}} e^{-i\frac{p^+}{2}t}. \quad (\text{B.8})$$

Note that modes with positive (negative) values of p^+ propagate forward (backward) in time.

A formal expression for the ‘scalar’ propagator, which is valid for an arbitrary background field but involves a path integral, has been presented in Eq. (2.10). Using this formal expression, we shall now to derive a fully explicit formula for the case where the target is a shockwave localized near $x^+ = 0$. When x^+ and y^+ are both positive, or both negative (i.e. they are on the same side of the shockwave), then the propagator in Eq. (2.10) reduces to the free propagator G_0 . Consider now the case where the gluon crosses the shockwave: $y^+ < 0$ and $x^+ > 0$. Then for a localized target field $A^-(t, \mathbf{z}) \sim \delta(t)$, one can approximate the Wilson line in Eq. (2.10) as

$$U_{x^+y^+}^\dagger[\mathbf{r}(t)] \simeq \text{P} e^{ig \int dt A^-(t, \mathbf{r}(0))} = \int d^2\mathbf{z} \delta^{(2)}(\mathbf{z} - \mathbf{r}(0)) \text{P} e^{ig \int dt A^-(t, \mathbf{z})}, \quad (\text{B.9})$$

and the path integral can be computed as follows:

$$\int [\mathcal{D}\mathbf{r}(t)] \exp \left\{ i \frac{p^+}{2} \int_{y^+}^{x^+} dt \dot{\mathbf{r}}^2(t) \right\} \delta^{(2)}(\mathbf{z} - \mathbf{r}(0)) = \mathcal{G}_0(x^+, \mathbf{x} - \mathbf{z}; p^+) \mathcal{G}_0(-y^+, \mathbf{z} - \mathbf{y}; p^+), \quad (\text{B.10})$$

where $\mathcal{G}_0 = 2p^+G_0$ is the free ‘reduced’ propagator. The last remaining case, where $y^+ > 0$ and $x^+ < 0$, can be deduced by using the symmetry property (2.11). One finally has

$$\begin{aligned} G(x^+, \mathbf{x}; y^+, \mathbf{y}; p^+) &= G_0(x^+ - y^+, \mathbf{x} - \mathbf{y}; p^+) [\theta(x^+)\theta(y^+) + \theta(-x^+)\theta(-y^+)] \\ &\quad + 2p^+ \int_{\mathbf{z}} G_0(x^+, \mathbf{x} - \mathbf{z}; p^+) G_0(-y^+, \mathbf{z} - \mathbf{y}; p^+) \\ &\quad \times [\theta(x^+)\theta(-y^+)U_{\mathbf{z}}^\dagger - \theta(-x^+)\theta(y^+)U_{\mathbf{z}}]. \end{aligned} \quad (\text{B.11})$$

C A sum rule for the light-cone gauge propagator

In this Appendix, we shall demonstrate the identity (2.13) which has played an important role in the construction of the high-energy evolution equations, notably in relation with the probability conservation and the cancellation of ultraviolet divergences. The careful treatment of the ϵ -dependence introduced by the adiabatic prescription will be essential for this purpose. Specifically, we shall show that the double time integral in the l.h.s. of (2.13) gives a result of $\mathcal{O}(\epsilon)$ and hence vanishes in the limit $\epsilon \rightarrow 0$.

We separately consider the two pieces in the decomposition (B.7) of the free propagator and use the mixed Fourier representation $G_0(t_2 - t_1, \mathbf{p}; p^+)$, cf. Eq. (B.8). We focus on the case $p^+ > 0$ for definiteness. Then the ‘radiation’ piece of the propagator is retarded ($\propto \theta(t_2 - t_1)$) and yields

$$\begin{aligned} \int dt_1 \int dt_2 G_{0,rad}^{--}(t_2 - t_1, \mathbf{p}; p^+) e^{-\epsilon(|t_1|+|t_2|)} &= \frac{p_\perp^2}{2(p^+)^3} \int_{-\infty}^{\infty} dt_2 \int_{-\infty}^{t_2} dt_1 e^{-ip^-(t_2-t_1)} e^{-\epsilon(|t_1|+|t_2|)} \\ &= \frac{p_\perp^2}{2(p^+)^3} \frac{1}{2\epsilon} \left[\frac{1}{ip^- + \epsilon} + \frac{1}{ip^- - \epsilon} \right] = -\frac{1}{\epsilon} \frac{i}{(p^+)^2} + \mathcal{O}(\epsilon), \end{aligned} \quad (\text{C.1})$$

where $p^- \equiv p_1^2/2p^+$. Note that, as compared to the previous, related, calculation in Eq. (3.12), the final result here is a purely divergent contribution, without any additional finite term. The respective contribution of the Coulomb piece is, clearly,

$$\int dt_1 \int dt_2 G_{0,Coul}^{\bar{-}}(t_2 - t_1, \mathbf{p}; p^+) e^{-\epsilon(|t_1|+|t_2|)} = \frac{i}{(p^+)^2} \int_{-\infty}^{\infty} dt e^{-2\epsilon|t|} = \frac{1}{\epsilon} \frac{i}{(p^+)^2}. \quad (\text{C.2})$$

As anticipated, this precisely cancels the divergent piece of the ‘radiative’ contribution, thus leaving a net result of $\mathcal{O}(\epsilon)$.

D Finite- N_c corrections within the mean field approximation

When constructing the evolution equation for a dipole in a medium, in Sect. 4.2, we have used the large- N_c limit to simplify some arguments and the various formulæ. But as also announced there, all the results obtained within the Gaussian approximation (4.14) for the medium correlations can be extended to finite values for N_c . In this Appendix, we present some tools which are useful in that sense. Such tools have been developed in applications of the CGC formalism and we refer to the original literature for their derivation and more details [34, 36–38, 40, 41].

As visible e.g. on (4.15), the evolution of the dipole S -matrix within the Gaussian approximation involves only two distinct Wilson line correlators: the dipole itself and a correlator built with three Wilson lines for the partonic system which exists during the fluctuation. For more generality, let us consider a dipole in some generic representation R of the $SU(N_c)$ algebra. Then, the relevant correlators read (within the mean field approximation, of course)

$$\mathcal{S}_R(\mathbf{x}, \mathbf{y}) \equiv \frac{1}{d_R} \left\langle \text{tr}_R [V_R^\dagger(\mathbf{x}) V_R(\mathbf{y})] \right\rangle = \exp \left\{ -g^2 C_R \int dt \Gamma(t, \mathbf{x}, \mathbf{y}) \right\}, \quad (\text{D.1})$$

and respectively (see e.g. Appendix B in Ref. [37] for a rapid derivation)

$$\left\langle U^{\dagger ab}(\mathbf{z}) \frac{\text{tr}_R}{d_R} \left(t_R^a V_R^\dagger(\mathbf{x}) t_R^b V_R(\mathbf{y}) \right) \right\rangle = C_R e^{-g^2 \int dt \left[\frac{N_c}{2} (\Gamma(t, \mathbf{x}, \mathbf{z}) + \Gamma(t, \mathbf{z}, \mathbf{y})) - \left(\frac{N_c}{2} - C_R \right) \Gamma(t, \mathbf{x}, \mathbf{y}) \right]} \quad (\text{D.2})$$

In these expressions, d_R is the dimension of the representation ($d_F = N_c$ for the fundamental, $d_A = N_c^2 - 1$ for the adjoint, etc.), C_R is the corresponding second Casimir ($C_F = (N_c^2 - 1)/2N_c$, $C_A = N_c$, etc.), and the integrals over t run over some arbitrary time interval (e.g. the width of the target, or a slice of it). Also, the transverse coordinates \mathbf{x} , \mathbf{y} , and \mathbf{z} need not be constant during that time interval, that is, Eq. (D.2) also holds for generic trajectories $\mathbf{x}(t)$, etc. Finally, the function $\Gamma(t, \mathbf{x}, \mathbf{y})$ is related to the function $\bar{\Gamma}(t, \mathbf{x}, \mathbf{y})$ which enters the 2-point function (4.14) of the background field via

$$\Gamma(t, \mathbf{x}, \mathbf{y}) = \frac{1}{2} [\bar{\Gamma}(t, \mathbf{x}, \mathbf{x}) + \bar{\Gamma}(t, \mathbf{y}, \mathbf{y})] - \bar{\Gamma}(t, \mathbf{x}, \mathbf{y}). \quad (\text{D.3})$$

Using these formulæ, it is straightforward to generalize the results in Sect. 4.2 to arbitrary N_c . For instance, for a dipole in the color representation R , the analog of Eq. (4.22) is obtained by replacing

$$\frac{N_c}{2} \left[\mathcal{S}_{t_2, t_1}(\mathbf{x}, \mathbf{r}) \mathcal{S}_{t_2, t_1}(\mathbf{r}, \mathbf{y}) \mathcal{S}_{t_2, t_1}^{-1}(\mathbf{x}, \mathbf{y}) - 1 \right] \rightarrow C_R \left\{ e^{-\frac{g^2 N_c}{2} \int_{t_1}^{t_2} dt [\Gamma_\omega(t, \mathbf{x}, \mathbf{r}) + \Gamma_\omega(t, \mathbf{r}, \mathbf{y}) - \Gamma_\omega(t, \mathbf{x}, \mathbf{y})]} - 1 \right\} \quad (\text{D.4})$$

within the r.h.s. of Eq. (4.22). Also, the respective l.h.s. should more generally read

$$-\frac{\partial \ln \mathcal{S}_R(\mathbf{x}, \mathbf{y})}{\partial \omega} = C_R \int_0^L dt \frac{\partial \Gamma_\omega(t, \mathbf{x}, \mathbf{y})}{\partial \omega}. \quad (\text{D.5})$$

After these replacements, the overall factor of C_R cancels out and Eq. (4.22) reduces to Eq. (4.24) for $\Gamma_\omega(\mathbf{x}, \mathbf{y})$ for *any* value of N_c . Hence, as already mentioned in the main text, this equation is independent of the color representation R of the dipole that we have started with.

References

- [1] Y. Mehtar-Tani, J. G. Milhano, and K. Tywoniuk, *Jet physics in heavy-ion collisions*, *Int.J.Mod.Phys.* **A28** (2013) 1340013, [[arXiv:1302.2579](#)].
- [2] A. Majumder and M. Van Leeuwen, *The theory and phenomenology of perturbative QCD based jet quenching*, [arXiv:1002.2206](#).
- [3] D. d’Enterria, *Jet quenching*, [arXiv:0902.2011](#).
- [4] J. Casalderrey-Solana and C. A. Salgado, *Introductory lectures on jet quenching in heavy ion collisions*, *Acta Phys. Polon.* **B38** (2007) 3731–3794, [[arXiv:0712.3443](#)].
- [5] A. Kovner and U. A. Wiedemann, *Gluon radiation and parton energy loss*, [hep-ph/0304151](#).
- [6] P. B. Arnold and W. Xiao, *High-energy jet quenching in weakly-coupled quark-gluon plasmas*, *Phys.Rev.* **D78** (2008) 125008, [[arXiv:0810.1026](#)].
- [7] S. Caron-Huot, *$O(g)$ plasma effects in jet quenching*, *Phys.Rev.* **D79** (2009) 065039, [[arXiv:0811.1603](#)].
- [8] A. Majumder, *Calculating the jet quenching parameter \hat{q} in lattice gauge theory*, *Phys.Rev.* **C87** (2013) 034905, [[arXiv:1202.5295](#)].
- [9] T. Liou, A. H. Mueller, and B. Wu, *Radiative p_\perp -broadening of high-energy quarks and gluons in QCD matter*, *Nucl.Phys.* **A916** (2013) 102–125, [[arXiv:1304.7677](#)].
- [10] M. Laine and A. Rothkopf, *Light-cone Wilson loop in classical lattice gauge theory*, *JHEP* **1307** (2013) 082, [[arXiv:1304.4443](#)].
- [11] M. Panero, K. Rummukainen, and A. Schfer, *A lattice study of the jet quenching parameter*, [arXiv:1307.5850](#).
- [12] A. H. Mueller, *Parton saturation: An Overview*, [hep-ph/0111244](#).
- [13] A. H. Mueller and S. Munier, *p_\perp -broadening and production processes versus dipole/quadrupole amplitudes at next-to-leading order*, *Nucl.Phys.* **A893** (2012) 43–86, [[arXiv:1206.1333](#)].
- [14] B. Wu, *On p_T -broadening of high energy partons associated with the LPM effect in a finite-volume QCD medium*, *JHEP* **1110** (2011) 029, [[arXiv:1102.0388](#)].
- [15] Y. L. Dokshitzer, V. A. Khoze, A. H. Mueller, and S. I. Troian, *Basics of perturbative QCD*, . Gif-sur-Yvette, France. Ed. Frontieres (1991) 274 p.
- [16] Y. V. Kovchegov and E. Levin, *Quantum chromodynamics at high energy*. Cambridge University Press, 2012.
- [17] I. Balitsky, *Operator expansion for high-energy scattering*, *Nucl. Phys.* **B463** (1996) 99–160, [[hep-ph/9509348](#)].
- [18] Y. V. Kovchegov, *Small- x F_2 structure function of a nucleus including multiple pomeron exchanges*, *Phys. Rev.* **D60** (1999) 034008, [[hep-ph/9901281](#)].

- [19] J. Jalilian-Marian, A. Kovner, A. Leonidov, and H. Weigert, *The BFKL equation from the Wilson renormalization group*, *Nucl. Phys.* **B504** (1997) 415–431, [[hep-ph/9701284](#)].
- [20] J. Jalilian-Marian, A. Kovner, A. Leonidov, and H. Weigert, *The Wilson renormalization group for low x physics: Towards the high density regime*, *Phys.Rev.* **D59** (1998) 014014, [[hep-ph/9706377](#)].
- [21] J. Jalilian-Marian, A. Kovner, and H. Weigert, *The Wilson renormalization group for low x physics: Gluon evolution at finite parton density*, *Phys. Rev.* **D59** (1999) 014015, [[hep-ph/9709432](#)].
- [22] A. Kovner, J. G. Milhano, and H. Weigert, *Relating different approaches to nonlinear QCD evolution at finite gluon density*, *Phys. Rev.* **D62** (2000) 114005, [[hep-ph/0004014](#)].
- [23] H. Weigert, *Unitarity at small Bjorken x* , *Nucl. Phys.* **A703** (2002) 823–860, [[hep-ph/0004044](#)].
- [24] E. Iancu, A. Leonidov, and L. D. McLerran, *Nonlinear gluon evolution in the color glass condensate. I*, *Nucl. Phys.* **A692** (2001) 583–645, [[hep-ph/0011241](#)].
- [25] E. Iancu, A. Leonidov, and L. D. McLerran, *The renormalization group equation for the color glass condensate*, *Phys. Lett.* **B510** (2001) 133–144, [[hep-ph/0102009](#)].
- [26] E. Iancu and L. D. McLerran, *Saturation and universality in QCD at small x* , *Phys. Lett.* **B510** (2001) 145–154, [[hep-ph/0103032](#)].
- [27] E. Ferreiro, E. Iancu, A. Leonidov, and L. McLerran, *Nonlinear gluon evolution in the color glass condensate. II*, *Nucl. Phys.* **A703** (2002) 489–538, [[hep-ph/0109115](#)].
- [28] E. Iancu, K. Itakura, and L. McLerran, *Geometric scaling above the saturation scale*, *Nucl. Phys.* **A708** (2002) 327–352, [[hep-ph/0203137](#)].
- [29] A. H. Mueller and D. N. Triantafyllopoulos, *The Energy dependence of the saturation momentum*, *Nucl.Phys.* **B640** (2002) 331–350, [[hep-ph/0205167](#)].
- [30] S. Munier and R. B. Peschanski, *Geometric scaling as traveling waves*, *Phys. Rev. Lett.* **91** (2003) 232001, [[hep-ph/0309177](#)].
- [31] Z.-B. Kang, E. Wang, X.-N. Wang, and H. Xing, *QCD factorization for semi-inclusive deeply inelastic scattering at twist-4 in next-to-leading order*, [arXiv:1310.6759](#).
- [32] E. Iancu, A. Leonidov, and L. McLerran, *The Color glass condensate: An Introduction*, [[hep-ph/0202270](#)].
- [33] F. Gelis, E. Iancu, J. Jalilian-Marian, and R. Venugopalan, *The Color Glass Condensate*, *Ann.Rev.Nucl.Part.Sci.* **60** (2010) 463–489, [[arXiv:1002.0333](#)].
- [34] A. Kovner and U. A. Wiedemann, *Eikonal evolution and gluon radiation*, *Phys. Rev.* **D64** (2001) 114002, [[hep-ph/0106240](#)].
- [35] E. Iancu, K. Itakura, and L. McLerran, *A Gaussian effective theory for gluon saturation*, *Nucl. Phys.* **A724** (2003) 181–222, [[hep-ph/0212123](#)].
- [36] J. P. Blaizot, F. Gelis, and R. Venugopalan, *High energy p A collisions in the color glass condensate approach. II: Quark production*, *Nucl. Phys.* **A743** (2004) 57–91, [[hep-ph/0402257](#)].
- [37] Y. V. Kovchegov, J. Kuokkanen, K. Rummukainen, and H. Weigert, *Subleading- N_c corrections in non-linear small- x evolution*, *Nucl. Phys.* **A823** (2009) 47–82, [[arXiv:0812.3238](#)].
- [38] F. Dominguez, C. Marquet, B.-W. Xiao, and F. Yuan, *Universality of Unintegrated Gluon Distributions at small x* , *Phys. Rev.* **D83** (2011) 105005, [[arXiv:1101.0715](#)].
- [39] E. Iancu and D. Triantafyllopoulos, *Higher-point correlations from the JIMWLK evolution*, *JHEP* **1111** (2011) 105, [[arXiv:1109.0302](#)].

- [40] E. Iancu and D. Triantafyllopoulos, *JIMWLK evolution in the Gaussian approximation*, *JHEP* **1204** (2012) 025, [[arXiv:1112.1104](#)].
- [41] A. Dumitru, J. Jalilian-Marian, T. Lappi, B. Schenke, and R. Venugopalan, *Renormalization group evolution of multi-gluon correlators in high energy QCD*, *Phys.Lett.* **B706** (2011) 219–224, [[arXiv:1108.4764](#)].
- [42] R. Baier, Y. L. Dokshitzer, A. H. Mueller, S. Peigne, and D. Schiff, *Radiative Energy Loss of High Energy Quarks and Gluons in a Finite-Volume Quark-Gluon Plasma*, *Nucl. Phys.* **B483** (1997) 291–320, [[hep-ph/9607355](#)].
- [43] R. Baier, Y. L. Dokshitzer, A. H. Mueller, S. Peigne, and D. Schiff, *Radiative Energy Loss and $P(T)$ -Broadening of High Energy Partons in Nuclei*, *Nucl. Phys.* **B484** (1997) 265–282, [[hep-ph/9608322](#)].
- [44] B. G. Zakharov, *Fully Quantum Treatment of the Landau-Pomeranchuk-Migdal Effect in QED and QCD*, *JETP Lett.* **63** (1996) 952–957, [[hep-ph/9607440](#)].
- [45] B. G. Zakharov, *Radiative Energy Loss of High Energy Quarks in Finite-Size Nuclear Matter and Quark-Gluon Plasma*, *JETP Lett.* **65** (1997) 615–620, [[hep-ph/9704255](#)].
- [46] R. Baier, Y. L. Dokshitzer, A. H. Mueller, and D. Schiff, *Radiative Energy Loss of High Energy Partons Traversing an Expanding QCD Plasma*, *Phys. Rev.* **C58** (1998) 1706–1713, [[hep-ph/9803473](#)].
- [47] R. Baier, Y. L. Dokshitzer, A. H. Mueller, and D. Schiff, *Medium-Induced Radiative Energy Loss: Equivalence Between the Bdmpps and Zakharov Formalisms*, *Nucl. Phys.* **B531** (1998) 403–425, [[hep-ph/9804212](#)].
- [48] U. A. Wiedemann, *Gluon Radiation Off Hard Quarks in a Nuclear Environment: Opacity Expansion*, *Nucl. Phys.* **B588** (2000) 303–344, [[hep-ph/0005129](#)].
- [49] U. A. Wiedemann, *Jet Quenching Versus Jet Enhancement: a Quantitative Study of the Bdmpps-Z Gluon Radiation Spectrum*, *Nucl. Phys.* **A690** (2001) 731–751, [[hep-ph/0008241](#)].
- [50] P. B. Arnold, G. D. Moore, and L. G. Yaffe, *Photon Emission from Ultrarelativistic Plasmas*, *JHEP* **11** (2001) 057, [[hep-ph/0109064](#)].
- [51] P. B. Arnold, G. D. Moore, and L. G. Yaffe, *Photon Emission from Quark Gluon Plasma: Complete Leading Order Results*, *JHEP* **12** (2001) 009, [[hep-ph/0111107](#)].
- [52] P. B. Arnold, G. D. Moore, and L. G. Yaffe, *Photon and Gluon Emission in Relativistic Plasmas*, *JHEP* **06** (2002) 030, [[hep-ph/0204343](#)].
- [53] J.-P. Blaizot and Y. Mehtar-Tani, *to appear*, .
- [54] Z. Chen and A. H. Mueller, *The Dipole picture of high-energy scattering, the BFKL equation and many gluon compound states*, *Nucl.Phys.* **B451** (1995) 579–604.
- [55] J. P. Blaizot, F. Gelis, and R. Venugopalan, *High-energy pA collisions in the color glass condensate approach. 1. Gluon production and the Cronin effect*, *Nucl.Phys.* **A743** (2004) 13–56, [[hep-ph/0402256](#)].
- [56] A. H. Mueller, *A Simple derivation of the JIMWLK equation*, *Phys.Lett.* **B523** (2001) 243–248, [[hep-ph/0110169](#)].
- [57] S. Jeon, *Color Glass Condensate in Schwinger-Keldysh QCD*, *Annals Phys.* **340** (2014) 119–170, [[arXiv:1308.0263](#)].
- [58] S. Caron-Huot, *When does the gluon reggeize?*, [arXiv:1309.6521](#).

- [59] D. Binosi, A. Quadri, and D. Triantafyllopoulos, *High-energy QCD evolution from BRST symmetry*, [arXiv:1402.4022](#).
- [60] Y. Hatta, E. Iancu, K. Itakura, and L. McLerran, *Odderon in the color glass condensate*, *Nucl. Phys.* **A760** (2005) 172–207, [[hep-ph/0501171](#)].
- [61] L. D. McLerran and R. Venugopalan, *Computing quark and gluon distribution functions for very large nuclei*, *Phys. Rev.* **D49** (1994) 2233–2241, [[hep-ph/9309289](#)].
- [62] L. D. McLerran and R. Venugopalan, *Green’s functions in the color field of a large nucleus*, *Phys. Rev.* **D50** (1994) 2225–2233, [[hep-ph/9402335](#)].
- [63] P. B. Arnold, *Simple Formula for High-Energy Gluon Bremsstrahlung in a Finite, Expanding Medium*, *Phys. Rev.* **D79** (2009) 065025, [[arXiv:0808.2767](#)].
- [64] Y. V. Kovchegov and K. Tuchin, *Inclusive gluon production in DIS at high parton density*, *Phys.Rev.* **D65** (2002) 074026, [[hep-ph/0111362](#)].
- [65] L. Lipatov, *Reggeization of the Vector Meson and the Vacuum Singularity in Nonabelian Gauge Theories*, *Sov.J.Nucl.Phys.* **23** (1976) 338–345.
- [66] E. Kuraev, L. Lipatov, and V. S. Fadin, *The Pomernchuk Singularity in Nonabelian Gauge Theories*, *Sov.Phys.JETP* **45** (1977) 199–204.
- [67] I. Balitsky and L. Lipatov, *The Pomernchuk Singularity in Quantum Chromodynamics*, *Sov.J.Nucl.Phys.* **28** (1978) 822–829.
- [68] J.-P. Blaizot, F. Dominguez, E. Iancu, and Y. Mehtar-Tani, *Probabilistic picture for medium-induced jet evolution*, [arXiv:1311.5823](#).
- [69] Y. Hatta, E. Iancu, and A. Mueller, *Deep inelastic scattering off a $N=4$ SYM plasma at strong coupling*, *JHEP* **0801** (2008) 063, [[arXiv:0710.5297](#)].
- [70] Y. Hatta, E. Iancu, and A. Mueller, *Jet evolution in the $N=4$ SYM plasma at strong coupling*, *JHEP* **0805** (2008) 037, [[arXiv:0803.2481](#)].
- [71] F. Dominguez, C. Marquet, A. Mueller, B. Wu, and B.-W. Xiao, *Comparing energy loss and p -perpendicular - broadening in perturbative QCD with strong coupling $N = 4$ SYM theory*, *Nucl.Phys.* **A811** (2008) 197–222, [[arXiv:0803.3234](#)].
- [72] Y. Hatta, E. Iancu, and A. Mueller, *Deep inelastic scattering at strong coupling from gauge/string duality: The Saturation line*, *JHEP* **0801** (2008) 026, [[arXiv:0710.2148](#)].
- [73] Y. Mehtar-Tani, *Relating the Description of Gluon Production in Pa Collisions and Parton Energy Loss in Aa Collisions*, *Phys. Rev.* **C75** (2007) 034908, [[hep-ph/0606236](#)].
- [74] J. Casalderrey-Solana and E. Iancu, *Interference Effects in Medium-Induced Gluon Radiation*, *JHEP* **08** (2011) 015, [[arXiv:1105.1760](#)].
- [75] J.-P. Blaizot, F. Dominguez, E. Iancu, and Y. Mehtar-Tani, *Medium-induced gluon branching*, *JHEP* **1301** (2013) 143, [[arXiv:1209.4585](#)].
- [76] Y. Mehtar-Tani, C. A. Salgado, and K. Tywoniuk, *Antiangular Ordering of Gluon Radiation in QCD Media*, *Phys. Rev. Lett.* **106** (2011) 122002, [[arXiv:1009.2965](#)].
- [77] Y. Mehtar-Tani, C. A. Salgado, and K. Tywoniuk, *Jets in QCD Media: from Color Coherence to Decoherence*, *Phys. Lett.* **B707** (2012) 156–159, [[arXiv:1102.4317](#)].
- [78] N. Armesto, H. Ma, Y. Mehtar-Tani, C. A. Salgado, and K. Tywoniuk, *Coherence Effects and Broadening in Medium-Induced QCD Radiation Off a Massive $Q\bar{Q}$ Antenna*, *JHEP* **01** (2012) 109, [[arXiv:1110.4343](#)].

- [79] J.-P. Blaizot, E. Iancu, and Y. Mehtar-Tani, *Medium-induced QCD cascade: democratic branching and wave turbulence*, *Phys.Rev.Lett.* **111** (2013) 052001, [[arXiv:1301.6102](#)].
- [80] D. Triantafyllopoulos, *The Energy dependence of the saturation momentum from RG improved BFKL evolution*, *Nucl.Phys.* **B648** (2003) 293–316, [[hep-ph/0209121](#)].
- [81] J. L. Albacete and Y. V. Kovchegov, *Solving high energy evolution equation including running coupling corrections*, *Phys.Rev.* **D75** (2007) 125021, [[arXiv:0704.0612](#)].
- [82] I. Balitsky and G. A. Chirilli, *Rapidity evolution of Wilson lines at the next-to-leading order*, *Phys.Rev.* **D88** (2013) 111501, [[arXiv:1309.7644](#)].
- [83] A. Kovner, M. Lublinsky, and Y. Mulian, *Complete JIMWLK Evolution at NLO*, [arXiv:1310.0378](#).
- [84] J. L. Albacete and C. Marquet, *Gluon saturation and initial conditions for relativistic heavy ion collisions*, [arXiv:1401.4866](#).
- [85] S. S. Gubser and A. Karch, *From gauge-string duality to strong interactions: A Pedestrian’s Guide*, *Ann.Rev.Nucl.Part.Sci.* **59** (2009) 145–168, [[arXiv:0901.0935](#)].
- [86] J. Casalderrey-Solana, H. Liu, D. Mateos, K. Rajagopal, and U. A. Wiedemann, *Gauge/String Duality, Hot QCD and Heavy Ion Collisions*, [arXiv:1101.0618](#).
- [87] S. S. Gubser, D. R. Gulotta, S. S. Pufu, and F. D. Rocha, *Gluon energy loss in the gauge-string duality*, *JHEP* **0810** (2008) 052, [[arXiv:0803.1470](#)].
- [88] P. M. Chesler, K. Jensen, A. Karch, and L. G. Yaffe, *Light quark energy loss in strongly-coupled $N = 4$ supersymmetric Yang-Mills plasma*, *Phys.Rev.* **D79** (2009) 125015, [[arXiv:0810.1985](#)].
- [89] P. Arnold and D. Vaman, *Jet quenching in hot strongly coupled gauge theories revisited: 3-point correlators with gauge-gravity duality*, *JHEP* **10** (2010) 099, [[arXiv:1008.4023](#)].
- [90] D. Binosi and L. Theussl, *JaxoDraw: A Graphical user interface for drawing Feynman diagrams*, *Comput.Phys.Commun.* **161** (2004) 76–86, [[hep-ph/0309015](#)].